The DEAH helicase RHAU is essential for embryogenesis and hematopoiesis

Inauguraldissertation

zur

Erlangung der Würde eines Doktors der Philosophie
Vorgelegt der
Philosophisch-Naturwissenschaflichen Fakultät
der Universität Basel

von

Ching Janice Lai

aus Sonderverwaltungszone Hongkong der Volksrepublik China

Basel 2012

creative commons

Attribution-Noncommercial-No Derivative Works 2.5 Switzerland

---

You are free:

to Share — to copy, distribute and transmit the work

Under the following conditions:

Attribution. You must attribute the work in the manner specified by the author or licensor (but not in any way that suggests that they endorse you or your use of the work).

Noncommercial. You may not use this work for commercial purposes.

No Derivative Works. You may not alter, transform, or build upon this work.

- For any reuse or distribution, you must make clear to others the license terms of this work. The best way to do this is with a link to this web page.
- Any of the above conditions can be waived if you get permission from the copyright holder.
- Nothing in this license impairs or restricts the author's moral rights.

Your fair dealing and other rights are in no way affected by the above.

This is a human-readable summary of the Legal Code (the full license) available in German:
http://creativecommons.org/licenses/by-nc-nd/2.5/ch/legalcode.de

Disclaimer:
The Commons Deed is not a license. It is simply a handy reference for understanding the Legal Code (the full license) — it is a human-readable expression of some of its key terms. Think of it as the user-friendly interface to the Legal Code beneath. This Deed itself has no legal value, and its contents do not appear in the actual license. Creative Commons is not a law firm and does not provide legal services. Distributing of, displaying of, or linking to this Commons Deed does not create an attorney-client relationship.

Quelle: http://creativecommons.org/licenses/by-nc-nd/2.5/ch/deed.en Datum: 3.4.2009

Genehmigt von der Philosophisch-Naturwissenschaftlichen Fakultät
auf Antrag von

Prof. Radek Skoda, Prof. Patrick Matthias, and Prof. Nancy Hynes and Dr. Yoshikuni Nagamine.

Basel, den 22. June 2010

Prof. Dr. Martin Spiess
Dekan

Abstract

The DEAH helicase RHAU (alias DHX36, G4R1) was recently identified as a shuttle protein localized mainly in the nucleus. It is the only helicase shown to have G4-RNA resolvase activity and the major source of G4-DNA resolvase activity in HeLa cell lysate. Its ablation reduces the proliferation rate of various human cell lines in culture. The Human Gene Atlas database (GNF, Novartis) shows ubiquitous expression of RHAU, with prominently elevated levels in lymphoid and CD34+ bone marrow cells, suggesting a potential role in hematopoiesis. To investigate the biological role of RHAU, we generated mice in which the RHAU gene was targeted conventionally or specifically in the hematopoietic system.

Conventional RHAU ablation caused embryonic lethality before 7.5 days after fertilization but without disturbing embryo implantation, suggesting a fundamental role for RHAU in early development (gastrulation).

Because conventional RHAU-ablation caused embryonic lethality, we then targeted the RHAU gene specifically in the hematopoiesis system. To achieve this we used vav1-iCre system, in which iCre gene (an optimized variant of Cre recombinase) was expressed under the control of *vav1* oncogen promoter that was active solely in the hematopoietic system. Results showed that RHAU-ablation in the hematopoietic system strongly affected the process of hematopoiesis in a lineage- and stage-specific manner. Notably, RHAU ablation caused hemolytic anemia and strong impairment of lymphoid cell differentiation at early its stages.

Finally, by micro-array analysis we examined the effect of RHAU ablation on the change of transcriptome in proerythroblasts. We found that within a group of genes involved in cell death and cell cycle regulation, RHAU-ablation deregulated those genes that contained G-quadruplex motifs in their promoter regions. This result suggests that RHAU plays a role in the regulation of gene expression through involving its G4 resolvase activity.

TABLE OF CONTENT

1 Introduction

RNAs are an important group of molecules for gene regulation in organisms. From transcription to signaling, RNA molecules can be found playing roles in all aspects. The biological roles of RNA molecules were extensively investigated in the last few decades. Since the discovery of siRNA in the early 90s of the last century, more people started to realize the important role of RNA metabolism in cell development and survival. In recent years, there is a huge increase of studies concerning the role of RNA binding molecules that directly regulate the RNA metabolisms. However, there is still numerous of proteins that regulate RNA metabolism but have never been looked at. Here, I am going to present a study using knockout mice model in which an RNA helicase, RHAU, is targeted I wish that this mouse model can also give some hints of how the other DEAH helicases function in mammals.

The biological function and the mechanism of RHAU are still almost unknown. In order to start to investigate this new protein, the best way is to get some information from other helicases. Here, I will guide you to know more about helicase, how the helicase structure is related to its function and biology of helicases.

1.1 RNA helicases

RNA helicases are proteins with enzymatic activity. They associate with RNA molecules and regulate various aspects of RNA metabolism. They can resolve complex RNA structures and displace proteins from RNA-protein complex with or without the hydrolysis of nucleoside triphosphates (Hilbert et al., 2009). Usually RNA helicases share conserved core domains. These core domains are critical for RNA binding and NTP hydrolysis. Each RNA helicase evolved with unique C and N termini that contribute to its specific functions (Jankowsky and Fairman, 2007). Although helicases are ancient molecules like RNA polymerase, the knowledge we have is too little compare to the level of importance of these protein in life.

1.2 Evolution and RNA helicases

RNA helicase was evolved in the necessity of resolving complex RNAstructures. Correct folding of RNA molecules in secondary, tertiary and quaternary structures is critical for their proper functions in transcription, splicing, processing and editing of transcripts, translation, RNA degradation and its regulation (Herschlag, 1995) (Anantharaman et al., 2002). According to a comparative genomics and protein evolution study on RNA metabolism carried by Anantharaman and his colleagues and published in 2002, around 3 to 11% of the complete proteome are related to RNA metabolism in bacteria, archaea and eukaryotes. Interestingly, half of these RNA metabolism-related domains are

shared amongst all three bacterial, archaeal and eukaryotic kingdom. These protein domains are even traceable to the last universal common ancestor from which all organisms on Earth descended (Anantharaman et al., 2002) (Doolittle, 2000) (Glansdorff et al., 2008). Amongst these RNA metabolism related proteins, RNA helicases form the largest group.

1.3 The structure of RNA helicases

The name "Helicases" was initially used to descript the proteins that harbor the catalytic activity of separating duplex DNA or RNA into two single strands in an ATP-dependent reaction. These helicases were grouped into two types based on the mode of activity, (1) unwinding duplexes in a 3' to 5' direction and (2) unwinding 5' to 3' direction (Caruthers and McKay, 2002). All of the helicases carry the classical Walker 'A' (phosphate-binding loop or 'P-loop') and Walker 'B' (Mg^{2+}-binding aspartic acid) motifs (Walker et al., 1982). Later in 1993, Gorbalenya and Koonin proposed to divide helicases into five major groups based on the conserved motifs or signatures found in the core catalytic domains. These groups are superfamily (SF) I, II and III, DnaB like family and Rho-like family (Gorbalenya and Koonin, 1993). SF1 includes some RNA helicases; superfamilies 2 (SF2) contributes the largest size of the helicase population; SF3 and SF4 include some viral RNA helicases.

SF2 include DNA and RNA helicases from the three primary kingdoms and viruses. They unwind nucleic acids in either directions of nucleic acid duplex (Caruthers and McKay, 2002). With the increasing knowledge of helicases, some SF2 helicases were found to remodel nucleic acid structures rather than unwind nucleic acid duplex (Staley and Guthrie, 1998). Based on the homology of primary structure of the helicases, SF2 are divided into DExH/D, the RecQ and SWI/SNF families. DExH/D proteins are further divided into DEAD-box, DExH and DEAH subfamilies (Jankowsky and Fairman, 2007). In mammals, DEAD-box proteins were assigned with gene symbol of DDX-, where DEAH or DExH proteins were assigned with DHX- (Abdelhaleem et al., 2003). For example, RHAU share the maximum homology with a series of DEAH RNA helicase in SF2, and this protein was assigned with DHX36 symbol even though it contains DEIH amino acid sequence rather than DEAH (Figure 1.1 and Figure 1.2A).

A total of at least eight motifs, motif I, Ia, Ib, II, III, IV, V and VI, were identified from the SF2 helicases (Figure 1.2.A). Motifs I and II are the classical Walker A and B, respectively. These eight motifs distribute on two helicase core domains (1 and 2) which are connected via a flexible linker region. This special structure is named RecA-like helicase domains which are involved in an ATP hydrolysis and nucleic-acid binding (Figure 1.2.B). Motifs Ia, Ib, Ic, IV and IVa locate at the surface of the helicase domains where it contacts the nucleic acid backbone. In the inner side of the cleft between the two helicase domains, motifs I, II and VI bind to nucleic acids while motifs III and V coordinate polynucleotide binding and ATPase activity. When SF2 helicases are bound to ATP, the two RecA domains transform from an open confirmation to a closed conformation.

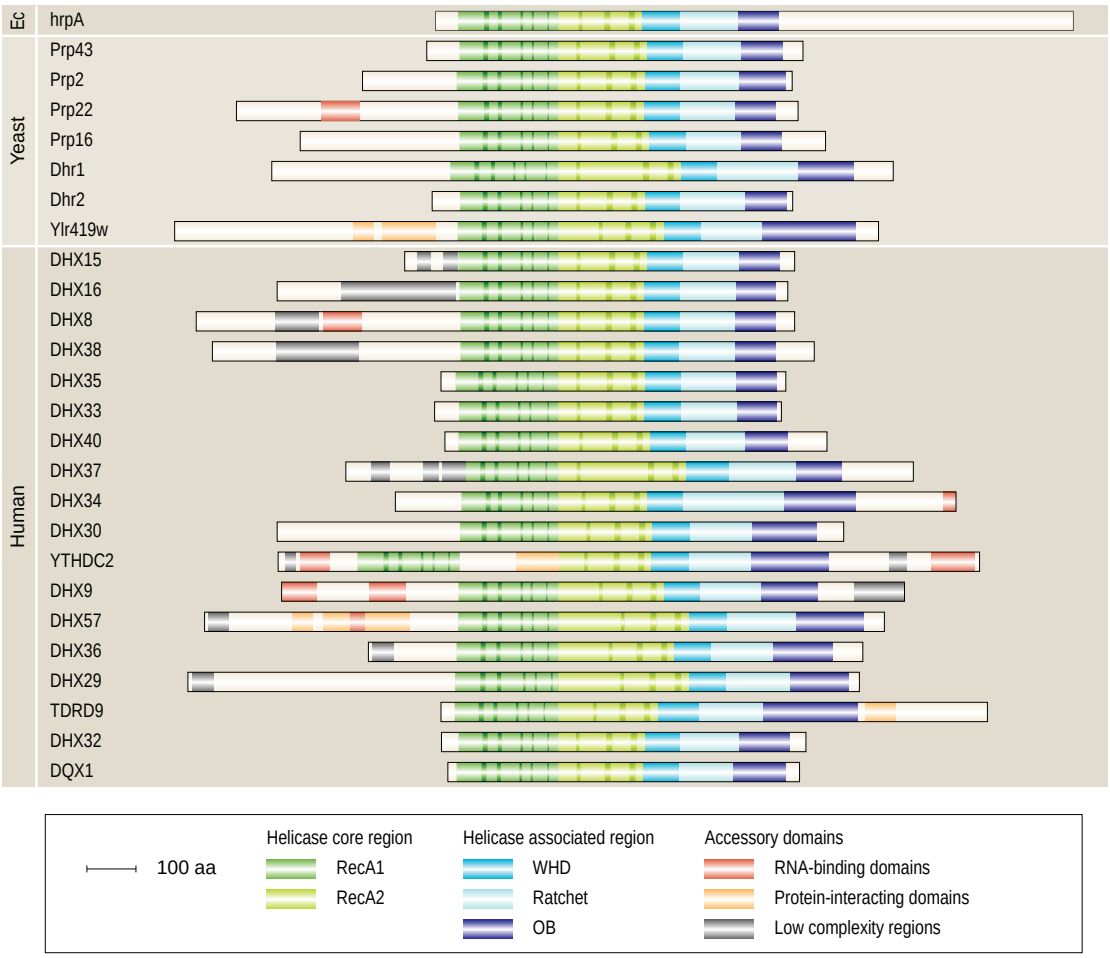

Figure 1.1. Alignment of the amino acid sequences of mammalian DEAH helicases. RHAU (DHX36) gene is in the human protein group. The dark and light green boxes represent the RecA domains 1 and 2 (Helicase core domain). Strips in the domains represent consevered motifs I to VI in the helicase core domain across all SF1 and SF2 helicases. Dodgerblud boxes are winged-helix domain (WHD), lightskyblue boxes are Ratchet domain, and navyblue boxes are oligonucleotide/oligosaccharide-binding fold (OB-fold) domain. The alignment shows that all the members share specific WHD, Ratchet and OB domains (unpublished data from Simon Lattmann, 2007).

A

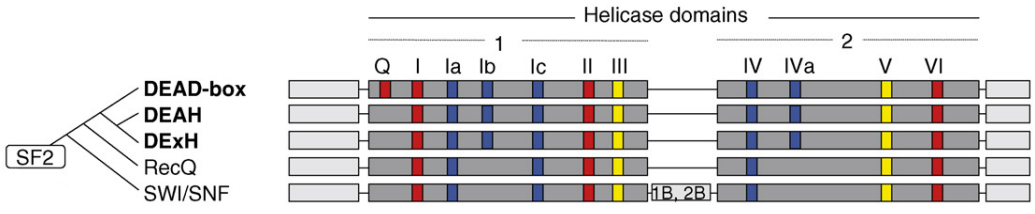

B

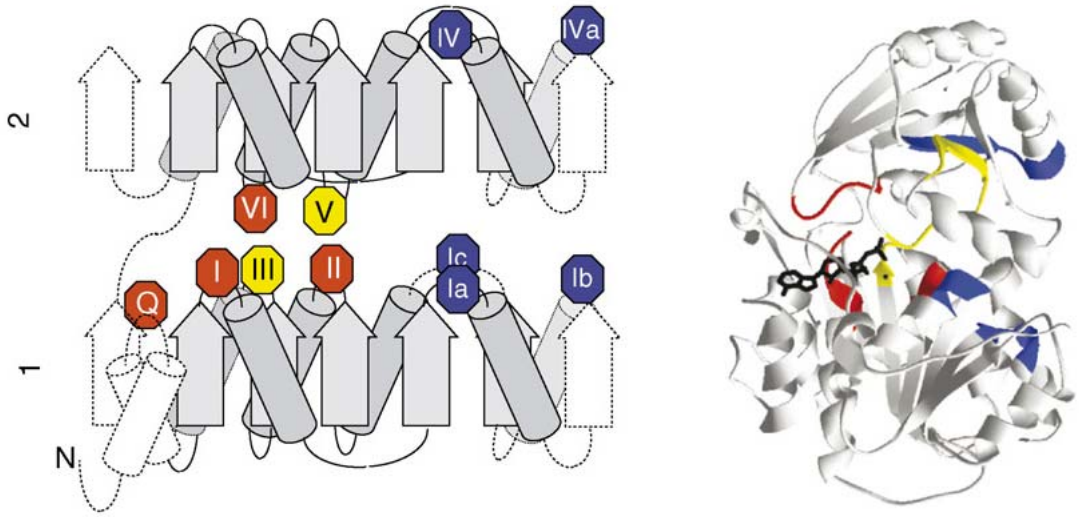

Figure 1.2. (A) Summary of sequence characteristics found in SF2 helicases. The tree diagram (left) shows the phylogenetic relationship of SF2 subfamilies helicases. Helicase domains are represented as dark gray blocks, and C and N termini are in light gray blocks. Insertions in the helicase domains are labeled. The blocks are not to scale in length. Colored blocks represent conserved functional motifs: red, ATP binding and hydrolysis; yellow, coordination between polynucleotide binding and ATPase activity; blue, nucleic acid binding. The DExH/D group helicases includes DEAD-box, DExH and DEAH subgroups. B (Left) The topology of the two RecA-like helicase domains. Solid outlined elements are presented in all SF2 helicases and dashed outlined elements are not present in all proteins. The position of the conserved sequence motifs is indicated by numbered octagons, colored as in (A). (B) The structure of the SF2 helicase DEAD-box protein VASA with bound ATP analog (black) (Sengoku et al., 2006). Conserved sequence motifs are colored as in (A) [Figure is modified from (Jankowsky and Fairman, 2007)]. The updated gene list of SF2 family is available on line http://www.dexhd.org/index.htm

Most of knowledge of RNA helicase structure are derived from studies on SF2 DEAD-box helicases (Andersen et al., 2006; Mackintosh et al., 2006) (Kim et al., 1998) (Bono et al., 2006; Sengoku et al., 2006). The mechanism of ATP hydrolysis is different among different helicases even though all SF2 helicases have the ATP binding and hydrolysis site in the core domain; DEAD-box helicase require nucleic acid to hydrolyze ATP while DEAH helicases can hydrolyze ATP in the absence of nucleic acid (Talavera and De La Cruz, 2005) (Iost et al., 1999) (Lorsch and Herschlag, 1998) (Polach and Uhlenbeck, 2002). Only last February, the first paper about the crystal structure of a DEAH helicase, Prp43p from yeast, appeared (He et al., 2010). This exciting data provides a bit more structural information of DEAH helicases outside the core RecA domains for the first time. Prp43p is a yeast homolog of mammalian DHX15 that is involved in per-messenger RNA splicing and pre-ribosomal RNA processing in yeast (Tanaka et al., 2007). This study has demonstrated that the structural building blocks in Prp43p are also represented in other DEAH helicases (Figure 1.1). Like DEAD-box helicases, DEAH helicases contain two RecA domains. Surprisingly, the sequence outside the core domains of these DEAH helicases share high homology with that of Hel308 and Hjm DNA helicases. In this region, there is a degenerated winged-helix domain (WHD) with a weakly defined β-sheet followed by a ratchet domain and then a C-terminal domain (CTD). The

CTD shows a structural homology to eIF1A. The WHD, ratchet domain and CTD all contact with the amino-terminal domain. The hairpin 5'HP, extending from the motifs V and VI of RecA2, is inserted into a cleft between the WHD and CTD (Figure 1.3). This hairpin is close to the 5'end of the putative binding pocket for ssRNA in the ATP state. Similar to the Hel308, this helix may be used to unwind very stable nucleic acid duplex (Zhang et al., 2009) (Pena et al., 2009) (He et al., 2010). Though we have some knowledge about the DEAH helicase structure by looking at this Prp43p protein, the N-terminus of RHAU is very unique not only among all DEAH helicases but any other proteins with known structural information. In order to know how RHAU function in the cell, elucidation of the crystal structure of this region is particularly critical.

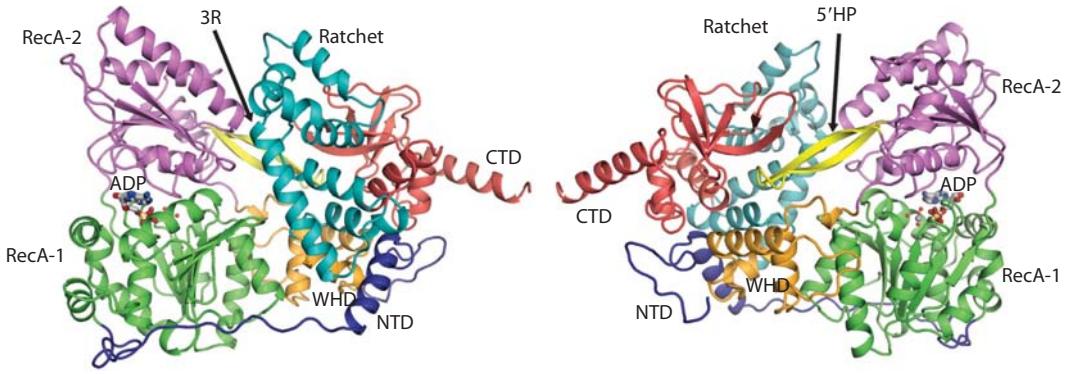

Figure 1.3. The structure of Prp43p. The extended NTD region is coloured blue, RecA domain 1 green, RecA domain 2 magenta, the 5'HP yellow, the WHD orange, the ratchet domain cyan and the CTD red. 3R is a long helix with the ratchet domain involved in RNA interaction [figure is modified from (He et al., 2010)].

1.4 The mechanism of RNA helicase

Based on the available biochemistry analysis, we knew that some RNA helicases firstly bind to a single stranded over-hanged nucleic acid and then slide along the RNA strands. Take Helicases nucleoside triphosphate phosphohydrolase II (NPH-II) and NS3 from viruses as examples. They just slide along one of the strands of the RNA duplex in an ATP dependent activity rather than binding on both strands (Kawaoka et al., 2004) (Beran et al., 2006). To explain how the helicase move along the nucleic acid strand, three models were widely proposed. They are (1) active rolling mechanism, (2) inchworm mechanism and (3) Brownian motor model (Figure 1.4). In rolling mechanism hypothesis, helicases work as a dimer with different conformation, one is opened when the next one is closed. Some helicases bind at a single stranded nucleic acid and others bind double stranded regions. The conformation of the monomer is changed for every single step when sliding along the RNA strands. For the inchworm model, helicases work as monomers. In this model, the helicase opens and closes the RecA domain 1 and 2 and slide along the nucleic acid strands. This movement is coupled with NTP hydrolysis (Tanner and Linder, 2001). In the Brownian motor model, NTP hydrolysis at the helicase core domain leads to change of protein conformation.

The change of conformation also leads to changes in nucleic acid binding affinitys by the helicase. When the helicase bind on the nucleic acid tightly, the helicase cannot move along the nucleic acid strand. When the helicase becomes loosened, it can move along the nucleic acid chain (Bleichert and Baserga, 2007).

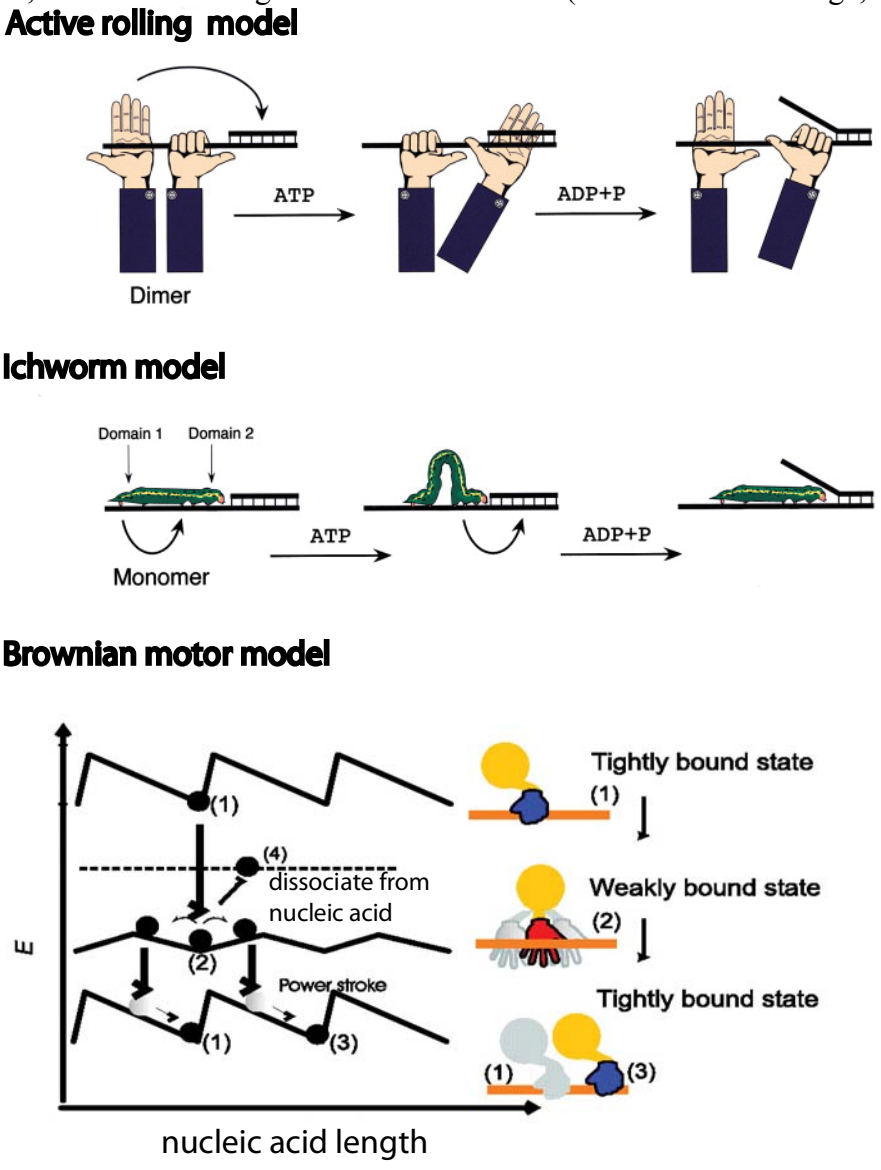

Figure 1.4. Three different models for helicase activity. (Top) Active rolling model. Each hand represents one helicase. The orientation of the hand does not represent the orientation of the helicase here. (Middle) Ichworm mechanismand. The anterior and posterior end of a worm represents the RecA domain 1 and domain 2. (Bottom) Brownian motor model. Image on the right shows a helicase undergoing nucleic acid affinity changes. (1) the helicase is the original position, (2) the helicase which, with an affinity to the nucleic acid is in a weak state, is fluctuating in either directions, (3) the helicase, resumed the original conformation, either moves forward or returns to the pervious place, (4) the helicase detaches from the nucleic acid. Graph on the left showes the energy change for tightly and loosely bound states. E on the x-axis is the energy state, whereas y-axis is the nucleic acid length. The underlying mechanisms were described in the text. (Figures were modified from (Tanner and Linder, 2001) and (Patel and Donmez, 2006))

1.5 Biological functions of RNA Helicases

DExH/D helicases are found in all aspects of RNA metabolism. In addition, one RNA helicase may have more than one function in a cell. It is very common that an RNA helicase originally found in mRNA splicing may also be involve in other pathways like mRNA decay. This interesting feature of helicases can be explained as follows. RNA metabolisms always involve large groups of proteins working together. Different steps of reactions will need different protein components in the complexes. The composition of the complexes rather than individual protein determines the function of the complexes. Therefore, one RNA helicase can be found in several different complexes in different regions of a cell for different functions.

1.5.1 RNA helicase in RNPase remodeling

RNA molecules will automatically form a structure of the lowest energy state. Improper folding of the RNA molecules will disrupt RNA metabolism including mRNA splicing, mRNA translation and RNA interference. DExH/D helicases are the proteins that remodel complicated RNA structures or RNA-protein complexes. Once RNAs are transcribeed, they form into complexes with other proteins called ribonucleoprotein complexes (RNPs). Since RNA needs to be handled differently at different sites, the compositions of RNPs are changing all the time as well. Correct composition of the RNPs and RNA folding at specific time and places are critical for specific functions. The composition of RNPs is dynamic and these dynamic processes are mediated by remodeling activity of various RNPases, DExH/D helicases being part of them.

The first model showing the ability of a DExH/D helicase to displace protein off from RNPs was reported in 2001 (Jankowsky et al., 2001). In this study, the DExH/D protein nucleoside triphosphate phosphohydrolase II (NPHII) from vaccinia virus could actively displace the U1 small nuclear ribonucleoprotein A (U1A), part of the pre-mRNA splicing machinery, in an ATP-dependent manner from a single strand overhang U1A binding site substrate. In this case, the RNA duplex unwinding and displacement happened concurrently. Later in 2004, another two models were proposed to showing that unwinding activity of an RNA helicase was not essential for the displacement of protein from RNPs by DExH/D helicase. Tryptophan RNA-binding attenuation protein (TRAP) formed a RNP with its specific 53-nt-long cognate RNA substrate in which secondary structure played no role for the RNP formation. NPH-II readily displaced TRAP from the RNA containing the single-stranded extension in an ATP-dependent way. Furthermore, another model using exon junction complex (EJC) with an RNA substrate, of which single-stranded regions being adjacent to the EJC-binding site, showed that two helicase NPH-II and DED1 were able to displace EJC from the RNA substrates. These studies also revealed that RNPase activity is substrate dependent; DED1 could not displace TRAP from the RNA substrate (Fairman et al., 2004). Although DExH/D RNA helicases have RNPase activities, the underlying molecular mechanisms still remain to be elucidated.

1.5.2 DExH/D Helicases in transcription

RNA helicases play a role in transcription. The most classic example of DEAH helicase being involved in transcription is the Drosophila maleless (Mle) protein encoded by MLE gene (Kuroda et al., 1991). Mle gene was found in Mle mutant Drosophila. Male Mle mutant are lethal and the female are viable. In Drosophila, the males have one X chromosome and one Y chromosome. Female have two X chromosomes. Since the male flies have one X chromosome less compared to their female counterparts, most genes on X chromosome in the male are needed to be transcribed 100% more efficient than that in female in order to compensate the gene dosages. This enhanced transcription activity is regulated by dosage compensation complex (DCC). DCC is composed of male-specific lethal-1(MSL1), male-specific lethal-2(MSL2), maleless on the third-132 (MSL3), maleless (MLE), male-absent-on-the-first (MOF) and two noncoding roX RNAs. The complex acetylates histone H4 at lysine 16 (H4K16ac) and leads to active transcription (Kotlikova et al., 2006). Mle protein and other components of the DCC were found associating along the whole X chromosome and mainly localized in actively transcribed regions in male Drosophila in an RNA dependent manner (Kotlikova et al., 2006) (Richter et al., 1996).

Mammalian DHX9 [also called RNA helicase A (RHA) or nuclear DNA helicase II (NDHII)] is an ortholog of Mle (Lee et al., 1997; Lee et al., 1998; Lee and Hurwitz, 1992; Zhang et al., 1995). Since the dosage compensation mechanisms for X chromosome in mammals is different from that in Drosophila, the above described case may not applicable in mammals. However, mammalian DHX9 has been shown to activate some transcription. It was reported that DHX9 acts as a bridging factor between the cAMP response element-binding, CREB-binding protein (CBP) and PolII. The N-terminal domain of DHX9 interacts with PolII independent of ATP activity but the CBP-dependent transcription is dependent on ATPase activity (Aratani et al., 2001). DHX9 also bridges the breast cancer-specific tumor suppressor (BRCA1) and PolII holoenzyme (Anderson et al., 1998). The interactions of DHX9 with other transcription factors like NF-kappaB and p16Ink4a were reported as well (Myohanen and Baylin, 2001) (Tetsuka et al., 2004).

DEAD-box helicases DDX5 (p68) and DDX17 (p72) were frequently found working as a dimer, and both proteins were found interacting with RHAU (Iwamoto, 2007). There are reports showing the involvement of the p68-p72 complex in transcription activation. It acts as transcription initiation components by bridging PolII and coactivators CBP/p300 (Rossow and Janknecht, 2003), interacts with a transcriptional activator Smad3, is localized at the ERα promoter upon estrogen treatment, acts as a coactivator of p53 and acts on p53 targeted promoter leading to gene expression enhancement in response to p53 pathway dependent stress response. Though p68 and p72 were initially reported as transcription activators, they also can repress transcription through the interaction with Histone deacetylase 1 (HDAC1).

1.5.3 DExH/D Helicases in splicing

In eukaryotic cells, pre-mRNA is processed by splicing factors once it is transcribed by DNA dependent RNA polymerases (Das et al., 2006). It is not surprise if an RNA helicase participates both in transcription and splicing at the same time. For example, DHX9 is associated with survival motor neuron protein (SMN) in nuclear Gem bodies and cytosolic spliceosomal small nuclear ribonucleoprotein complexes (Pellizzoni et al., 2001). The p68-p72 complex was found to be part of the spliceosomes. p68 alone acts as a splicing protein and acts at the U1 snRNA-5' site. p72 alone ws co-purified with U1 snRNP(Neubauer et al., 1998). In addition, the p62-p72 complex is known to be essential for alternative splicing of H-ras and CD44 (Fuller-Pace, 2006).

1.5.4 DExH/D RNA helicases in mRNA turnover

Regulation of RNA turnover is essential for cellular survival, because it plays an important role in gene expression, defense against virus infection and prevention of transposons RNA expression. These processes are highly regulated and involve a wide range of proteins. Many of these proteins are conserved across organisms (Meyer et al., 2004) (Coller and Parker, 2004) (Table 1.1). The half lives of mammalian mRNA range from 15 minutes to 50 hours (Stolle and Benz, 1988) (Shyu et al., 1989). Although cells are using the same basic machineries fordegradation of for different mRNAs, different mRNAs have different half lives in the same cell. This implies that each mRNA is regulated in a specific manner. Cells should be able to distinguish between mRNAs for degradation. In eukaryotic cells, the 5' m7GpppN cap and a 3'poly(A) tail on an mRNA protect it from undergoing decay. When the mRNAs are ready to be processed for decay, majority of mRNAs undergo deadenylation-dependent decapping pathway. Under this pathway, mRNAs first undergo the removal of the poly(A) tails and followed with hydrolysis of the 5'cap to give a 5'monophosate-mRNA. The decapped mRNA is then either degraded by a 5'exonuclease, 3' exonuclease or endonuclease (Meyer et al., 2004).

Table 1.1 A summary of the proteins participating mRNA decay with 5' or 3' exonucleolytic activity of eukaryotic cells. Activators and inhibitors of the mRNA decay were labeled as effectors (Meyer et al., 2004).

Reaction		Enzymes		Effectors
		Yeast	Mammals	
I	deadenylation	• Pan2p/Pan3p • CCR4-NOT complex	• Pan2/Pan3 • CCR4-NOT complex • PARN	PABPC PABPC cap
IIa	decapping	• Dcp1p/Dcp2p	• Dcp1/Dcp2	Edc1p; Edc2p; Edc3p; Pat1p; Lsm1-7; Dhh1p; PABPC
IIb	cap hydrolysis	• Dcs1p	• DcpS	
III	5′-3′exonucleolytic decay	• Xrn1p	• Xrn1	
IV	3′-5′exonucleolytic decay	• exosome	• exosome	Ski2p; Ski3p; Ski7p; Ski8p

DExH/D helicases have been found as the components of the basic machineries of RNA decay (Table 1.1). Dhh1 is a DEAD-box protein in yeast. It is a decapping activator and translation repressor. It converts mRNA from translation-active state in the cytoplasm to a non-active state the P-bodies(Coller and Parker, 2004).

Furthermore, there are pathways to remove aberrant mRNA produced by splicing errors. Nonsense-mediated decay (NMD) and nonstop decay are pathways to eliminate mRNAs that have a premature stop codon and lack a stop codon, respectively (Frischmeyer et al., 2002; Van Hoof, 2001). DNA rearrangements in B and T cells during maturation, nonsense mutations and splicing errors can produce harmful C-terminal truncated proteins. In mammals, NMD depends on the splicing activity. When a termination codon appears at the upstream of an exon with <50 to 55 nt away, it becomes a premature termination codon and triggers NMD. During translation, the ribosome scans along the mRNA and removes exon junction complexes (ECJ) that are formed during splicing in the nucleus. When a premature termination codon appears, ribosome is stopped and leaves the EJC unremoved at the downstream. This EJC becomes a platform for the recruitment of NMD machinery and starts mRNA decay. The human NMD involves UPF1, UPF2, UPF3, UPF3B, SMG1, SMG5, SMG6, SMG8, SMG9, NAG and DHX34(Nicholson et al.). DHX34 is a DEAH helicase and was recently identified as part of NMD in C. elegans (Longman et al., 2007). It was found that DHX34 was highly conserved in C. elegans and human. Knocking down of DHX34 in either C. elegans or human cells reversed NMD activity (Longman et al., 2007).

1.5.5 RNA Helicase in translation

Translation initiation is the slowest step in eukaryotic translation. When translation starts, a 40S ribosomal subunit forms an initiation complex with eIFs 1 and 1A, 2 and 3. This complex then is charged with a ternary tRNAMet complex (tRNAMet/eIF2/GFP) to form a 43S initiation complex. This initiation complex is

directed to the 5'untranslated region (5'UTR) of mRNA and scans for the start codon. It becomes a 48S complex when it meets the start codon. The mRNAs in eukaryotic cells usually are capped with m7G5'ppp5N structure at the 5' end in addition to a relatively unstructured 5'UTR less than 100 nucleotides. The landing of 43S ribosomes initiation complex on the mRNAs requires eIF4F, 4A and 4B. The eIF4F is composed of eIF4E, eIF4G and eIF4A. eIF4E recognizes the 5' cap of mRNAs. eIF4G is a scaffolding protein associate with eIF4E and eIF4A and eIF3. eIF4A is a DEAD-box helicase (Figure 1.5). Mammalian DDX3 and its yeast homologue DED1 were also found manipulating the translation efficiency.

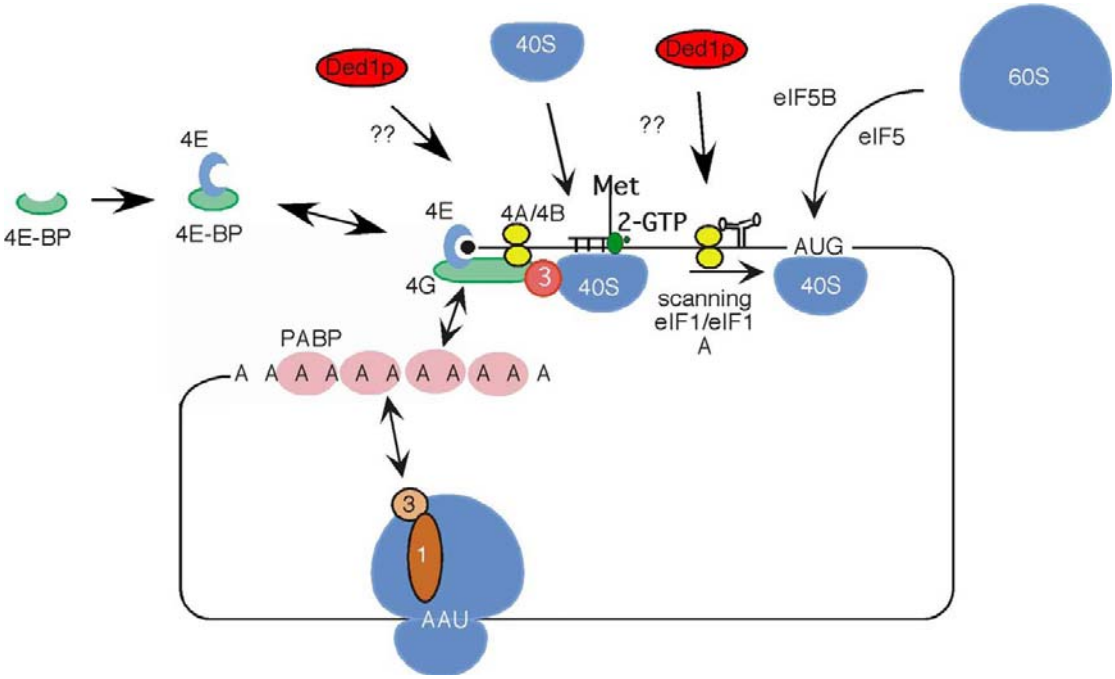

Figure 1.5. Overview of the translation initiation process in eukaryotic cells. 4E-BP is eIF4E-binding protein. (Figure was modified from (Linder, 2003)).

The binding affinity of regulatory proteins at the 5'UTR can be modulatedby changing the tertiary structure of mRNA, leading to changes in translation efficiency (Linder, 2003) (Baim and Sherman, 1988; Pelletier and Sonenberg, 1985). As mRNA structure takes part in the translation initiation regulation, helicases become important for gene expression regulation. However, the characterization of how helicases are involved in translational control has not been fully studied.

Some retroviruses pre-mRNA and some mammalian mRNAs from intronless genes contain highly structured and long 5'UTR. In these cases 5'UTR takes part in the translation initiation control (Short and Pfarr, 2002). These highly structured 5'UTRs that harbor translation initiation regulating function are called 5'-terminal post-transcriptional control elements (PCEs) and are present in several viral and human genes. It was published for the first time in 2006 (Hartman et al., 2006) that the DEAH helicase DHX9 was necessary for efficient translation of mRNA with PCE. The DHX9-PEC interaction is sequence specific

and enhances the polyribosome assembly and protein synthesis. Another DEAH helicase, DHX29, was shown to be important for translation initiation beside DHX9. DHX29 was shown to bind to 40S monomers and dimmers. Though the detailed mechanism is still unknown, this protein might directly unwind mRNA before loading of 40S initiation complex on the mRNA or remodeling the 43S complexes.

1.5.6 RNA helicases are essential for embryogenesis and differentiation

Differentiation is a process that involves continuous global changes of gene expression. Modulation of RNA metabolism is critical for proper differentiation. Distortions of the expression of RNA helicases have been demonstrated in knockout mouse models. Several RNA helicases are specifically expressed in germ cells and embryos. Analysis of global gene expression patterns suggests that these RNA helicases play roles in differentiation and embryogenesis. A few RNA helicases have been knocked out in mice. I will briefly describe three such cases in which the knocked out RNA helicases are related to RHAU and involved in embryogenesis.

DEAD-box helicases p68 and p72 are structurally closely related protein, being members of the same SF2 family, and are co-immunopreciptated with RHAU in HeLa cells (Iwamoto, 2007). Expression of these helicases was shown to be developmentally regulated (Stevenson et al., 1998), and later they were found to be involved in pre-mRNA processing (Lee, 2002; Liu, 2002). These two helicases showed specific expression pattern during muscle and adipocyte differentiation (Caretti et al., 2006) (Kitamura et al., 2001). As described before, p68, p72 form a complex with a noncoding RNA, SRA. It was reported that this p68-p72-SRA complex was essential for the activation of Myo D transcriptional factor and also for the formation of the transcription initiation complex and chromatin remodeling (Caretti et al., 2006). Konckdown of p68 and p72 in vitro led to differentiation defect in myoblasts (Caretti et al., 2006). p68 single gene knockout mice were embryonic lethal at around 11.5 dpc. p72 single gene knockout mice caused neonatal death at day 2 after birth. p68-p72 double knockout mice resulted in earlier lethality at least before 8.0 dpc (a stage before organogenesis start). The lethality of p68-p72 knockout mice compare to single gene knockout mice implied that functions of these two genes are partially but not totally redundant (Fukuda et al., 2007; Uhlmann-Schiffler et al., 2006).

DHX9 is able to bind and catalyze the unwiding of both DNA and RNA. It involves in transcription regulation (Nakajima et al., 1997), mRNA processing (Zhang et al., 1999), translation initiation (Bolinger et al., 2010) and RNA editing (Reenan et al., 2000). DHX9 ablated mice are lethal at 7.5 dpc. This model showed that DHX9 was not essential for gastrulation initaiton. It was because DHX9-ablated embryos showed some signatures of gastrulation initiation such as

the present of extraembryonic, yolk sac and structure with blood island markers (Lee et al., 1998).

1.5.7 RNA helicases in hematopoiesis

So far, only one member of the DEAH RNA helicase family has been suggested to play a role in hematopoiesis. Ubiquitously expressed DHX32 was found to be specifically downregulated in acute lymphoblastic leukemia (Abdelhaleem, 2002), possibly through suppressing apoptosis (Alli et al., 2007). A causal role for this helicase in leukemia development, however, has not yet been addressed.

1.5.8 The role of RNA helicases in cancer

Since RNA helicases regulate RNA metabolism, deregulation of these proteins could result in distortion of the downstream RNA processing and lead to global changes of cellular activity. Several RNA helicases were reported to be overexpressed in cancer as a result of chromosome aberration (Abdelhaleem, 2004). Some of them are shown to be co-immunoprecipitated with RHAU, such as DDX1 (Iwamoto, 2007), p68 (Iwamoto, 2007) and DHX9 (unpublished data).

It was reported that DDX1 gene was co-amplified with MYCN in neuroblastoma (Godbout et al., 1998) (Pandita et al., 1997) (Squire et al., 1995) (Manohar et al., 1995). MCYN is a member of the myc family and is a biomarker for poor prognosis of neuroblastoma (Schmidt et al., 1994). Although not all MCYN overexpressing tumors show co-amplification of DDX1, tumors with both genes amplifiedare usually of higher grade. DDX1 is known to be a nuclear protein which involves pre-mRNA processing at the 3'-end and interacts with the nuclear-ribonucleoprotein K (hnRNPK) (Bleoo et al., 2001).

p68 (Ford et al., 1988) (Yang et al., 2005) was found consistently overexpressed in the colon cancer (Causevic et al., 2001). Recombinant p68 was phosphorylated in cancer cell lines but not in normal tissues (Yang et al., 2005). Bale and his colleagues (ref) down regulated p68 by RNAi and found that p53 target genes were downregulated in response to DNA damage and p53-dependent apoptosis specifically. From these observations, they proposed that p68 was recruited together with p53 to the p21 promoter and regulated p21 gene expression. This implies that p68 may act as a tumor cosuppressor, in concert with p53, on the transcription of p53 target genes (Bates et al., 2005). In addition, p68 also promotes miR-21 maturation with association of activated R-SMADs and DROSHA (Davis et al., 2008). miR-21 suppresses the programmed cell death gene 4 (Pdcd4) that is a tumor suppressor protein (Singh et al., 2009).

DHX9 is capable of linking the C-terminus domain of breast cancer suppressor protein (BRCA1) to RNA polII (Aratani et al., 2003). It was also reported that

DHX9 bound specifically to the p16/INK4a promoter and upregulated p16 transcription (Myohanen and Baylin, 2001). DHX9 was also overexpressed specifically in lung cancer cells compared to normal counter parts (Wei et al., 2004).

Besides DHX9, other DHX family members, DHX32, DHX34 and DHX29, were also found related to carcinogenesis. DHX32 was found to be overexpressed in leukemia cell lines (Abdelhaleem, 2002). DHX34 is a NMD pathways component and found to be amplified in human neurohlastomas (Wimmer et al., 1999) (Scott et al., 2003). DHX29 is a translation initiation factor and is essential for cancer cell proliferation (Parsyan et al., 2009).

Deregulation of RNA transcription, processing, alternative splicing, translation and non-coding RNA processing are critical for the development of cancer (Abdelhaleem, 2004). Targeting the RNA surveillance accuracy will be a new direction for cancer therapy, and RNA helicases could be a new aspect for this purpose.

1.6 The RHAU gene

RHAU (alias DHX36, G4R1) belongs to DEAH RNA helicase family. It was initially identified as a putative RNA helicase in human cells regulating urokinase mRNA decay (Tran et al., 2004). Chromosomal location of the human RHAU gene is at 3q25.2 while that of mouse RHAU gene at Ch3E1. Since RHAU protein is a helicase and binds to the AU-rich element of urokinase mRNA, it was termed "RNA helicase-associated with AU-rich elements". This gene is conserved in chimpanzee, dog, cow, mouse, rat, chicken, zebrafish, fruit fly and mosquito (NCBI database) but neither in yeast nor nematoda. The lack of RHAU homologue in less complex organisms implies that this gene may be evolve for the cellular processes that appear in later stages of evolution. According to the gene portal system of the Human Gene Atlas database (BioGPS, GNF, Novartis), RHAU is relatively highly expressed in hematopoietic cells in both human and mouse (Figure 1.6 A and B). This specific expression pattern implies that RHAU is important in hematopoietic system.

A

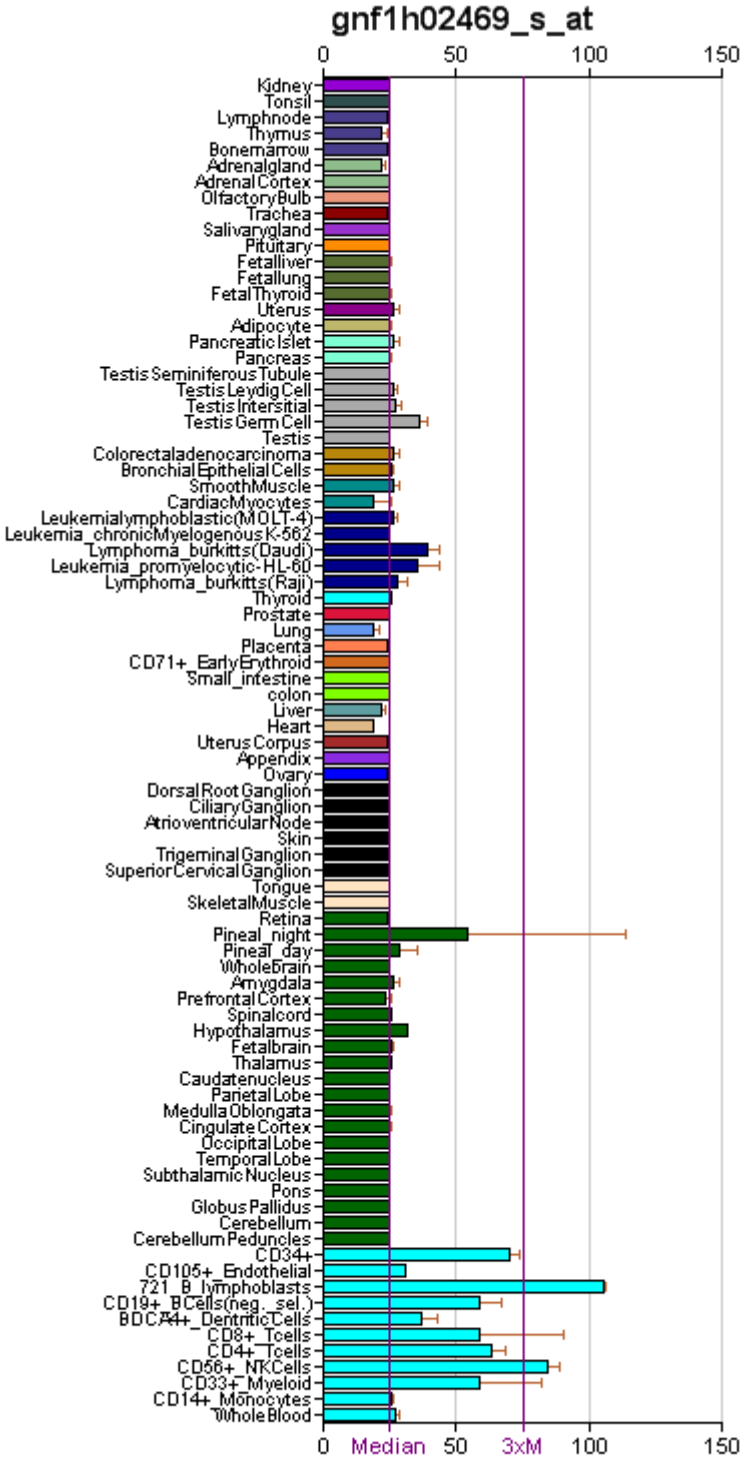
gnf1h02469_s_at
0
50
100
150
Kidney
Tonsil
Lymphnode
Thymus
Bonemarrow
Adrenalgland
Adrenal Cortex
OlfactoryBulb
Trachea
Salivarygland
Pituitary
Fetalliver
Fetallung
FetalThyroid
Uterus
Adipocyte
Pancreatic Islet
Pancreas
Testis SeminiferousTubule
Testis Leydig Cell
Testis Intersitial
Testis Germ Cell
Testis
Colorectaladenocarcinoma
Bronchial Epithelial Cells
SmoothMuscle
CardiacMyocytes
Leukemialymphoblastic(MOLT-4)
Leukemia_chronicMyelogenous K-562
Lymphoma_burkitts(Daudi)
Leukemia_promyelocytic-HL-60
Lymphoma_burkitts(Raji)
Thyroid
Prostate
Lung
Placenta
CD71+_EarlyErythroid
Small_intestine
colon
Liver
Heart
Uterus Corpus
Appendix
Ovary
Dorsal Root Ganglion
CiliaryGanglion
Atrioventricular Node
Skin
Trigeminal Ganglion
Superior Cervical Ganglion
Tongue
SkeletalMuscle
Retina
Pineal_night
Pineal_day
WholeBrain
Amygdala
Prefrontal Cortex
Spinalcord
Hypothalamus
Fetalbrain
Thalamus
Caudatenucleus
Parietal Lobe
Medulla Oblongata
Cingulate Cortex
Occipital Lobe
Temporal Lobe
Subthalamic Nucleus
Pons
Globus Pallidus
Cerebellum
Cerebellum Peduncles
CD34+
CD105+_Endothelial
721_B_lymphoblasts
CD19+_BCells(neg._sel.)
BDCA4+_DentriticCells
CD8+_Tcells
CD4+_Tcells
CD56+_NKCells
CD33+_Myeloid
CD14+_Monocytes
WholeBlood
0
Median
50
3xM
100
150

B

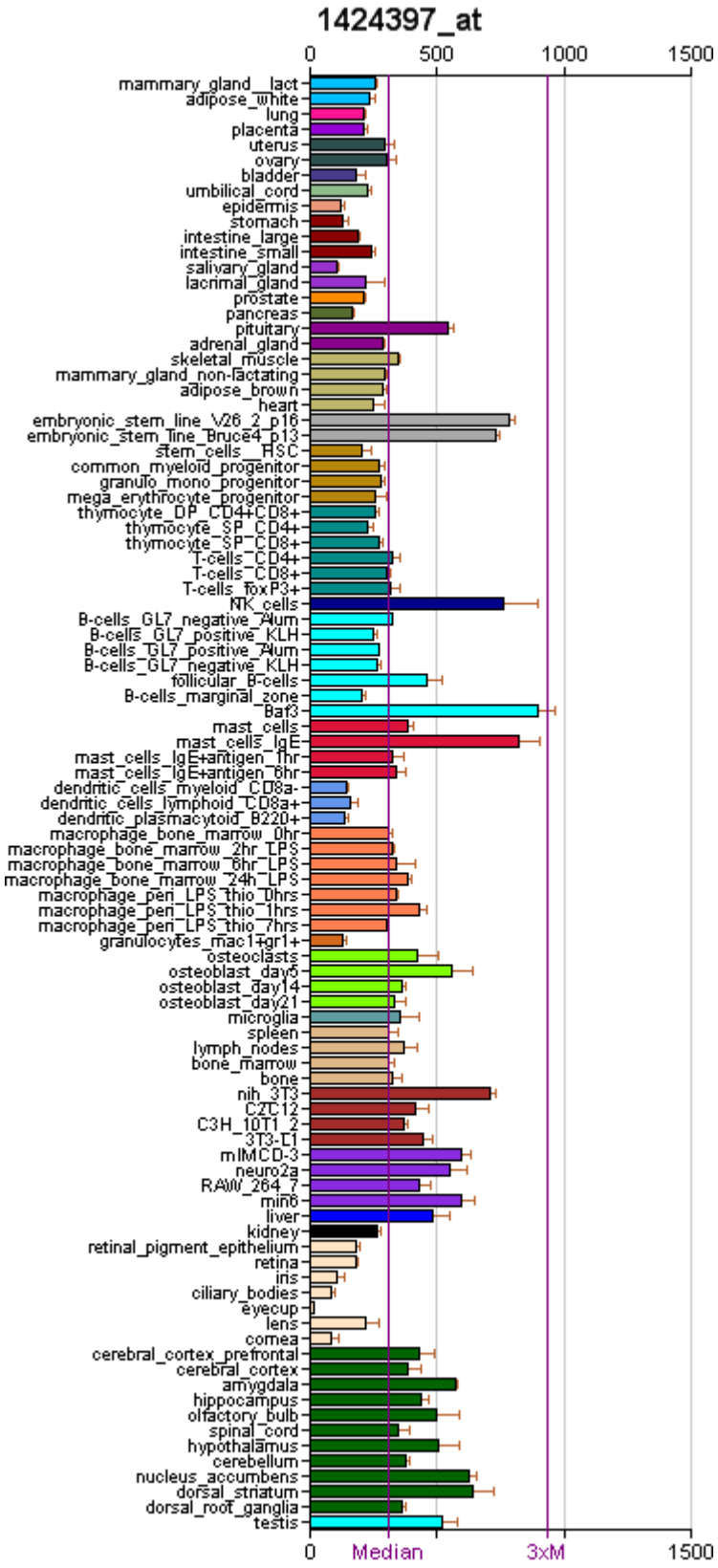

Figure 1.6. RHAU mRNA expression in different tissues in (A) human and (B) mouse. Data were obtained from (BioGPS, GNF, Novartis). The red lines represent the meadian value of expression.

.

1.6.1 RHAU promotes exosome-associated mRNA decay

Biological function of RHAU was firstly described in 2004 when one of the PhD students in Nagamine's group was studying how the urokinase plasminogen activator (uPA) (Alias: PLAU) mRNA stability was regulated. The presence of an AU-rich element (ARE) in the 3'UTR of uPA mRNA suggested that the uPA protein expression could be regulated at the mRNA stability level. In this study, the 3'UTR ARE of uPA mRNA (ARE(uPA)) was immobilized on agarose beads and incubated with HeLa cells nuclear extracts. Proteins interacted specifically with the (ARE(uPA)) were identified and RHAU was amongst them. Further analysis showed that RHAU promoted mRNA decay by recruiting the exoxome and poly(A) ribonuclease (PARN) to the message (Tran et al., 2004).

1.6.2 RHAU resolves RNA and DNA tetramolecular quadruplexes

One year after RHAU was found in RNA decay process, Akman's group identified RHAU/G4R1 as the major source of tetramolecular quadruplex G4-DNA resolvase activity in HeLa cells (Vaughn et al., 2005). G4-DNA, is also called G-quadruplex. G4 was first described in 1988. Single-stranded DNA with G rich region will self-associate to form a stable four strand structure at physiological concentration (Sen and Gilbert, 1988). This four strand structure involves a stack of G quartets arranged vertically. A G quartet involves four guanine molecules arranged on the same plane and stabilized by Hoogsteen hydrogen bonding and a monovalent cation (Figure 1.7). It was reported that G4-DNA structures were particularly enriched in certain regulatory elements, such as oncogene promoter regions (Siddiqui-Jain et al., 2002; Simonsson et al., 1998; Verma et al., 2009), guanine-rich regions of ribosomal DNA, and specific genetic control elements, such as immunoglobin heavy chain switch region (Sen and Gilbert, 1988). G4-DNA sequences in these regions are conserved across species, implying that G4 has biological importance. After finding that RHAU could resolve DNA G-quadruplex, RHAU was found to be able to resolve RNA G-quadruplex (G4-RNA) as well and even more efficiently than G4-DNA (Creacy et al., 2008). Like DNA, guanine rich RNA region can form G-quadruplex structure. There are more than fifty thousand G4-RNA sites predicted near mRNA splicing and polyadenylation sites in human and mouse genome (Kostadinov et al., 2006). G4-RNA structures can modulate translation initiation and repress mRNA turnover (Kumari et al., 2007).

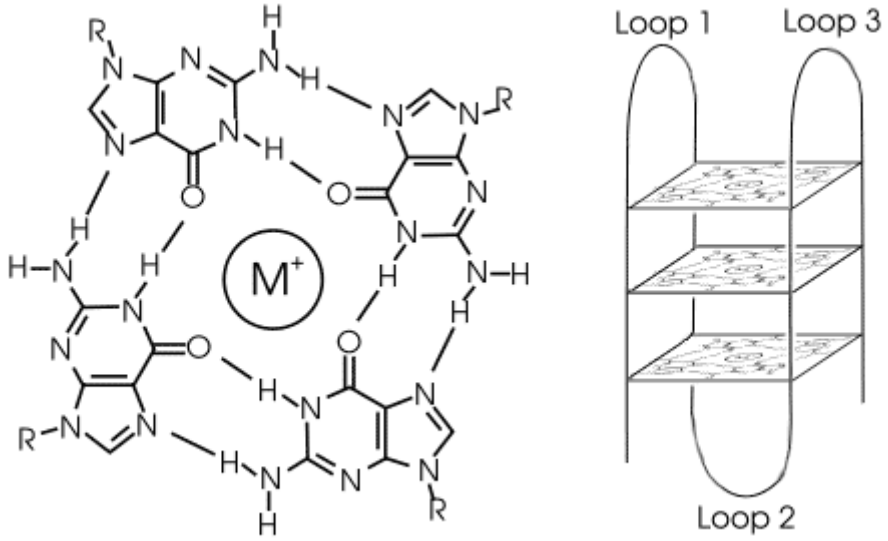

Figure 1.7. Structure of a G-quadruplex. Left: a G-tetrad. Right: an intramolecular G-quadruplex (Neidle and Balasubramanian, 2006). M^+ is monovalent cation.

1.6.3 RHAU localized to stress granules (SGs)

SGs are special cytoplasmic foci where translationally stalled RNP complexes are stored (Kedersha et al., 2005). The RNP complexes consists of polysome-free 48S preinitiation complexes, small ribosomal subunits, poly(A)-binding protein 1 (PABP1) and RNAs. Formation of SGs requires eIF2alpha phosphorylation that is induced by various stresses. It was presumed that when cells faces unfriendly environmental conditions, cells respond by sending mRNAs to P-bodies for degradation or to SGs for storage. These mechanisms allow the cell to quickly manipulate the profile of protein expression.

RHAU was found to associate with SGs upon various stresses. Protein deletion analysis showed that the first 105 amino acids of the N-terminal domain were essential for RNA binding. It was also shown that this RNA-binding domain fused with β-gal-EGFP could associate with SGs in response to stress. Furthermore, when the ATPase activity of RHAU was abolished by mutating the motif II of helicase core domain from DEIH to DAIH, the mutant RHAU was found to be recruited to and unable to leave SGs. This indicates that the ATPase activity of RHAU modulates the association of RHAU with SGs but the ATPase activity was not essential for the recruitment of RHAU to SGs (Chalupnikova et al., 2008).

1.6.4 RHAU is a nuclear protein

Although RHAU was found to be involved in mRNA decay process being associated with the exosome and localized in SGs in the cytoplasm, RHAU is predominantly localized in the nucleus. As many RNA helicases are multi-functional, it is not be surprised if RHAU also functions in the nucleus. In HeLa cells, GFP-RHAU is localized throughout the nucleoplams and aggregates at nuclear speckles. Using transcription initiation inhibitor, Actinomycin D, RHAU was found to be localized close to but never overlapping with p68 and p72. In vitro coimmunoprecipitation experiments further showed that the interaction between RHAU and p68 or p72 was RNA dependent. Previously, it was reported that p68-p72 dimer was involved in nuclear processing of miRNA and rRNA processing and transcription (Fukuda et al., 2007). The possiblilty cannot be ruled out that RHAU is also involved in these processes. By measuring the amounts of transcripts at the steady state level and their half lives using microarray analysis method, most genes that showed changes at the steady state level after RHAU knockdown were found to be regulated by RHAU at the transcription level rather than at the mRNA stability level (Iwamoto et al., 2008). These observations suggest RHAU also act as a multifunctional nuclear protein that can modulate transcription of subset of transcripts.

1.7 Hematopoiesis

In biological view, the hematopoietic system is an important part for maintaining healthy physiological condition because it produces all types of blood cells required for oxygen transportation, coagulation and fighting against infection. This is also a fascinating process because it involves continuous interaction of hematopoietic cells with the surrounding environment all over the body and tight control of the expression of various genes. Therefore, hematopoiesis is an excellent model for studying gene regulation mechanism.

Hematopoiesis is partially conserved in all vertebrates, from fish to amphibian, reptile, avian, and mammal (Cumano and Godin, 2007). In the last few decades, amphibians, avians and fish were used as model organisms to unravel distinct differentiation steps of hematopoiesis. However, due to similarity to humans and the availability of gene targeting technique, mouse model has been far more attractive and extensively used to dissect the hematopoietic system.

The hematopoietic system involves in at least eight different cell lineages and is discussed below.

1.7.1 Hematopoietic cells

1.7.1.1 Erythrocytes: oxygen delivery

Red blood cells are also called erythrocytes. They contribute to the largest cell population in the hematopoietic system. Every day, around 10^{12} new erythrocytes are produced in the body. The major task of erythrocytes is to carry oxygen from lungs to all tissues.

1.7.1.2 Blood platelets: hemostasis

Thrombocytes are called platelets in mice and human. They are derived from megakaryocytes. The major function of platelet is to regulate hemostasis by forming blood clot to prevent excessive bleeding. In addition, platelets also serve as inflammatory mediators (Roitt et al., 2001).

1.7.1.3 Cells for immunity

In humans and mice, the bone marrow and thymus are the primary lymphoid organs where the lymphocytic cells develop. The spleen, lymph nodes and lymphoid tissues of the respiratory tracts are the secondary lymphoid organs. Hematopoietic cells that are involved in the immune system are called leucocytes or white blood cells. There are three types of them: (1) lymphocytes, (2) phagocytes and (3) auxiliary cells. Lymphocytes include B cells, T cells and large granular lymphocyte. Phagocytes include mononuclear phagocytes, neutrophils and eosinophils. Auxiliary cells include basophile, mast cell and platelets. These

leukocytes play different roles in the immunity. They work either in innate immunity or adaptive immunity. Both immunities are responsible for defense against pathogen. Innate immunity respond to a pathogen the same way whether or not it was pre-exposed while adaptive immunity is specific for re-exposed pathogens with stronger intensity than innate immunity with life-long memory. Histocompatibility complex (MHC) plays an important role in the immunity. Class I MHC molecules bind to fragmented internal molecules while class II MHC molecules are expressed by specialized antigen-presenting cells (macrophages, B cells and dentric cells) and bind to fragmented and processed foreign particles.

1.7.1.3.1 Lymphocytes

Natural killer (NK) cells are part of large granular lymphocytes and they are cytotoxic CD8+ but lack T cell receptors. NK cells are part of innate immunity and specialized for attacking tumor cells and viral infected cells that have low expression level of major MHC class I on their surface. NK cells can target the cells that are bound by antibodies. By binding to the Fc portion of the antibody, NK cells are activated to release cytotoxic chemicals stored in the cytoplasmic granules. This cytotoxicity leads to apoptosis of the target cells (Hoffbrand et al., 2006d).

Dendritic cells (DCs) are antigen-presenting cells that interface between the innate and adaptive immunity. They process antigens and present it to the helper T (TH) cells. They are localized in the skin, lymph nodes and thymus. After taking up antigens at infected sites, DCs migrate to the lymph nodes and present to B and T cells the foreign molecules together with class II MHC for further immune response.

T cells express T cell antigen receptor (TCR). T cell progenitors are produced in the bone marrow but their development takes place in the thymus. More than 95% of T cells express α and β polypeptide heterodimers and around 5% T cells express γ and δ polypeptide heterodimers. These TCRs associate with the CD3 complex and form the T cell receptor complex (TCR-CD3 complex). The αβ T cells are further divided into CD4+ and CD8+ subsets. CD4+ cells help immune response and have no cytotoxic or phagocytic ability to kill the infected cells. Therefore they are called helper T (TH) cells. They recognize antigens presented on the class II MHC molecules on the antigen presenting cells. CD8+ T cells are cytotoxic T cells. They can recognize antigens on class I MHC cells. As soon as CD8+ cells recognize the infected or dysfunctional somatic cells through the antigen on the Class I MHC, they release cytotoxin and kill the cells. The different stages of T cell development will be described in the next section.

B cells express B cell receptors which are membrane bound immunoglobulins (Ig). B cells are responsible for antibodie production and present antigens to T cells. There are five classes of antibodies, IgG, IgA, IgM, IgD and IgE. The Ig molecules are formed by two heavy and two light chains. Somatic recombination

of three variable regions, variable (V), diversity (D) and joining (J) segments introduce diversity in the heavy chain (Tonegawa, 1983). The differentiation path of B cells will be described in the next section.

1.7.1.3.2 Phagocytes

There are two types of phagocytes, mononuclear phagocytes and polymorphonuclear granulocytes. These cells are able to engulf pathogens and internalize antigens in order to destroy them. Mononuclear phagocytes are a group of cells deprived from the same lineage and are long lived. The progenitors arose in the bone marrow are called monoblasts. They develop into monocytes in blood circulation. The monocytes migrate into the tissues and develop into tissue macrophages. Macrophages are particularly enriched in spleen, liver, kidney, brain, lung alveolar, bone marrow and lymph nodes. The macrophages in the liver are called Kupffer cells in and those in the brain microglias. The macrophages either engulf the antigens or present antigens to the T cells. Polymorphonuclear granulocytes are not specified for antigen recognition. They are essential for acute inflammation. Granulocytes include neutrophils and eosinophils. Neutrophils are the most abundant but short lived. Eosinophils are especially capable of targeting large parasitic worms by releasing the granulocyte content, there by damaging the parasites.

1.7.1.3.3 Audiliary cells

Basophils, mast cells and platelets are auxiliary cells. Basophils are relatively low in number in the circulation. Usually they are less than 0.2% of leucocytes. Basophils are polymorphonuclear granulocytes but they are not true phagocytes. Basophils and mast cells contain granules where heparin, leukotrienes, histamine are stored. Basophils and mast cells acts against parasites but also play a critical role in autoimmune disorder (Benoist and Mathis, 2002) (Arinobu et al., 2009). Platelets are anuclear cells derived from megakaryocytes. Megakaryocytes migrate from bone marrow to the lung capillaries and are fragmented into blood platelets (Levine et al., 1990). They are not only involved in blood clotting but also play a role in inflammation.

Different cell types can be identified by their distinct pattern of markers expressed on the cell surface.

1.7.2 Origin of hematopoiesis in mouse

The first hematopoietic stem cells detectable in mouse embryo are in extraembryonic yolk sac at 7.25 days postcoitus (dpc). Yolk sac is derived from mesodermal layer of gastrulation. Certain mesoderm cells differentiate into hemangioblasts which are common progenitors of endothelial cells and hematopoietic cells (Ueno and Weissman, 2006). Then the cells are arranged in a structure in which endothelial cells surround the blood cells. The blood cells inside the structure are called blood islands. The first wave of hematopoiesis produces primitive erythrocytes followed by primitive megakaryocytes and

macrophages (Cumano and Godin, 2007). At 8 dpc, the yolk sac blood islands are connected with intraembryonic blood vessels (McGrath et al., 2003). Then at 8.5 dpc, intraembryonic hematopoietic precursors appear at aorta-gonad-mesonephros (AGM) (Cumano and Godin, 2007; Mikkola and Orkin, 2006). These cells have multipotent differentiation potential. It was demonstrated that the hematopoietic cells in AGM could come from the yolk sac (Samokhvalov et al., 2007). At 10 dpc, HSCs seedling to fetal liver occurs after the establishment of the circulatory network. Fetal liver is the primary site for hematopoiesis and expands during 13 to 16 dpc. Seedlings of HSCs then migrate to the thymus, and then the spleen. On 17 dpc, HSCs are seeded in the bone marrow (BM), and thereafter the BM remains the primary site of hematopoiesis including the time after birth (Cumano and Godin, 2007). However, in case of certain diseases, such as osteopetrosis, anemia, thrombocytopenia and splenomegaly, hematopoiesis takes place in sites other than bone marrow, for example in spleen. This situation is called extra medullary hematopoiesis (Adams and Smuts, 1989).

1.7.3 Differentiation road of hematopoietic cells in adult mice

The cells in the hematopoietic system are continuously lost by mechanical damage and aging. The cells that have the ability to replenish all the blood cells are called hematopoietic stem cells (HSCs). These special cells are capable of self-renewal and give rise to all kinds of cells in the blood system when induced by appropriate cytokines and environment (Curry and Trentin, 1967) (Trentin et al., 1989). The scheme below shows that all the cell types are originated from the HSCs which first differentiate into lineage-restricted progenitors and eventually fully differentiated cells of various types (Figure 1.8).

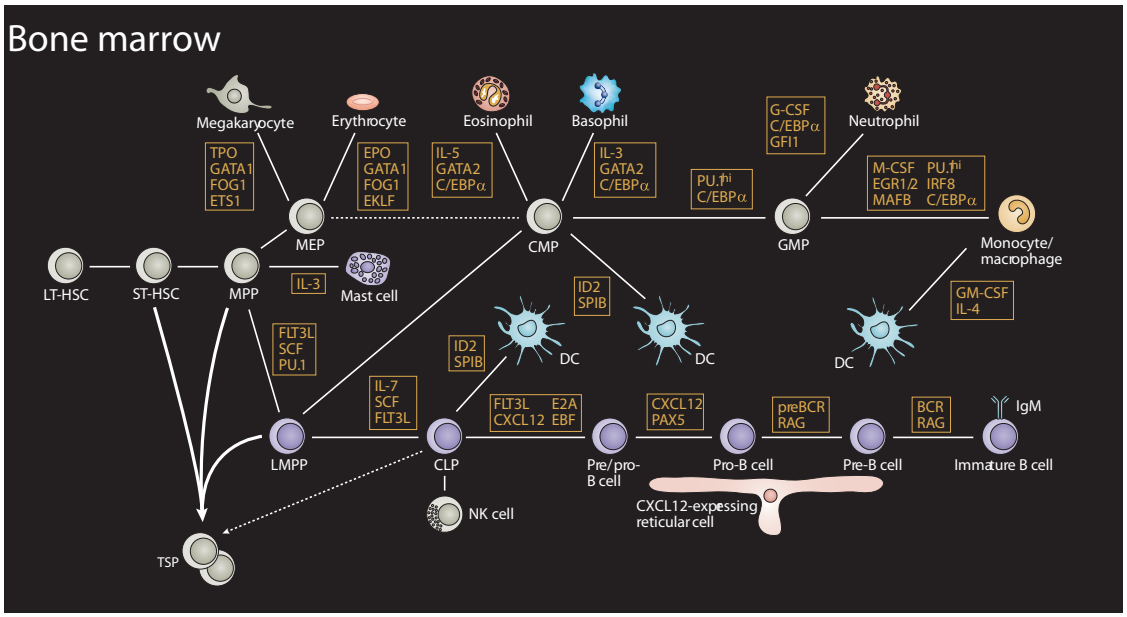

Figure 1.8. Hematopoietic cells differentiation pathways. Abbreviations: HSC, haematopoietic stem cell; LT-HSC, long-term repopulating HSC;ST-HSC, short-term repopulating HSC; MPP, multipotent progenitor; LMPP, lymphoid primed MPP; MEP, megakaryocyte/erythroid progenitor; CMP, common myeloid

progenitor; GMP, granulocyte/macrophage progenitor; CLP, common lymphoid progenitor; DC, dendritic cell; NK, natural killer. The yellow boxes represent the transcription factors and chemokines or cytokines required for the differentiation to occur. The dotted lines represent the pathways which are not yet determined (Figure adapted from (Graf and Trumpp, 2007)).

There are two types of HSCs, long-term repopulating HSC (LT-HSC) and short-term repopulating HSC (ST-HSC). Only LT-HSCs are capable of colonizing lethally irradiated bone marrow in human or mice and reconstitute the entire hematopoietic system for years. ST-HSCs are cells still capable to differentiate to different cell types as LT-HSCs but the repopulation period is limited to a few weeks only (Morrison et al., 1995). HSCs differentiate into MPPs which have the potential to differentiate into the myeloid lineage and the lymphoid lineage. When MPPs are committed to the megakaryocyte and erythroid lineage, it becomes megakaryocyte/erythroid progenitors (MEPs). In MEPs the differentiation potential of the lymphoid lineage is lost. When MPPs become committed to the lymphoid lineage, these cells become lymphoid-primed multipotent progenitors (LMPPs). In this case, in LMPPs the differentiation potential of the erythroid lineage and the megakaryocyte lineage is lost. LMPPs differentiate into common lymphoid progenitors (CLPs), common myeloid progenitors (CMPs) or granulocyte/macrophage progenitors (GMPs) (not drawn in the picture). CMPs can differentiate into GMPs, and GMPs are capable to differentiate into neutrophils, monocytes, eosinophils and basophils and mast cells. Esinophils and basophils are mainly differentiated directly from CMPs. And evidence shows that GMPs can also produce esinophils and basophils in a limited number (Laiosa et al., 2006) (Iwasaki et al., 2005) (Arinobu et al., 2005). The CLPs derived from LMPPs are capable of differentiating into B cells, T cells and natural killer cells (Kondo et al., 1997). In fact, CLPs and CMPs retain plasticity in that CLPs can differentiate to macrophages and CMPs to B cells (Laiosa et al., 2006).

1.7.3.1 Differentiation of enucleated erythrocytes

Differentiation of enucleated erythrocytes in mammals is called erythropoiesis. Transcription factors Gata-1, Gata-2 and FOG-1 are critical for the whole erythropoiesis (Ferreira et al., 2005; Kaneko et al., 2010). The first erythrocyte lineage committed progenitor cells, proerythroblast, are derived from MEPs (Figure 1.9). The development of erythrocytes in bone marrow can be divided into four stages. The proerythroblasts undergo cell division and form smaller basophilic erythroblasts, which differentiate to smaller polychromatophilic erythroblasts, which further develop to still smaller orthrochromic erythroblasts. Different stages of erythroblast differentially express CD71 and Ter119 on the cell surface. These two markers together with the cell size therefore can be used to determine the stage of differentiation of these cells by FACS analysis (Figure 1.9). The cells are progressively making more hemoglobin at basophilic erythroblast stage. After this stage, the nuclei become progressively condensed and the amounts of cytoplasmic protein and RNA are decreased. The nuclei are finally extruded from orthrochromic erythroblasts which still have some ribosomal RNA used for hemoglobin synthesis (Hoffbrand et al., 2006a).

Erythropoiesisis regulated by erythropoietin which is a hormone produced by interstitial cells in kidney. Erythropoietin is a glycosylated protein of 34 kDa with 165 amino acids. Its secretion is regulated by oxygen concentration in the blood. When an animal is suffering from anemia or other cardiac dysfunction, less oxygen is delivered to the kidney. Hypoxia in the blood leads to decrease of degradation of transcription factor hypoxia-inducible factor-1 (HIF-1) in cells, resulting in the binding of HIF-1 to hypoxia response element at the promoter of erythropoietin gene (Shams et al., 2005) (Lok and Ponka, 1999). As a result, erythropoietin secretion is enhanced. Erythropoietin activates the GATA-1 gene through erythropoietin receptor (EpoR). Activation of GATA-1 expression increases bcl-xL protein expression that is essential for maintaining the viability of MEP and proerythroblast (Gregory et al., 1999).

The half-lives of normal erythrocyte are around 120 days in humans and 40 days in mice (Abbrecht and Littell, 1972; Shemin and Rittenberg, 1946). Erythrocytes are constantly exposed to various stresses throughout the circulation. When erythrocytes pass through the lung, they are under oxidative stress. When they pass through the kidney, they undergo osmotic shock. When they pass through in peripheral tissues the capillaries the diameter of which is smaller than theirs, they are under mechanical stress. Erythrocyte cell membrane flexibility is progressively decreased with age. If the erythrocytes are rigid more than normal, these erythrocytes may have tendency torupture when passing through narrow capillaries, ensuing haemolysis. The lysed cells will release hemoglobin in the extracellular fluid, which will eventually cause renal failure. Therefore, aged erythrocytes must be removed from circulation systematically. The aged erythrocytes have higher degree of asymmetric distribution of phosphatidylserine (PS) on the cell membrane like what is happening during apoptosis in nucleated cell. The externalization of PS signals the macrophage in the reticuloendothelial system in the spleen and liver to engulf the aged erythrocytes. This process is called eryptosis. The iron released from haem (composed of iron and protoporphyrin) of erythrocytes is carried to the bone marrow for recycling, while the protoporphyrin is broken down to bilirubin. Bilirubin is transported to the liver and then combines with glucuronides there and excreted into the gut via bile. In the gut, the bilirubin glucuronide is converted to stercobilinogen and stercobilin. Part of stercobilin is excreted in faeces and stercobilinogen and remaining stercobilin are converted to urobilinogen and urobilin and excreted in urine. When the rate of eryptosis or hemolysis is increased, the body compensates the loss by increasing the erythropoiesis. However, if erythropoiesis cannot compensate the loss of erythrocytes, anaemias ensues (Alvarez et al., 2007; Bosch et al., 1994; Bosman et al., 2008; Chen et al., 1999; Cherukuri et al., 2004; Hebbel, 1991; Lorenz et al., 1999; Rivera et al., 2006). The basic features of haemolytic anemias are jaundice of the mucous membranes and splenomegaly. Jaundice is due to unconjugated bilirubin in the blood (Hoffbrand et al., 2006b).

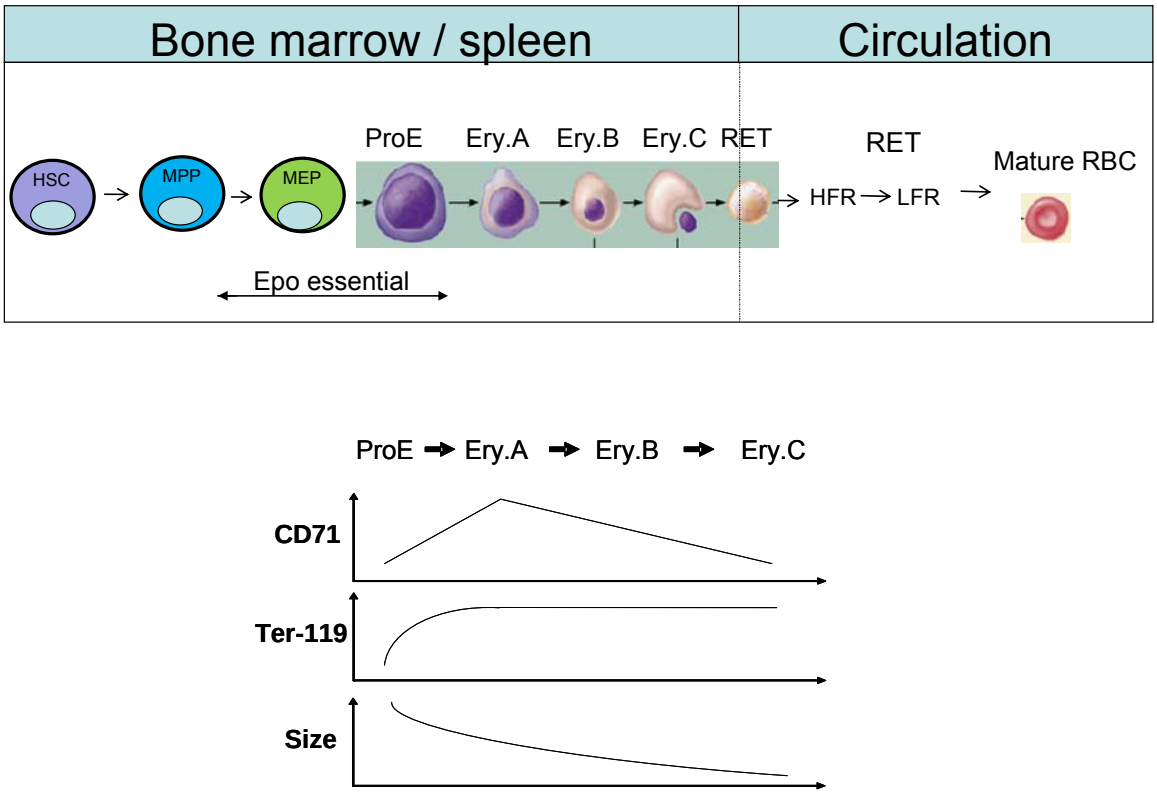

Figure 1.9. (Top) Description of erythroblast development in the erythropoiesis organs. (Bottom) Differential expressions of cell markers, Ter-119 and CD71, on erythroblasts of different erythroblasts stages. ProE represents proerythrocytes, Ery.A represents Basophilic erythroblasts, Ery.B represents polychromalophilic erythroblasts and Ery.C represents orthrochromic erythroblasts. CD71 expression increased from ProE and reaches the maximum value at Ery.A stage. The CD71 expression then decreased from Ery.A stage until the end of erythropoiesis. On another hand, the Ter-119 expression is increased to the highest level once the ProE progenitors are committed to the erythrocytes lineage stage. The Ter-119 expression remains high until the end of mature red blood cells. The size of cells is decreased progressively throughout the erythropoiesis.

1.7.3.2 Differentiation of lymphocytes

The differentiation of lymphoid cells startd when the LMPPs differentiate into early lymphoid progenitors (ELPs) that is accompanied by the increased expression of recombination-activating gene 1 (Rag1) and Rag2. Rag 1 and Rag 2 are enzymes that are essential for somatic recombination during formation of B cell and T cell receptors (Spanopoulou et al., 1996). ELPs can either migrate to thymus to differentiate to T cells or remain in the bone marrow for B cell development. The ELPs further develop into CLPs which express interlukein 7 receptor alpha on the cell surface(Kondo et al., 1997). CLPs still have the potential to develop into B cells, T cells, DCs and NK cells (Figure 1.8).

1.7.3.2.1 B cells differentiation

Those CLPs that express B220 are considered to be the earliest B cell progenitors and are called ProB cells. It was shown that transcription factors E2A, early B-

cell factor (EBF), paired box protein 5 (Pax5), lymphoid-enhancer-binding factor1 (LEF1) and sex-determining region Y (SRY) box 4 (Sox4) are essential for differentiation of CLP to ProB cells (Zhuang et al., 1996) (Cobaleda et al., 2007; Hagman et al., 1995; Reya et al., 2000). Then ProB cells develop into Pre-BI cells where somatic recombination start to occurs. The immunoglobin in B cells is composed of two light chains and two heavy chains. The viable region in the heavy chain is composed of V, D and J segments. These three segments are the gene products of random DNA recombination taking place at V, D and J segment genes in the immunoglobin heavy chain locus. PreBI cells undergo recombination between D and J segment. Then PreBI develops to be Large PreBII cell and V segment joins to DJ segment through DNA recombination. VDJ gene is rearranged. This rearranged immunoglobin heavy chain assembles with the surrogate light chain to form per-B-cell receptor and is presented on the cell surface. Large PreBII cells expand in population. Then RAG1 and RAG2 expression is enhanced again, and light chain rearrangement occurs joining the V and J segments of light chain at the light chain locus. Immature B cells that are not autoreactive leave the bone marrow, move to the spleen and become transitional B cells (Hoek et al., 2006). Transitional B cells finally develop into mature B cells. Mature B cells are mainly either follicular B cells or marginal-zone B cells. Follicular B cells form germinal centres together with T cells in the spleen after immunization. The B cells in germinal centers undergo proliferation and somatic hypermutation at the variable gene segment and undergo isotype switching [Reviewed in (Matthias and Rolink, 2005)]. The markers that help to identify different stages of B cells are summarized in the figure 1.10.

Stages	CLP	Pro-B cells	Pre-BI cells	Large Pre-BII cells	Small Pre-BII cells	Immature B cells	Mature B cells
Heavy chain	germline	undergoes D-J rearrangement	undergoes V-DJ rearrangement	VDJ rearranged	VDJ rearranged	VDJ rearranged	VDJ rearranged
Light chain		germline	germline	germline	undergoes V-J rearrangement	VJ rearranged	VJ rearranged
lineage	-	+	+	+	+	+	+
IgM	-	-	-	-	-	+	+
IgD	-	-	-	-	-		+
B220	-	+	+	+	+	+	+
CD19	-	-	+	+	+	+	+
CD43	-	+	+	+/-	-	-	-
CD25	-	-	-	+	+	+/-	-
Kit	+	+	+	-	-	-	-

Figure 1.10. Summary of markers for identifying different stage of B cells.

1.7.3.2.2 T cell differentiation

T cells develop in the thymus in mice and humans. Different stages of developing T cells can be identified by specific markers (Figure 1.11). The thymus does not produce T cells progenitors and relies on continuous seedling of progenitors produced in bone marrow and transported via blood circulation (Wallis et al., 1975). The cells that are seeded in the thymus from bone marrow are the early lymphoid progenitors (ELPs) (Lind et al., 2001; Medina et al., 2001). It has been

shown that CLPs are also capable of reconstituting T cell development in the thymus but that circulating CLPs are rare and thus unlikely the major source of T cell progenitors in vivo (Schwarz and Bhandoola, 2004). The cells migrate to specific sites in the thymus at specific stages throughout the T-cell development. ELPs enter the thymus via blood vessels at cortico-medullary junctions. The commitment of the T cell lineage from ELPs or CLPs to early T cell precursors (ETPs) requires the molecular interaction of Notch-1 ligand with stromal cells in the thymus. ETPs proliferate and migrate to the thymus cortex where they develop into double-negative 2 stage (DN2). The cells further migrate to sub-capsular zones where theyare shifted to the DN3 stage and undergo T cell receptor (TCR) gene rearrangement of V, D and J segments at the β, γ,δ loci. TCR-β combines with pre-Tα to form pre-TCR and is presented on the cell surface for β-selection (Fischer and Malissen, 1998). T cells with gene arrangement at β chain become αβT cells while those with gene arrangement at γ,δ loci become γ,δ T cells. Only those DN3 cells which contain in-frame TCR genes are selected for further development (Burtrum et al., 1996). Before fully developed into double positive (DP) cells, DN3 cells that pass the β-selection migrate to the thymus cortex again and develop into DN4. DN4 then develop into immature single positive cells (ISPs), which then develop into the DP stage. During this transition, the α chain of TCRt occurs by joining V and J segments. At DN4 to ISP transition stage, around 10% of cells undergo TCR α chain rearrangement. At ISP to DP transition stage, more than 90% of cell undergo TCR α chain rearrangement (Mertsching et al., 1997). After the α chain is rearranged, αβTCR is presented on the cell surface and the cells become double positive for CD4 and CD8. A knockout mice model revealed that the nuclear factor of activated T cells (NFAT) and Sox4 are essential for T cell development from DN to DP stage (Schilham et al., 1997). DP cells in the thymus cortex undergo positive selection in which only those cells that bind to MHC molecules survive. (Those cells that bind to class I MHC molecules become CD8+ T cells and those that can bind to class I MHC molecules become CD4+ T cells eventually.) Then survival cells migrate towards the medulla of thymus and undergo negative selection. During negative selection, T cells areexposed to antigen-presenting cells with self-antigen on MHC molecules and those T cells that react to self-antigen are eliminated. Finally, survival cells develop into SPCD4+ and SPCD8+ cells (Figure 1.12) [Reviewed in (Ceredig and Rolink, 2002; Rothenberg et al., 2008)].

Stages	DN1	DN2	DN3	DN4	ISP	DP	CD4	CD8
βγδchains	undergo D-J rearrangement	undergo V-DJ rearrangement	Pre-TCR formation					
α chain					undergo V-J rearrangement			
CD117	+++	+++	+	low	-	-	-	-
CD44	+++	+++	+	low	-	-	-	-
CD25	-	++	++	-	-	-	-	-
CD127	-	+	low	-	-	-	-	-
CD3	-	-	low	low	low	+	+	+
CD4	-	-	-	-	-	+	+	-
CD8	-	-	-	-	+	+	-	+

Figure 1.11. Summary of markers for identifying different stage of T cells.

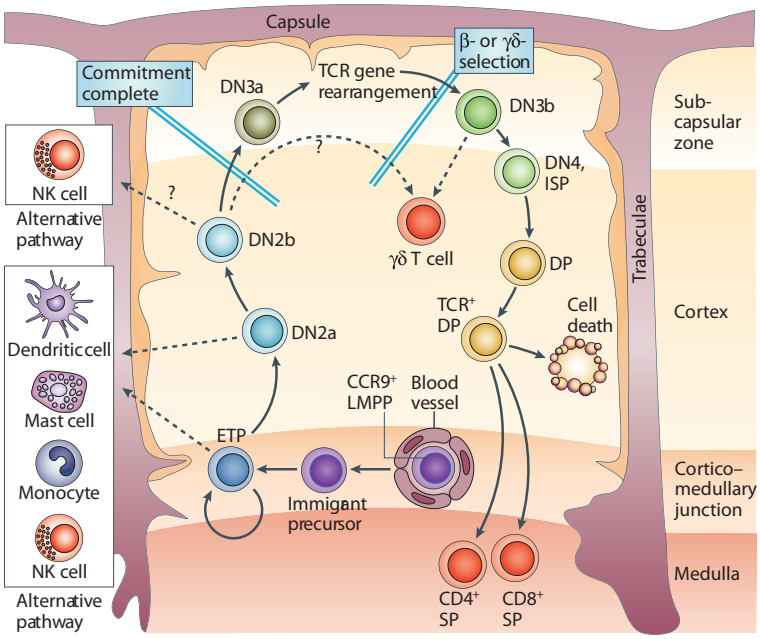

Figure 1.12. Cross-section of adult thymic lobule. Cell migration paths during T cell development are shown with arrows. Broken arrows represent the possible pathway of cell differentiation. The differentiation path is described in the text. Abbreviation: the early T-cell precursors (ETP); double negative (DN); immature single positive (ISP); double positive (DP); single positive (SP) stages (figure is adapted from (Rothenberg et al., 2008)).

Differentiation of T cells involve a network of interacting signals like transcription factors, cytokines and chemokines throughout the differentiation path (Laiosa et al., 2006). The components that instruct the differentiation of hematopoietic cells are found based on knockout mice models. Figure 1.13 shows a list of transcription factors that are or might be involved in lineage commitments. From the figure, it is demonstrated that loss of function of a single transcription factors may have effects on several lineages or only affect one lineage. For example, PU.1 and Ikaros knockout mice show defect in most lineages, FOG-1 deficiency mice show a defect in T-cell and erythroid cell maturation only (Laiosa et al., 2006).

Regulator	Family	HSC	B	T	NK	GM	MegE	DC
Ikaros	ZnF	func	lack	lack/ matur	lack	matur	decr	lack
PU.1	ets	func	lack/ matur	lack/ matur	decr/ matur	lack		lack
EBF	HLH		matur					
Pax5	paired		matur					
E2A	HLH		matur	matur				
HEB	HLH			matur				
GATA-3	ZnF			lack				
Notch1	transmem			lack				
Id3	HLH		func	matur				
C/EBP α	bZip	func				lack		
C/EBP β	bZip		decr/ func			func		
GATA-1	ZnF						lack/ matur	
FOG-1	ZnF			matur			lack/ matur	
Id2	HLH				decr			decr
RelB	RHD		func					decr

Figure 1.13. List of transcription factors involved in hematopoietic lineage commitment. Blue boxes indicate affected cell types labeled on the top. Knockout mouse models mentioned here are restricted to loss of function of gene by using germ line specific Cre (conventional) and hematopoietic Mx1-Cre or lineage-specific-Cre. Empty boxes representing no phenotype was reported or observed. Labels denotes as follow: lack, indicates the loss of the lineage; matur, maturational block; func, defect of cellular function; decr, decrease in cell numbers; inc, increase in cell numbers. Abbreviations: bZip, basic leucine zipper; HLH, helix-loop-helix domain; transmem, transmembrane; HMG box, high motility group box; HTH, helix-turn-helix domain; RHD, Rel homology domain; ZnF, zinc finger domain. References of each knockout mice model refer to the review (Laiosa et al., 2006).

2 Materials and Methods

2.1 Generation of RHAU-targeted mice

We targeted the exon 8 of RHAU gene in which the motif II of DExH helicase essential for the APTase activity of RHAU resides. The homologous arms 4.5 kb upstream and 5.5 kb downstream of exon 8 and exon 8 were amplified by PCR from 129/Sv mouse genomic DNA using linker-primers AscI-5'arm-fw (5'-ACC AGG CGC GCC GTT CAA ACT ATC TCG TGT TCT ATG CTG C-3'), AscI-5'arm-rev (5'-ACC AGG CGC GCC GGA TGA GGA GGA AGA GTG TCA TGT AG-3'), FseI-3'arm-fw (5'-TGT AGG CCG GCC AGA TAC AGA TCA GAT AGT GGG C-3'), FseI-3'arm-rev (5'-ACA AGG CCG GCC AGA AGA CTG AAC TAG ATG CCC T-3'), PacI-exon8-fw (5'-CCA GTT AAT TAA AAA TGT ACC ACC ACT GTC C-3') and PacI-exon8-rev (5'-CGT ATT AAT TAA GCA AAC TGT CAG CTT AGC C-3'). These fragments were sub-cloned into the pGEMT vector (Promega). As a backbone for the replacement targeting vector we used pOZIII (Ozgene) with the neomycin resistance gene (NeoR) flanked by flippase recognition target (FRT) sites and loxP sites and unique restriction sites to introduce the targeted exon and the homologous arms. The homologous arms, exon 8 and the HSV-TK gene (for negative selection with Ganciclovir, which was not used in this work), each flanked by unique restriction sites, were inserted sequentially into the pOZIII vector. The final vector RHAU-KO was linearized with PvuI and NotI and electroporated into 129Ola ES cells. The G418-resistant clones were screened by PCR and Southern blot for homologous recombination and the correctly targeted ES cells were used to generate chimeric mice with the genotype $RHAU^{fl,neo/+}$. These were crossed to C57BL/6 mice to obtain germ line transmission of the targeted allele. The progeny were crossed to B6.129S4-Meox2CreSor (Meox2Cre) to achieve deletion of exon 8 and the neomycin cassette from the targeted allele, resulting in $RHAU^{\Delta/+}$;cre^{tg} mice. $RHAU^{\Delta/+}$;$Meox2Cre^{g}$ mice were crossed with $RHAU^{+/+}$ mice to generate $RHAU^{\Delta/+}$ mice free of the Cre transgene.

To remove only the neomycin cassette from targeted alleles, floxed mice with the neomycin cassette ($RHAU^{fl,neo/+}$) were crossed with 129S4/SvJaeSor-Gt(ROSA)26Sortm1(FLP1)Dym/J mice (Jackson Laboratory) that bore the FLP1 transgene and expressed FLP1 recombinase (FLPtg). F1 offspring with the genotype $RHAU^{fl/+}$; FLP^{tg} were then selfed to derive $RHAU^{fl/fl}$ mice lacking the neomycin cassette and the FLP1 transgene. These new $RHAU^{fl/fl}$ mice were then crossed with vav-iCre mice (de Boer et al., 2003) that expressed Cre specifically in the hematopoietic system (Almarza et al., 2004) (Zhao et al., 2007). Expression of cre can be detectable from stem cells. Offsprings with the genotype $RHAU^{fl/+}$; $iCre^{tg}$ were then crossed with $RHAU^{fl/fl}$ or $RHAU^{fl/+}$ mice to derive $RHAU^{fl/fl}$; $iCre^{tg}$ mice for further experiments. $RHAU^{fl/fl}$ littermates were used as a control in

most experiments and $RHAU^{fl/+}$ littermates were used as a control in bone marrow transplantation experiments.

We have also established an interferon-inducible RHAU knockout mice specific in the hematopoietic system using the MxCre system (Behrens et al., 2002; Natarajan et al., 2007). Cre is under the control of Mx1 promoter. When induced by interferon, transcription of Cre gene increased in interferon response cells. For the production of $RHAU^{fl/fl}$; $MxCre^{tg}$ mice, the breeding plan was similar to that for $RHAU^{fl/fl}$; $iCre^{tg}$ mice generation. $RHAU^{fl/fl}$ littermates were used as a control.

Animal experimentation was carried out according to regulations effective in the canton of Basel-Stadt, Switzerland. The mice were housed in groups of one to eight animals at 25°C with a 12-h light-dark cycle (12 h light, 12 h dark). They were fed a standard laboratory diet containing 0.8% phosphorus and 1.1% calcium (NAFAG 890; Kliba, Basel, Switzerland). Food and water were provided ad libitum.

2.2 Genotyping

A 0.5-mm tail section or a whole embryo was lysed in 300 µL of lysis buffer (100 mM Tris pH 8, 5 mM EDTA, 200 mM NaCl 0.2% SDS and 50 µg/µL Proteinase K). Samples were incubated at 55ºC overnight. DNA was precipitated with 700 µL absolute ethanol and collected by centrifugation at 20'000 g for 10 min. Pellets were washed once with 500 µL 70% ethanol and dried at room temperature. DNA was dissolved in 10 mM Tris-HCl pH 8 buffer and incubated at 55ºC for 1 h. DNA concentration was measured with 280 nm UV light (NanoDrop Technologies, Inc.). For genotyping with PCR, we always use PrimeSTARTM HS DNA polymerase (Takara Bio Inc.) and 20 µL reaction volume as mentioned in the protocol. For optimal reaction, 100 ng of DNA was used. For embryos that were earlier than 7 dpc, all DNA was purified with phenol chloroform extraction. Purified DNA sample finally was dissolved in 30 µL of 10mM Tris-HCl buffer, pH 8.0, and 10 µL of DNA was submitted for every PCR reaction. $Meox2Cre^{tg}$ allel was identified by PCR using primer one (common: 5'-GGG ACC ACC TTC TTT TGG CTT C-3'), primer two (Cre: 5'-AAG ATG TGG AGA GTT CGG GGT AG-3') and primer three (wild type: 5'-CCA GAT CCT CCT CAG AAA TCA GC-3') (Tallquist and Soriano, 2000). The wild-type and mutant bands were 411 bp and 311 bp, respectively. To identify vav-$iCre^{tg}$ mice, forward primer (5'- TCA CAC CAG TGA GTG GAA GC-3') and reverse primer (5'-TCC CTC ACA TCC TCA GGT TC-3') were used. The PCR product was ~800 bp. To identify $MxCre^{tg}$ mice, forward primer (5'- GCA AGA ACC TGA TGG ACA TGT TCA G-3') and reverse primer (5'- GCA ATT TCG GCT ATA CGT AAC AGG G-3') were used. The PCR product was 462 bp. To analyze for exon 8 of the RHAU gene, we used primers KO3-fw (5'-TGT ACA TTT TGA TAC TAC TTA ATC TAC CCT TTG A-3') and KO3-rev (5'- TAT GGA AAT GCT CCT AGT TAA AGT TTA GAG CT-3'). The wild-type band was 2664 bp, the transgenic band with the targeting vector loxP-Exon8-flp-NEO-flp-loxP was 4010 bp, the transgenic band with targeting vector loxP-Exon8-loxP (without neomycin cassette) was 2229 bp and the mutant band with both exon 8

and the neomycin cassette removed by Cre was 1509 bp. To confirm correct integration of the targeting vector into the genome, we used two pairs of primer sets that flanked the boundaries of the 5' and 3' homologous recombination arms of the targeting vector. To probe correct integration of the 5' arm, we used primers mod2 (5'- GGG AGA TGG GTG TGT ACT TAT AGA GAA CAG ATG TTG-3') and mod8 (5'-GGC CGA TCC CAT ATT GGC TGC AGG TC-3'). To probe the 3' arm, we used primers mod7 (5'-GAT GCG GTG GGC TCT ATG GCT TCT GAG GC-3'); and mod4 (5'- CAA ACT TTC AAT TCC TTT GGC TCT TAC AAT CTT AAG TG-3'). Correct integration gave PCR products of 6365 bp and 6192 bp with primers mod2/8 and mod7/4, respectively. These PCR fragments were verified by sequencing.

2.3 Analysis of the efficiency of implantation

Three types of crossing were carried out: male $RHAU^{\Delta/+}$ mice × female $RHAU^{\Delta/+}$, male $RHAU^{\Delta/+}$ × female $RHAU^{+/+}$ and female $RHAU^{\Delta/+}$ × male $RHAU^{+/+}$. To determine the efficiency of implantation of embryos, the numbers of corpora lutea (CL) from $RHAU^{\Delta/+}$ (n=25) and $RHAU^{+/+}$ (n=25) female mice were counted. The ratio of the number of implanted embryos to the number of CL denotes the efficiency of embryo implantation.

2.4 Western blot analysis

Protein from cells and tissues were extracted with RIPA buffer (10mM Tris pH 7.0, 150 mM NaCl, 1%w/v Na-deoxycholate, 1% w/v Triton-X 100 and 0.1% sodium dodecyl sulfate). Samples were centrifuged at 14000 rpm at 4ºC for 1 minute. Supernatants were transferred to new 1.5 mL microcentrifuge tubes and cell debris pellets were discarded. Protein concentrations in the supernatant were determined by micro BCA protein assay (Pierce). Samples were mixed with 6x SDS loading buffer (Sambrook, 2001) and submit for SDS-PAGE. Separated proteins were transferred to PVDF membrane (Immobilon-P, 0.45 μm, Millipore) for western blot analysis. Mouse monoclonal anti-RHAU antibody (YN1) generated against a 20-aa peptide, CKKKSDKFLIIPLHSLMPTV, which except for the first three amino acids corresponds to amino acids 515-531 of the human RHAU and is conserved across species. HRP-conjugated anti-mouse and anti-rabbit secondary antibodies were used. Signals were developed by ECL detection reagent (Amersham Biosciences, RPN2106V1) and detected by Fuji Medical X-Ray film (FUJIFILM Corporation, Japan).

2.5 Histology

Eight weeks old mice were sacrificed and perfixed with ALPHELYS RCL2®-CS100. Organs were embedded after fixation in PBS containing 4% paraformaldehyde. Bones were incubated in decalcification solution (20% EDTA w/v, 2% NaOH, pH 7.5) for 7 days twice. Decalcificated bones and other organs

were subsequently sectioned and stained with hematoxylin and eosin for microscopic examination.

2.6 Complete blood count analysis

Blood (*ca* 200 µL) was collected by tail bleeding into EDTA-coated BD Microtainer K2E tubes (BD Pharmingen). Samples were mixed with EDTA by shaking the tubes upside down for ten times and kept at room temperature until analysis. Complete blood cell counting was performed by the Advia 120 Hematology Analyzer and results were analyzed by Multispecies Software, version 2.3.01-MS (Bayer, Leverkusen, Germany).

2.7 FACS analysis

Eight to ten weeks old mice were used for all FACS analysis. Bone marrow cells were recovered by flushing femur and tibia with PBS containing 3% FCS (FACS buffer). Splenocytes and thymocytes were collected from whole spleen and thymus by pressing gently with a sterile plunger from a 2 mL syringe into the FACS buffer. Cells were stained with different antibodies conjugated to a chromophore and processed by flow cytometer using appropriate antibodies for different cell markers. A list of the reagents, target cells and suppliers is given in Suppl. Table 1. A FACSCalibur cytometer (Becton Dickinson) with dual lasers (488 and 635 nm) was used for the detection of T cells, B cells, NK cells, monocytes and neutrophils, and a MoFlo (DakoCytomation) with three lasers (355, 488, and 633 nm) for the detection of LT-HSC, ST-HSCF, MPP, LMPP, CMP, GMP, MEP, and CLP cells. Cell sorting was steered with the Summit software (DakoCytomation) and the data obtained were analyzed using the FlowJo (Tree Star) software.

We determined the absolute number of viable cells in the bone marrow (two femurs and two tibias per mouse), spleen and thymus by the trypan blue exclusion method and counting in a ViCell counter (Beckman Coulter Inc.). Total cells number was multiplied by the percentage of the viable cell gate (DAPI or 7-AAD negative) and then by the percentage of cells in each sub-gate thereafter, to determine the absolute number of each subpopulation per mouse.

2.8 Bone marrow transplantation

Bone marrow cells were collected from femora and tibiae by flushing with PBS containing 3% FCS (FACS buffer) and filtered through 40-µm mesh. 3 x 10^6 cells in 200 µL HBSS were injected into the tail vein of lethally irradiated (1100 cGy in 2 doses, separated by 3 hours) seven- to ten-week-old recipient mice. C57BL/6SJL-PtprcaPep3b/BoyJ (B6.CD45.1) mice and (GFP)–expressing C57BL/6-Tg(UBC-GFP)30Scha/J [Tg(GFP)] mice were used as the recipients. Five weeks after bone marrow transplantation, recipient mice which received

bone marrow cells from $RHAU^{fl/fl}$; $MxCre^{tg}$ and $RHAU^{fl/fl}$ control mice were treated with poly(inosinic acid)-poly(cytidylic acid) (polyI:C). Chimerism of recipient mice was analyzed for CD45.1 positive and CD45.2 positive cells by flow cytometry using anti-CD 45.1-APC (eBioscience) and anti-CD 45.2 PerCP Cy5.5 (BD Pharmingen) (Pan et al., 2007).

2.9 Colony forming assay

Bone marrow cells and splenocytes were collected as described for FACS analysis. $2x10^4$ bone marrow cells or $1x10^5$ of splenocytes were seeded in 1 mL of methylcellulose medium provided from the kit of Mouse Colony-Forming Cell Assays Using MethoCult® (M3434, StemCell Technology). Protocol was followed as described by the manufacturer. After 12 days, the number of BFU-E, CFU-GM, CFU-G, CFU-M and CFU-GEMM in the dish cultured with bone marrow cells and spleen cells were counted.

2.10 Determination of the half lives of erythrocytes by in vivo biotin labeling

The half lives of erythrocytes were determined by in vivo biotinylation of red blood cells. 20 mg/mL of biotin-x-HNS (Sigma) in DMSO was diluted ten folds with 0.9% (v/w) NaCl solution. Each mouse was injected with 300 µL (600µg) of diluted biotin-x-HNS. Blood samples were collected every day starting one day after the injection. Around 2 µL of blood were collected from each mouse into 1 mL PBS. Cells were counted, and 1 x 10^6 cells were incubated on ice with 125 µL FACS buffer containing 5µg/ mL PE Streptavidin (BD Pharmingen) for 20 minutes. Cells were washed twice with FACS buffer and submitted for FACS analysis. The numbers of biotin positive cells were compared with that obtained on the first day. Survival slopes were linear. The Half lives of cells were calculated by the formula $y = mx + C$, where C is the y intercept and is always equal to 1, y is the ratio of biotin positive cells, x is the days and m is the slope (de Franceschi et al., 2004; Hoffmann-Fezer et al., 1997).

2.11 Determination of the half lives of erythrocytes by in vitro biotin labeling

Blood of$RHAU^{fl/fl}$ mice or $RHAU^{fl/fl}$; iCre mice was collected in 1.5 centrifuge tubes containing 5 µL 5000 IE/UI heparin in each tube (Pfizer Inc., NY, US). Blood cells of the same genotype were pooled and washed twice with twenty volumes of PBS. Cells were resuspended in 35 mL PBS (about 20 volumes of the blood cell pellet). 5 µL of 20 mg/mL biotin-x-HNS (Sigma) in DMSO was added directly in the suspended cells and rotated for 30 min at room temperature. Cells were washed three times with 50 mL PBS and resuspended in 1.75 mL PBS to give 50% hematoitcrit. Around 200 µL of cell suspension were injected into each $RHAU^{fl/fl}$ or $RHAU^{fl/fl}$; $iCre^{tg}$ mouse using a 30G needle. Blood samples were

collected every day starting one day after the injection. The numbers of biotin positive cells were counted in the same way as above mentioned in vivo biotinylation experiment, but using $5x10^6$ cells instead.

2.12 Determination of the osmotic resistance

Blood samples were collected by tail bleeding into EDTA-coated BD Microtainer K2E tubes (BD Pharmingen). 2 μL of well mixed blood were added to 200 μL of solutions with different NaCl concentrations (0~0.9%) in a 96-well-plate. After centrifugation for 5 min at 500g, 80 μL of the supernatant were transferred to another 96-well-plate and the absorption at 405 nm was determined, which showed the extent of haemolysis. The value of the absorption at different NaCl concentrations wase normalized to the absorption at 0% NaCl, which was set as 100% haemolysis (Foller et al., 2009). The enucleated erythrocytes were sorted for osmotic resistance as well. To identify cells with and without nuclei, 2×10^7 erythrocytes were suspended in 10 mL RPMI containing 10% serum in 15 mL tube and incubated with Hoechst 33324 (10 μg/mL) for 10 minutes at room temperature. During cell sorting, erythrocytes with appropriate cell sizes were selected by gating with forward and side scatterings. Cells with appropriate cell sizes and without Hoechst 33324 signals were collected and submitted for osmotic resistance test as above.

2.13 Quantization of plasma concentrations of erythropoietin

Blood samples were collected by tail bleeding into 1.5 centrifuge tubes. Samples were allowed to clot for 16 h at 4ºC. Clotted blood was centrifuged at 2000 g for 20 min. The supernatant was diluted with Calibrator Diluent RD6Z provided together with the Mouse/Rat Epo Immunoassay kit (R&D System, Minneapolis, USA). The concentration of Epo in the samples was determined according to the instructions provided by the manufacture of the kit.

2.14 Annexin V staining of erythrocytes

2μL of blood samples were collected into 1 mL PBS and counted. 1×10^6 cells were counted and resuspended in 1 mL Annexin V binding buffer (10mM Hepes, pH 7.4, 140mM NaCl, and 2.5 mM $CaCl_2$. 100μL of cells were transferred into a new tube and incubated with 5 μL of Annexin V-APC solution (BD Pharmingen) for 15 min at room temperature. The cells were mixed with 400μL of Annexin V binding buffer and submitted for FACS analysis.

2.15 mRNA microarray analysis

Bone marrow cells were treated as the same way as for FACS data analysis and stained with Ter-119 and CD71 for ProE cell sorting mentioned above. Cells were sorted in FACS solution and centrifuged for 5 minutes at 4ºC. mRNA were

extracted with RNeasy Micro Kit (QIAGEN). RNA was quantified with NanoDrop. 200 ng of RNA per sample was submitted for one cycle labeling kit from Affymetric according to the manufacturer's instructions. Samples were hybridized on Mouse Gene 1.0 chips. Gene expression values and fold changes were analysis by R written by Genome Facility in FMI.

3 Results

3.1 Comparison of the primary structure of human and mouse RHAU

The amino acid sequences of human RHAU and mouse RHAU are aligned. According to the alignment results, human RHAU and mouse RHAU are of 91% identity and 95% similarity (Figure 3.1).

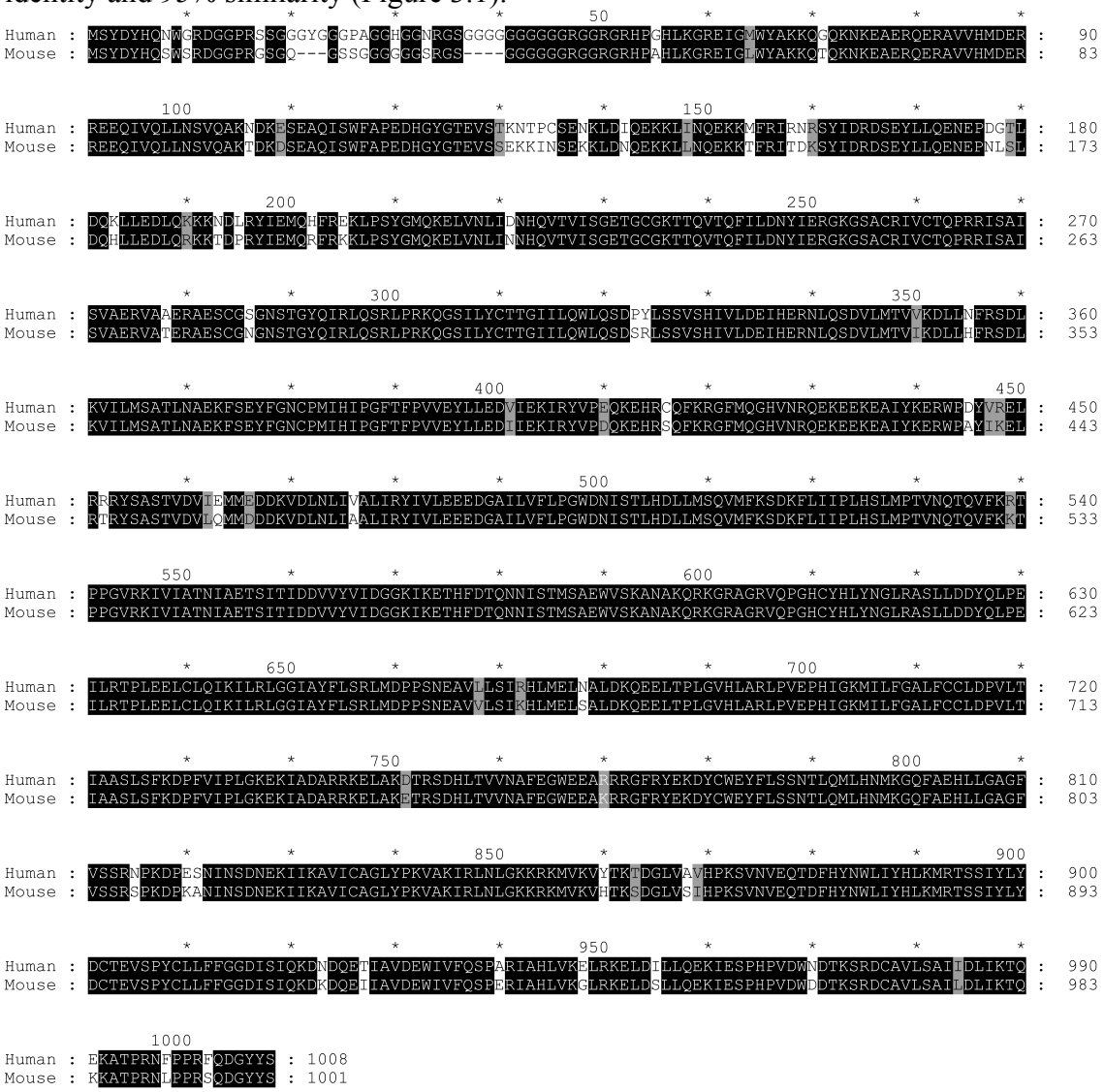

Figure 3.1 Primary structure comparison of human and mouse RHAU showed 91% identity and 95% similarity done by MAFFT (Katoh and Toh, 2008) edited in GeneDoc (Nicholas et al., 1997). The black boxes represent the same amino acids shared by human and mouse RHAU. The grey boxes represent the amino acids that are different between human and mouse RHAU but share similar chemical properties.

3.2 RHAU protein is ubiquitously expressed in adult mouse

RHAU was detectable by western blot in most tissues collected from adult mice. We tested male and female mice in parallel and both showed similar expression pattern. Figure 3.2 shows a representative western blot detecting the RHAU protein in various organs from a male adult mouse. Due to the low expression level of RHAU in the bone marrow cells, we loaded 50µg and 100µg of protein from bone marrow cells in the last two lanes in order to detect the expression of RHAU. The mouse RHAU is 1008 amino acids in length and the molecular weight is 113.8 kDa (predicted by ExPASy Proteomic Server). We could see a band corresponding to 113.8 kDa in the gel. The identity of this band was confirmed by probing the blot with another anti-RHAU rabbit polyclonal antibody (clone 399).

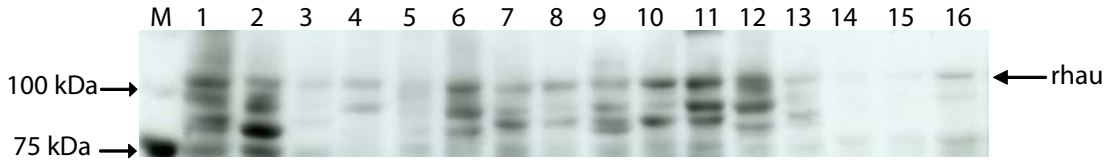

M is protein marker
1 Brain
2 Heart
3 Lung
4 Pancrease
5 Stomach
6 Intestine
7 colon
8 spleen
9 kidney
10 Thymus
11 Liver
12 muscles from leg
13 spinal cord
14 bone marrow (25 µg)
15 bone marrow (50 µg)
16 bone marrow (100 µg)

Figure 3.2. Detection of RHAU protein in different tissues of a 16-week old male mouse by western blot. Tissues were collected and homogenized in RIPA buffer (10mM Tris pH 7.0, 150 mM NaCl, 1%w/v Na-deoxycholate, 1% w/v Triton-X 100 and 0.1% sodium dodecyl sulfate) using a microcentrifuge pestle in 2 mL microcentrifuge tubes. Samples were centrifuged at 14,000 rpm at 4ºC for 1 min. Proteins in supernatants were transferred to new 1.5 mL microcentrifuge tubes and cell debris pellets were discarded. 25µg of protein from each sample were loaded on each lane for all organs. 50 µg and 100 µg of bone marrow protein were loaded in the last two lanes. Arrows on the left shows the protein molecular weight markers of 100 kDa and 75 kDa (Precision Plus Protein, BioRad). Arrow on the right shows the band corresponding to the RHAU protein.

3.3 Generation of RHAU-targeted mice

To enable conditional deletion of the RHAU gene, we designed a targeting vector in which loxP sites flanked the exon 8 of the RHAU gene and the neomycin-resistant gene (NeoR) cassette, which itself was flanked by flp sites, was inserted downstream of exon 8,. In the targeted genome, CRE deletes both exon 8 and the neomycin cassette while FLP1 deletes only the neomycin cassette (Figure 3.3A). The exon 8 encodes the DEIH box of the RHAU that is essential for its ATPase activity (Tran et al., 2004) and deletion of this exon introduces a frameshift downstream that led to the total decay of the message through the nonsense-mediated mRNA decay mechanism. The linearized vector was transfected into ES cells and cells with a correctly targeted allele (clones 2 and 42) with the genotype $RHAU^{fl,neo/+}$ were detected by Southern blot analysis (Figure 3.3B). PCR analysis of these clones using the primer pairs mod4/7 and mod2/8 yielded products of the correct sizes (Figure 3.3C). Genotyping of the F1 mice and their offspring using the primer pair KO3fw and KO3rev showed three different combinations of two alleles (Figure 3.3D). $RHAU^{\Delta/+}$ mice were derived by crossing $RHAU^{fl,neo/+}$ with Meox-CRE mice as described in Materials and Methods. $RHAU^{fl/fl}$ mice were obtained by first deleting the neo cassette from $RHAU^{fl,neo/+}$ and then crossing with $RHAU^{fl/+}$ mice, as described in Methods.

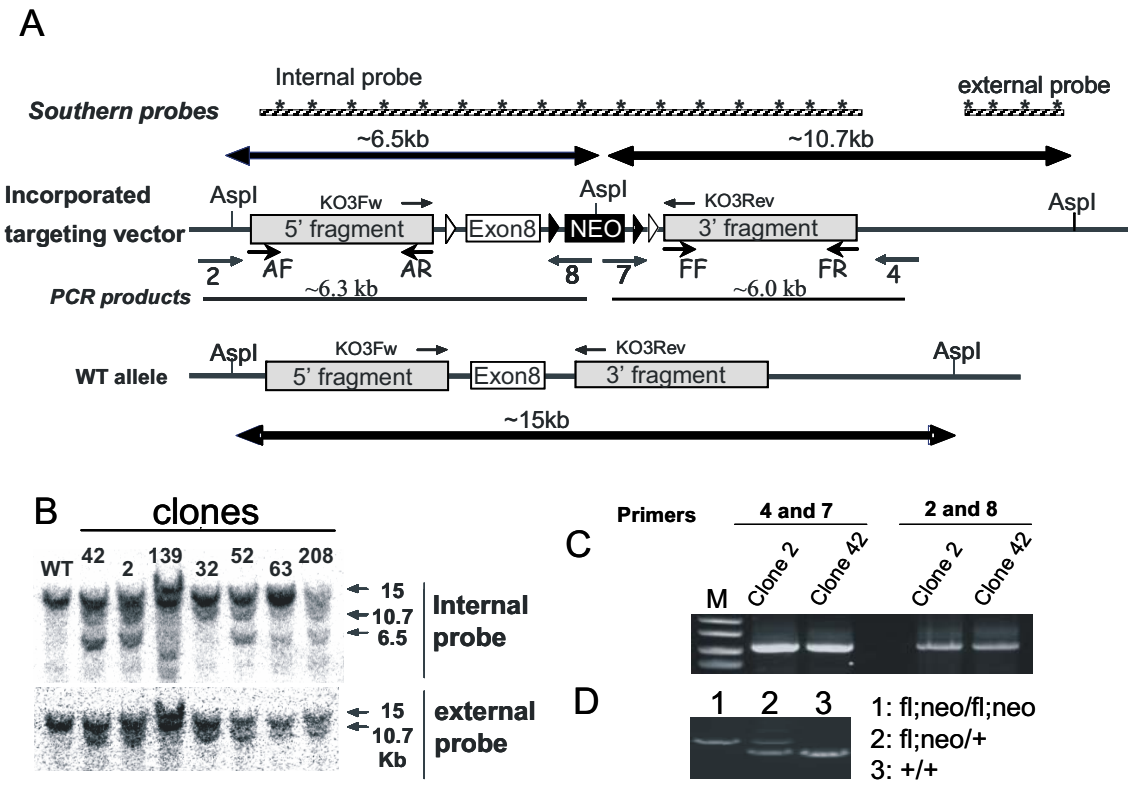

Figure 3.3. Generation of RHAU-targeted mice. (A) Schematic representation of the RHAU-targeting vector. A targeting vector was constructed by inserting two loxP sites flanking the exon 8 of RHAU and a NeoR. Open arrowheads denote the loxP sites and closed arrowheads denote the flp sites. The striped bars indicate the positions of the internal and external probes used in Southern hybridizations. Vertical lines indicate AspI

restriction sites. (B) Identification of the targeted clones. G418-resistant ES cells were screened for homologous recombination by Southern hybridization. DNA samples from ES cells were digested with AspI restriction enzyme. One AspI site is introduced into the genome when recombination of targeting vector occurs. Internal and external probes were used to identify the clones with correct homologous recombination of the targeting vector. The internal probe detected three bands, 15, 10.7 and 6.5 kb, while the external probe detected two bands, 15 and 10.7 kb, from the ES cell samples with correct homologous recombination in one of the two alleles. Cells without recombination (WT) gave rise to a 15-kb band with both internal and external probes. Clones number 42, 2, 52, 63 and 208 contained one allele with the correct integration of the targeting vector and a wild-type allele. (C) PCR fragments amplified with primer pairs 2 and 8 and 7 and 4; confirmed by sequencing. DNA marker ladders are 10, 8, 6 and 5 kb from the top of the image. (D) Genotyping of mice. A primer pair KO3fw and KO3rev was used for genotyping. Crossing mice with heterozygous recombination gave rise to mice of three genotypes with the expected Mendelian ratio.

3.4 Loss of RHAU caused embryonic lethality but had no effect on the implantation efficiency

Inbreeding of $RHAU^{\Delta/+}$ mice produced either $RHAU^{+/+}$ or $RHAU^{\Delta/+}$ but no $RHAU^{\Delta/\Delta}$ offsprings. This indicates that the $RHAU^{\Delta/\Delta}$ phenotype is embryonic lethal. $RHAU^{\Delta/+}$ mice did not show differenct phenotype from wildtype mice.

Following $RHAU^{\Delta/+} \times RHAU^{\Delta/+}$ crosses, we found degenerated embryos at 11.5 days post coitus (dpc). However, genotyping of them was not possible due to poor recovery of material. At 8.5 dpc, degenerated fetuses were recovered and genotyped as $RHAU^{\Delta/\Delta}$ (Table 3.1, upper panel). Morphological differences between $RHAU^{\Delta/\Delta}$ and $RHAU^{\Delta/+}$ or $RHAU^{+/+}$ embryos were observed at 7.5 dpc (Figure 3.4). However, at 6.5 dpc, morphologically degenerated embryos were not observed although some were $RHAU^{\Delta/\Delta}$ (Table 3.1 upper section, and data not shown). Therefore, $RHAU^{\Delta/\Delta}$ embryos probably died at around 7.0 dpc.

We also had examined the effect of RHAU ablation on embryo implantation. This was achieved by calculating the efficiency of embryonic implantation (the number of implanted embryos at 6.5~8.5 dpc divided by the number of corpus luteum). The crosses $RHAU^{\Delta/+} \times RHAU^{\Delta/+}$ and $RHAU^{\Delta/+} \times RHAU^{+/+}$ gave rise to almost identical numbers of embryos born and the same implantation efficiency (Table 3.1, Bottom). These results suggest that RHAU ablation does not impair embryonic implantation but plays a critical role in embryonic development manifested after 6.5 dpc.

Table 3.1. RHAU knockout causes embryonic lethality but does not affect implantation. Top. Embryos produced from crossing $RHAU^{\Delta/+}$ and $RHAU^{\Delta/+}$ mice were counted and genotyped. As a control, breeding RHAUΔ/+ mice were crossed with $RHAU^{+/+}$ mice. Embryos with homozygous recombination were not detected at 11.5 days after coitus (dpc). Homozygous embryos at 7.5 dpc had already degenerated.

		Genotype			Genotype	
	Total	+/+	+/Δ	Δ/Δ	+/+	+/Δ
6.5 dpc	56	17	34	5	-	-
7.5 dpc	59	12	32	15	-	-
8.5 dpc	24	6	14	4	-	-
11.5 dpc	22	6	16	0	-	-
13.5 dpc	-	-	-	-	96	107

Breeding	+/Δ x +/\Δ	+/+ x +/Δ
female mice	25	25
total CL counts	257	245
implanted embryos	228	218
rate of implanted embryo	88.72%	88.98%

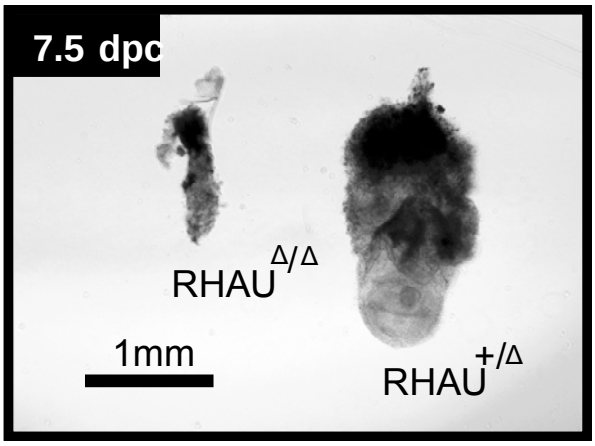

Figure 3.4. RHAU $^{\Delta/\Delta}$ embryos was degenerated at 7.5 dpc. Left is RHAU $^{\Delta/\Delta}$ embryo and right is control RHAU $^{\Delta/+}$ embryo.

3.5 Conditional knockout of RHAU in hematopoietic system causes anemia

We examined the role of RHAU in hematopoiesis by ablating the RHAU gene specifically in hematopoietic cells by means of vav-iCre system as described in Materials and Methods. Unlike conventional RHAU knockout mice, $RHAU^{fl/fl}$; $iCre^{tg}$ mice were alive at birth and survived for up to at least 6 months old. Mice were kept for six months only because of limited space. Pups with a relatively pale color at birth (Figure 3.5A) were shown by PCR genotyping to be $RHAU^{fl/fl}$; $iCre^{tg}$. This suggested that these RHAU mutant mice were anemic with a possible defect in red blood cell differentiation. Western blot analysis confirmed that the RHAU gene was efficiently and specifically deleted in hematopoietic organs as RHAU protein was expressed in the spinal cord of $RHAU^{fl/fl}$; $iCre^{tg}$ but not in the bone marrow, spleen and thymus (Figure 3.5B). Interestingly, $RHAU^{fl/fl}$; $iCre^{tg}$ mice developed splenomegaly and hepatomegaly manifested by increased size and higher weight relative to the body mass (Figure 3.5C, D), a phenotype frequently associated with anemia (Hoffbrand et al., 2006c). Accordingly, the livers and kidneys of $RHAU^{fl/fl}$; $iCre^{tg}$ mice were jaundice. In addition, $RHAU^{fl/fl}$; $iCre^{tg}$ mice developed thymic hypoplasia manifested by the smaller size and lower weight relative to the body mass (Figure 3.5C, D). However, RHAU ablation in hematopoietic cells gave no effect on the total body mass or relative weight of kidney (Figure 3.5C, D). $RHAU^{fl/fl}$; $iCre^{tg}$ mice developed smaller bone marrow cavities and thicker bones (Figure 3.5E). The distinct structures of red and white pulp were absent from the spleens of $RHAU^{fl/fl}$; $iCre^{tg}$ mice (Figure 3.5E) and, although the thymus of $RHAU^{fl/f}$l; $iCre^{tg}$ mice were smaller than those of the wild type, there were no obvious structural changes (Figure 3.5E).

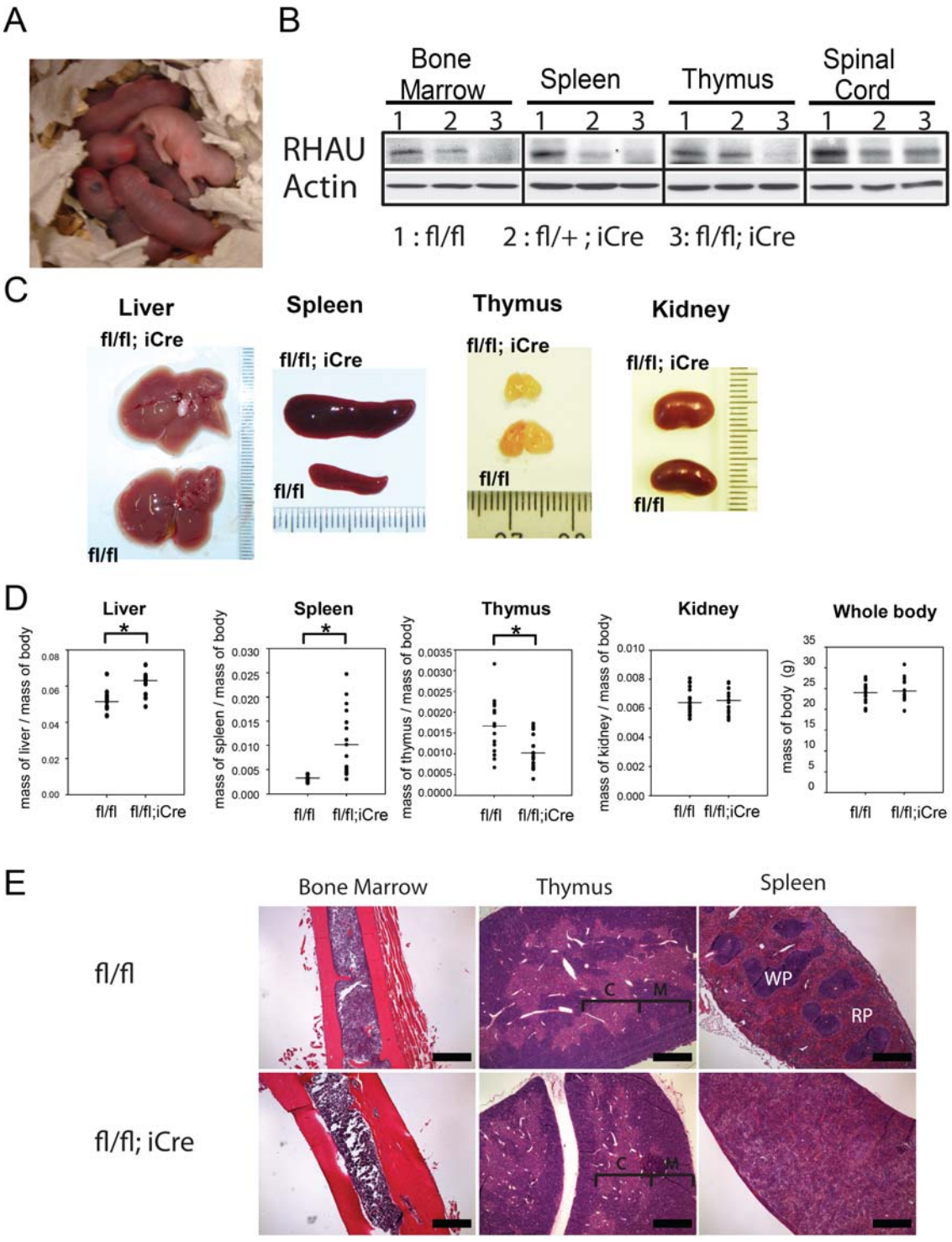

Figure 3.5. Phenotypes of RHAU$^{fl/fl}$; iCre^{tg} mice. (A). Anemic appearance of newborn RHAU$^{fl/fl}$; iCre^{tg} mice with RHAU ablation specifically in the hematopoietic system. (B) Western blot analysis of the efficiency of RHAU ablation in hematopoietic organs. Bone marrow cells were recovered by flushing the femur and tibia. Spleen and thymus were pressed gently with a sterile plunger from a 2-mL syringe into PBS. Spleen and bone marrow cells were treated with RBC lysis buffer for 7 min on ice. Spinal cord was collected from the internal tissue of the backbone. Protein was extracted with RIPA buffer. Aliquots of 50μg of protein from bone marrow and 25μg of protein from other tissues were loaded in each lane. 1, 2, and 3 denote the genotypes of RHAU$^{fl/fl}$, RHAU$^{fl/+}$; iCre^{tg} and RHAU$^{fl/fl}$; iCre^{tg}, respectively. (C) Liver, spleen, thymus and kidney of RHAU$^{fl/fl}$; iCre^{tg} and control RHAU$^{fl/fl}$ mice. (D) Total body mass and relative body mass of each organ from RHAU$^{fl/fl}$; iCre^{tg} and RHAU$^{fl/fl}$ mice. Each dot represents the relative body mass which was calculated by dividing the weight of the organ by total body weight. (E) Hematoxylin and eosin staining of

paraffin-embedded sections of femur (for bone marrow), spleen and thymus from RHAU$^{fl/fl}$ and RHAU$^{fl/fl}$; iCretg mice. Imagines were taken by Nikon ECLIPSE E600 with 4X magnification using Imagic ImageAccess for image calibration with scale bar representing 500μm.

3.6 Effects of RHAU knockout on different lineages in peripheral blood

To study the effects of RHAU ablation on hematopoietic cells, peripheral blood samples from eight-week-old RHAU$^{fl/fl}$, RHAU$^{fl/+}$; iCretg and RHAU$^{fl/fl}$; iCre^{tg} mice were analyzed (Table 3.2 Group A). Furthermore, in order to confirm that the phenotypes observed in RHAU$^{fl/fl}$; iCre^{tg} mice were cell autonomous effects in the hematopoietic cells, we performed two bone marrow transplantation experiments. Firstly, we used RHAU$^{fl/+}$; iCretg and RHAU$^{fl/fl}$; iCre^{tg} mice as bone marrow cell donors, and used UBC-GFP and BL6.CD45.1 as recipients. Complete blood count was performed every two to three weeks after the fifth week of transplantation (Table 3.2 Group B1 and B2). Unfortunately, two out of three UBC-GFP mice transplanted with bone marrow cells from RHAU$^{fl/fl}$; iCre^{tg} mice died at the sixth week post-transplantation. Therefore, counting at the fifth week was available only for Group B1. We repeated bone marrow transplantation using RHAU$^{fl/fl}$;Mx-Cre^{tg} mice and RHAU$^{fl/fl}$ mice as donors and UBC-GFP and BL6.CD45.1 as recipients. Mx-Cre recombinase activity is interferon inducible and can be achieved by injecting polyI:C to the mice. Complete blood count was performed every two to three weeks since the fifth week after transplantation (Table 3.2A and B, Group C1 and C2).

By comparing the results of complete blood counting between the control mice and the target mice (whose hematopoietic cells are RHAU-ablated), we found that the mice responded to RHAU ablation consistently in eleven parameters in all groups, A, B and C (Table 3.2A and B). Firstly, all RHAU ablated mice were anemic with low red blood cell counts (RBC), lowered total hemoglobin (Hb) and hematocrit (Hct) counts. These data agree with the phenotypes of the new born pups of RHAU$^{fl/fl}$; iCre^{tg} mice which were born anemic. In addition, the mice developed reticulocytosis as shown by the enhancement of reticulocytes percentages. Secondly, all mice showed reduced platelet counts. Furthermore, all RHAU-ablated mice showed decreased counts of white blood cells (WBC). The reduction of WBC numbers was mainly due to reduced lymphocytes (lympho) because the counts of monocytes (mono), esinophils (esino) and basophils (Baso) were not reduced (Table 3.2A and B). Since recipient RHAU$^{fl/fl}$ mice transplanted with RHAU-ablated bone marrow cells showed similar phenotypes as RHAU$^{fl/fl}$; iCre^{tg} mice, the effects of RHAU ablation in RHAU$^{fl/fl}$; iCre^{tg} mice was cell autonomous. Therefore, RHAU$^{fl/fl}$; iCre^{tg} mice were used in the following studies on the effect of RHAU ablation on hematopoiesis.

Table3.2 A

Group A vaviCre (Data were collected at 8 weeks old)

Sex	Genotype		WBC x10⁹	RBC x10¹²	Hb g/L	Hct L/L	MCV fL	MCH pg	MCHC g/L	RDW %	hypochrome %	platelet x10⁹	MPV fl	Reti 10⁻¹ %	Reti x10⁹	neutro %	neutro x10⁹	lympho %	lympho x10⁹	mono %	mono x10⁹	eosino %	eosino x10⁹	baso %	baso x10⁹	LUC %	LUC x10⁹
male	fl/fl; iCre	average	6.86	6.43	95	0.339	52.83	14.85	281.5	25.43	1.775	713.5	10.95	68.25	430.25	17	1.195	67.45	4.57	3.45	0.235	9.025	0.63	1.65	0.115	1.45	0.115
(n=4)		SD	2.61	0.77	10.89	0.03	1.58	0.17	5.07	1.43	0.92	44.49	0.19	16.40	58.79	1.96	0.55	4.11	1.63	1.80	0.19	1.26	0.27	0.06	0.04	0.88	0.07
male	fl/+; iCre	average	11.96	9.55	150.5	0.485	50.75	15.8	311.5	13.38	0.1	1153	9.325	42.75	406.4	17.25	2.075	78	9.31	2.2	0.265	2.1	0.26	0.1	0.005	0.4	0.05
(n=4)		SD	1.72	0.18	4.43	0.02	0.99	0.35	2.38	0.49	0.00	148.94	0.53	5.74	49.01	5.30	0.79	6.11	1.38	0.71	0.11	0.41	0.08	0.08	0.01	0.22	0.03
male	fl/fl	average	14.685	9.885	151.5	0.487	49.28	15.3	310.75	13.98	0.075	1135	9.325	44.5	432.4	7.3	1.06	87.98	12.97	2.55	0.335	1.675	0.25	0.075	0.015	0.375	0.06
(n=4)		SD	3.27	0.66	5.74	0.02	2.22	0.67	2.50	0.97	0.05	234.75	0.39	12.77	101.55	1.69	0.30	2.57	3.24	1.63	0.16	0.33	0.06	0.05	0.01	0.10	0.02
	fl/+; iCre vs fl/fl	T-test p value	0.103	0.195	0.396	0.429	0.145	0.124	0.340	0.164	0.196	0.451	0.500	0.407	0.333	0.014	0.039	0.020	0.053	0.357	0.251	0.079	0.426	0.312	0.104	0.421	0.325
	fl/fl; iCre vs fl/fl	T-test p value	0.005	0.000	0.000	0.000	0.022	0.137	0.000	0.000	0.017	0.017	0.001	0.032	0.486	0.000	0.343	0.000	0.004	0.243	0.227	0.000	0.031	0.000	0.005	0.046	0.113

Group B1 (Bone Marrow transplantation, data were collected at 5 weeks after transplantation)

sex	recipients	donar		WBC x10⁹	RBC x10¹²	Hb g/L	Hct L/L	MCV fL	MCH pg	MCHC g/L	RDW %	hypochrome %	platelet x10⁹	MPV fl	Reti 10⁻¹ %	Reti x10⁹	neutro %	neutro x10⁹	lympho %	lympho x10⁹	mono %	mono x10⁹	eosino %	eosino x10⁹	baso %	baso x10⁹	LUC %	LUC x10⁹
female	UBC-GFP;BL6	fl/fl; vav-iCre	Mean	5.3	4.0	60.0	0.2	51.3	14.9	288.7	29.2	1.5	473.3	8.8	68.0	276.1	11.5	0.6	70.1	3.7	4.6	0.2	11.2	0.6	2.1	0.133	0.5	0.0
(n=3)			SD	1.13	0.14	4.00	0.00	2.30	1.32	12.66	5.75	0.60	191.26	0.21	38.16	161.21	2.56	0.24	2.86	0.62	0.45	0.05	1.30	0.17	0.71	0.06	0.46	0.02
female	UBC-GFP;BL6	fl/+; vav- iCre	Mean	39.3	11.0	144.0	0.5	41.1	13.0	317.5	14.8	0.1	1486.0	7.5	38.0	417.0	8.0	3.2	88.8	34.9	1.0	0.4	1.7	0.6	0.1	0.0	0.4	0.2
(n=4)			SD	2.43	0.40	13.06	0.04	2.53	0.82	5.32	1.65	0.00	238.41	0.10	6.22	63.63	10.60	4.23	11.78	4.86	0.45	0.19	0.45	0.20	0.00	0.00	0.26	0.11
			T-test p value	0.000	0.000	0.000	0.000	0.002	0.060	0.023	0.021	0.028	0.001	0.001	0.153	0.133	0.279	0.158	0.023	0.000	0.000	0.080	0.002	0.395	0.019	0.059	0.449	0.027

Group B2 (Bone Marrow transplantation, data collected at 12 weeks after transplantation)

sex	recipients	donar		WBC x10⁹	RBC x10¹²	Hb g/L	Hct L/L	MCV fL	MCH pg	MCHC g/L	RDW %	hypochrome %	platelet x10⁹	MPV fl	Reti 10⁻¹ %	Reti x10⁹	neutro %	neutro x10⁹	lympho %	lympho x10⁹	mono %	mono x10⁹	eosino %	eosino x10⁹	baso %	baso x10⁹	LUC %	LUC x10⁹
female	BL6.CD45.1	fl/fl; vav-iCre	Mean	3.6	7.1	105.0	0.3	49.5	15.1	305.0	21.3	0.8	781.0	8.4	63.3	425.7	11.4	0.4	78.4	2.8	2.8	0.1	6.0	0.2	0.6	0.110	0.8	0.0
(n=4)			SD	0.78	1.35	17.40	0.05	2.84	0.45	9.13	3.91	0.73	62.43	0.63	24.10	112.63	2.55	0.09	3.20	0.67	0.69	0.05	1.14	0.03	0.49	0.19	0.46	0.02
female	BL6.CD45.1	fl/+; vav-iCre	Mean	15.7	11.2	160.0	0.5	42.6	14.3	335.0	13.5	0.1	1275.0	8.6	27.0	302.4	7.1	1.1	88.3	13.8	3.1	0.5	1.1	0.2	0.0	0.000	0.5	0.1
(n=4)			SD	2.06	0.30	4.62	0.01	0.48	0.25	6.73	1.02	0.00	11.49	0.28	2.58	25.22	2.08	0.43	2.53	1.74	3.33	0.47	0.50	0.09	0.05	0.00	0.14	0.03
			T-test p value	0.000	0.004	0.003	0.004	0.008	0.014	0.001	0.012	0.070	0.000	0.295	0.028	0.057	0.020	0.020	0.002	0.000	0.446	0.107	0.001	0.281	0.050	0.170	0.127	0.024

Group-C1 (Bone Marrow transplantation, data collected at 12 weeks after poly I:C treatment)

sex	recipients	donar		WBC x10⁹	RBC x10¹²	Hb g/L	Hct L/L	MCV fL	MCH pg	MCHC g/L	RDW %	hypochrome %	platelet x10⁹	MPV fl	Reti 10⁻¹ %	Reti x10⁹	neutro %	neutro x10⁹	lympho %	lympho x10⁹	mono %	mono x10⁹	eosino %	eosino x10⁹	baso %	baso x10⁹	LUC %	LUC x10⁹
female	UBC-GFP;BL6	Rhau fl/fl; MxCre	Mean	8.7	9.0	143	0.44	48.7	15.9	328	18.6	0.2	921	8.75	32.5	292	5.2	0.45	85.9	7.43	2.13	0.18	6.3	0.54	0.1	0	0.53	0.04
(n=4)			SD	0.70	0.68	11.94	0.02	1.44	0.10	9.33	2.19	0.06	168.96	0.54	3.87	43.39	1.83	0.19	3.42	0.55	0.33	0.02	2.09	0.19	0.00	0.00	0.10	0.03
female	UBC-GFP;BL6	Rhau fl/fl																									
(n=3)			Mean	22.9	11.1	150.7	0.45	41	13.7	334	14.1	0.1	1100	7.8	19.33	214	3.2	0.72	92.9	21.2	1.2	0.27	2.3	0.52	0.1	0.013	0.37	0.09
			SD	3.86	0.39	6.11	0.02	0.42	0.45	7.02	0.35	0.00	125.92	0.26	2.52	24.25	1.08	0.22	1.64	3.73	0.61	0.14	0.26	0.04	0.10	0.02	0.06	0.02
			T-test p value	0.011	0.002	0.162	0.127	0.000	0.006	0.160	0.012	0.091	0.085	0.016	0.001	0.016	0.070	0.084	0.009	0.011	0.050	0.199	0.015	0.426	0.500	0.211	0.022	0.026

Group-C2 (Bone Marrow transplantation, data collected at 12 weeks after poly I:C treatment)

sex	recipients	donar		WBC x10⁹	RBC x10¹²	Hb g/L	Hct L/L	MCV fL	MCH pg	MCHC g/L	RDW %	hypochrome %	platelet x10⁹	MPV fl	Reti 10⁻¹ %	Reti x10⁹	neutro %	neutro x10⁹	lympho %	lympho x10⁹	mono %	mono x10⁹	eosino %	eosino x10⁹	baso %	baso x10⁹	LUC %	LUC x10⁹
male	UBC-GFP;BL6	Rhau fl/fl; MxCre		6.4	9.0	129	0.40	45.2	14.5	320	16.9	0.1	930	8.73	40	358	5.3	0.35	83.5	5.32	5.75	0.37	4.8	0.31	0.15	0	0.5	0.03
(n=4)				0.6	0.7	6	0.01	2.274	0.545	7.438638	0.635	0.1	121	0.377	3.7417	30	1.5	0.09	0.4	0.5	1.794	0.128	1.5	0.11	0.1	0	0.141	0.02
male	UBC-GFP;BL6	Rhau fl/fl	Mean	17.0	10.6	148	0.44	41.3	13.9	336	13.9	0.1	1616	8.93	26.33	279	5.7	0.96	89.6	15.2	2.9	0.51	1.3	0.24	0.03	0.000	0.43	0.08
(n=3)			SD	2.22	0.08	4.00	0.01	0.40	0.20	2.65	0.35	0.00	502.33	0.25	3.21	36.71	2.16	0.35	1.76	1.97	0.96	0.23	0.44	0.11	0.06	0.00	0.06	0.00
			T-test p value	0.006	0.009	0.002	0.003	0.020	0.068	0.008	0.000	0.196	0.068	0.211	0.002	0.020	0.398	0.044	0.012	0.005	0.023	0.210	0.007	0.215	0.056	-	0.220	0.008

Group-C3 (Bone Marrow transplantation, data collected at 12 weeks after poly I:C treatment)

sex	recipients	donar		WBC x10⁹	RBC x10¹²	Hb g/L	Hct L/L	MCV fL	MCH pg	MCHC g/L	RDW %	hypochrome %	platelet x10⁹	MPV fl	Reti 10⁻¹ %	Reti x10⁹	neutro %	neutro x10⁹	lympho %	lympho x10⁹	mono %	mono x10⁹	eosino %	eosino x10⁹	baso %	baso x10⁹	LUC %	LUC x10⁹
female	BL6.CD45.1	Rhau fl/fl; MxCre	Mean	7.4	8.9	134	0.40	44.7	15.1	337	15.3	0.1	918	8.68	43.25	384	7.3	0.53	84.5	6.25	4.18	0.31	3.3	0.24	0.18	0.010	0.6	0.05
(n=4)			SD	1.1	1.0	9.5219	0.03	1.718	0.666	2.217356	1.5	0.1	155	0.35	9.3229	75	1.5	0.02	0.8	1.0	1.069	0.105	0.5	0.05	0.096	0.02	0.365	0.04
female	BL6.CD45.1	Rhau fl/fl	Mean	19.0	10.3	147.5	0.43	41.7	14.3	342	14.1	0.1	1298	7.8	26.75	278	5.4	1	91.4	17.3	1.2	0.23	1.6	0.31	0.05	0	0.35	0.06
(n=3)			SD	2.87	0.18	5.26	0.01	1.52	0.56	6.70	0.73	0.00	184.10	0.48	3.10	30.29	2.29	0.34	2.20	2.80	0.39	0.10	0.35	0.09	0.06	0.00	0.10	0.02
			T-test p value	0.001	0.032	0.030	0.066	0.020	0.063	0.118	0.098	0.196	0.010	0.014	0.016	0.030	0.117	0.034	0.002	0.001	0.004	0.143	0.001	0.116	0.038	0.196	0.134	0.296

Table 3.2 B


Group A vaviCre (Data were collected at 8 weeks old)
Group B1 (Bone Marrow transplantation, data were collected at 5 weeks after transplantation)
Group B2 (Bone Marrow transplantation, data collected at 12 weeks after transplantation)
Group-C1 (Bone Marrow transplantation, data collected at 12 weeks after poly I:C treatment)
Group-C2 (Bone Marrow transplantation, data collected at 12 weeks after poly I:C treatment)
Group-C3 (Bone Marrow transplantation, data collected at 12 weeks after poly I:C treatment)

Table 3.2. (A) Effects of RHAU ablation in the hematopoietic system on peripheral blood counts. Peripheral blood was collected by tail bleeding and characterized as described in Materials and Methods. Parameters obtained by this analysis are: white blood cell count (WBC), red blood cell count (RBC), hemoglobin (HB), hematocrit (Hct, ratio of blood occupied by RBC), mean corpuscular volume (MCV), mean corpuscular hemoglobin (MCH), mean corpuscular hemoglobin concentration (MCHC), red blood cell distribution width (RDW), mean platelet volume (MPV), reticulocyte count (RET), neutrophils (neutro), lymphocytes (lympho), monocytes (mono), eosinophils (eosino) and basophils (baso), large unstained cell (LUC). (A) Data of complete blood count. Group A: complete blood cell counts were analyzed from male $RHAU^{fl/fl}$, $RHAU^{fl/+}$; iCretg and $RHAU^{fl/fl}$; $iCre^{tg}$ mice at the age of eight weeks old. Group B1 and B2: Complete blood cell counts of UBC-GFP and B6.CD45.1 mice after five and twelve weeks of bone transplantation, in which the bone marrow was provided from either control $RHAU^{fl/+}$; iCretg mice or target $RHAU^{fl/fl}$; $iCre^{tg}$ mice.) Group C1 and C2: Complete blood counts of recipient UBC-GFP and BL6Ly5.1 mice after twelve weeks of polyI:C treatment. These mice received bone marrow cells isolated from control $RHAU^{fl/fl}$; $MxCre^{tg}$ mice or target $RHAU^{fl/fl}$; $MxCre^{tg}$ mice. Mice were treated with polyI:C after five weeks of bone marrow transplantation. The detail of bone marrow transplantation and polyI:C treatment was described in the Materials and Methods. Efficiency of RHAU knockout induced by polyI:C treatment wasf determined by genotyping of individual clone formed in colony forming assay. Results showed 98% and 47% of progenitors in bone marrow and spleen, respectively, were RHAU knockout. (B) Summary of blood counts. Red arrows show a significant decrease in RHAU-ablated mice compare to the control mice with t- test p value < 0.05. Blue arrows show a significant increase in RHAU-ablated mice compare to the control mice with t- test p value < 0.05. Dashed arrows show a decrease or increase of values in RHAU-ablated mice compare to the control mice with t- test $0.05 <$ p value < 0.09. Student-t test p value is shown at the bottom of each control group. The red values indicate that there are significant differences between the target groups and the control groups. SD indicates standard deviation. “n” for each subgroup is presented in first column of the table.

3.7 FACS analysis of different hematopoietic cell lineages in spleen, bone marrow and thymus

Unlike in humans, the spleen of adult mice continues to be an accessory hematopoietic organ although its role is limited largely to erythropoiesis and megakaryocytopoiesis (Slayton et al., 2002). In certain diseases that cause defects in hematopoiesis in the bone marrow of mammals including humans, extramedullary hematopoiesis in spleens may occur. Therefore, we analyzed cell populations in both spleen and bone marrow of control $RHAU^{fl/fl}$ and target $RHAU^{fl/fl}$; $iCre^{tg}$ mice.

3.7.1 Loss of RHAU leads to erythropoiesis defect

There are four major differentiation stages of erythroblasts that can be identified in hematopoietic organs: ProE, Ery.A, Ery. B and Ery.C. An examination of of these erythroblasts (Figure 3.6) in the bone marrow RHAU-ablated mice showed dramatic increases in ProE from 1.8 to 10.9% and in Ery.A from 24.3 to 41.7% (Figure 3.6B). In contrast, Ery.B and Ery. C decreased from 25.4 to 13.6% and from 48.5 to 33.6%, respectively (Figure 3.6A). In the spleen, ProE increased markedly from 0.7 to 11.8% and Ery.A from 6.7 to 22.9%. The proportion of Ery. B did not change and Ery. C decreased from 84.7 to 54.9% (Figure 3.5A). In terms of total numbers of erythroblasts, a marked difference in the response to RHAU ablation was found between the two organs (Figure 3.6C). Since it would also be interesting to see whether RHAU ablation affects the total number of erythroblasts, we calculated the total cell number of each population. By multiplying the cell numbers by the percentages of particular cell types determined by FACS, we obtained the absolute numbers per organ. In bone marrow, total erythroblasts decreased by 37%, in which Pro.E increased and Ery.B and Ery.C decreased significantly. In contrast, total erythroblasts in the spleen increased dramatically 4.7-fold, with all subgroups contributing to the increase.

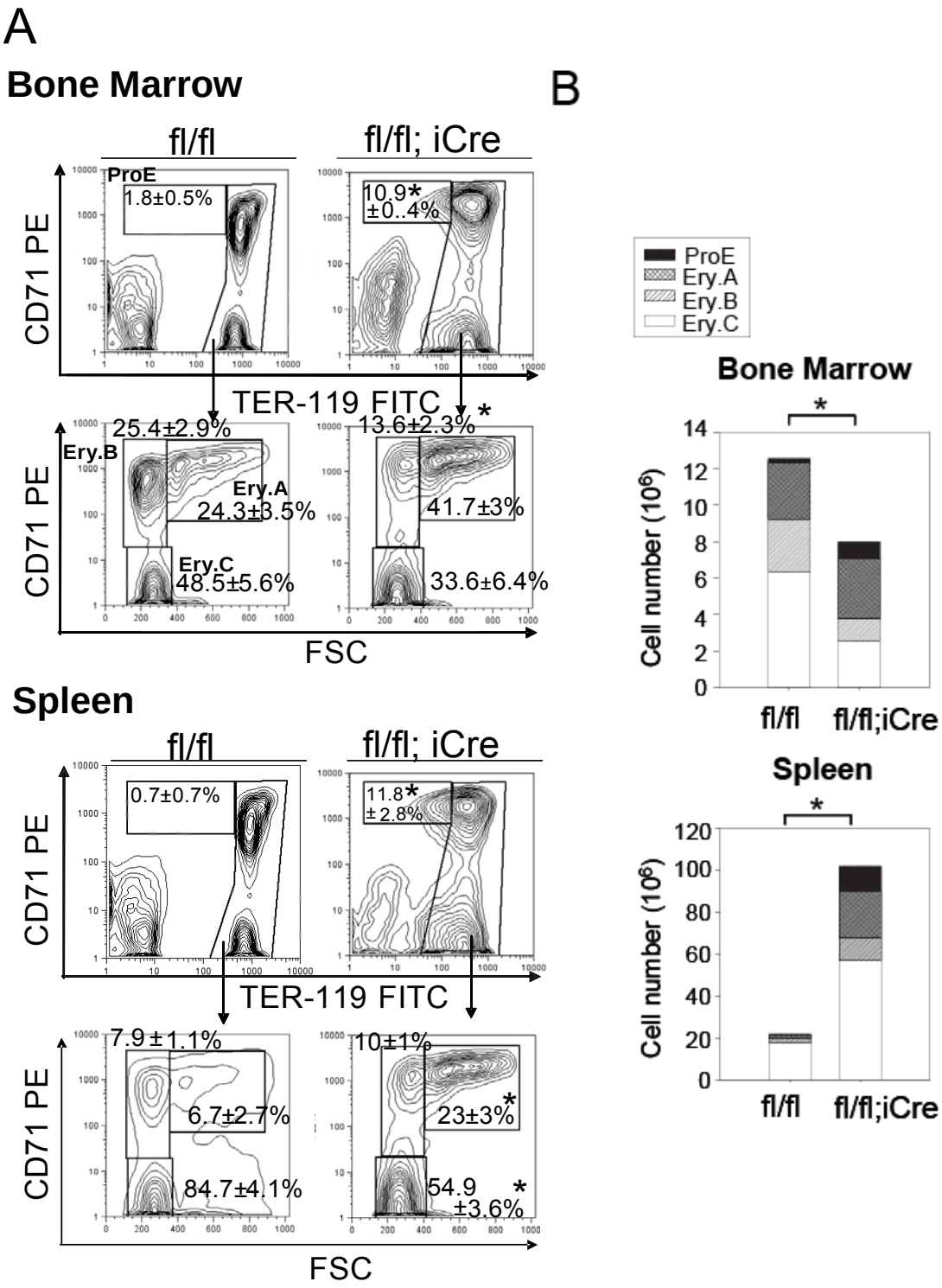

Figure 3.6. Differential effects of RHAU ablation on erythroid cell differentiation in the bone marrow and spleen. (A) Effect of RHAU ablation on the distribution of four stages of erythroblasts. The different stages were identified in FACS by probing Ter-119 and CD71 together with a forward scatter (FSC) parameter (Liu et al., 2006). All Ter119-positive cells are classified into four subgroups: ProE (Ter119med CD71hi), Ery.A (Ter119hiCD71hiFSChi), Ery.B (Ter119hiCD71hiFSClow) and Ery.C (Ter119hiCD71lowFSClow). The mean proportions of each subgroup with standard errors (n=4) are shown at the top of the boxes in dot plot graphs. (B) Effect of RHAU ablation on total numbers of erythroid cells in bone marrow and spleen. Cell numbers of the four subgroups were also calculated based on their percentages and are indicated in the bars by different shades that denote, from the top, Pro.E, Ery.A, Ery.B and Ery.C. *$p<0.05$, n=4.

3.7.2 Loss of RHAU leads to changes in granulocyte and lymphoid cell numbers

Monocytes and neutrophils can be distinguished with two markers, Mac-1 and Gr-1 (Lagasse and Weissman, 1996). As shown in Figure 3.7, monocytes were more abundant in both bone marrow and spleen of RHAU-ablated mice than in wild-type mice, while neutrophils were less abundant. When total cell number in each organ was considered, monocytes appeared to have declined in the bone marrow but increased in the spleen (Figure 4A, lower panel). Total cell number neutrophils were decreased in both organs (Figure 3.7A).

Lymphoid cells include natural killer (NK) cells, B cells and T cells. The percentage of DX5+ NK cells was not affected by RHAU ablation either in the bone marrow or the spleen (Figure 3.7B). However, the total number of NK cells was strongly reduced in bone marrow and slightly increased in spleen of RHAU-ablated mice (Figure 3.7B, bottom panel).

B cell maturation proceeds in the bone marrow from the very early Pro-B cell to immature B cells. Immature B cells enter the peripheral circulation, seed in the spleen and undergo further differentiation (Matthias and Rolink, 2005). CD19 is a marker that is expressed on all B stages cells from early Pro-B cells. Loss of RHAU strongly reduced the fraction of CD19+ cells in both bone marrow and spleen (Figure 3.7C, dot plots). Despite the splenomegaly in RHAU-ablated mice, the total number of B-cells in the spleen of these mice was still much lower than in control spleens, suggesting that not all cell types were increased to the same degree of splenomegaly (Figure 3.7C, lower panels).

Progenitors of T cells leave the bone marrow and migrate to thymus for T cell differentiation. T cell maturation in the thymus proceeds from double negative cells (DN, CD3-CD4-CD8-) to immature single positive cells (ISP, CD3-CD4-CD8+), then to double positive cells (DP, CD3+CD4+CD8+), and finally to either single CD4+ (CD3+ CD4+CD8-) or single CD8+ cells (CD3+CD4-CD8+)(Ceredig and Rolink, 2002; MacDonald et al., 1988). Different differentiation stages of T cells in the mice were analyzed with CD3, CD4 and CD8 markers. The percentages of ISP8 and DN cells were elevated in the thymus of RHAU-ablated mice (Figure 3.7D, dot plots). However, the percentage of mature SP cells did not change (Figure 3.7D, histograms). When we compare the absolute number of thymocytes in RHAU-ablated mice to control mice, we found that there were less DN cells, no change in ISP8 cells and finally less SPCD4+ and SPCD8+ cells. Furthermore, we also found that the majority of ISP8 cells from RHAU-ablated mice were CD3low. Thus, progression from the ISP8 stage to the mature SP stage appears to be retarded when RHAU was removed.

A

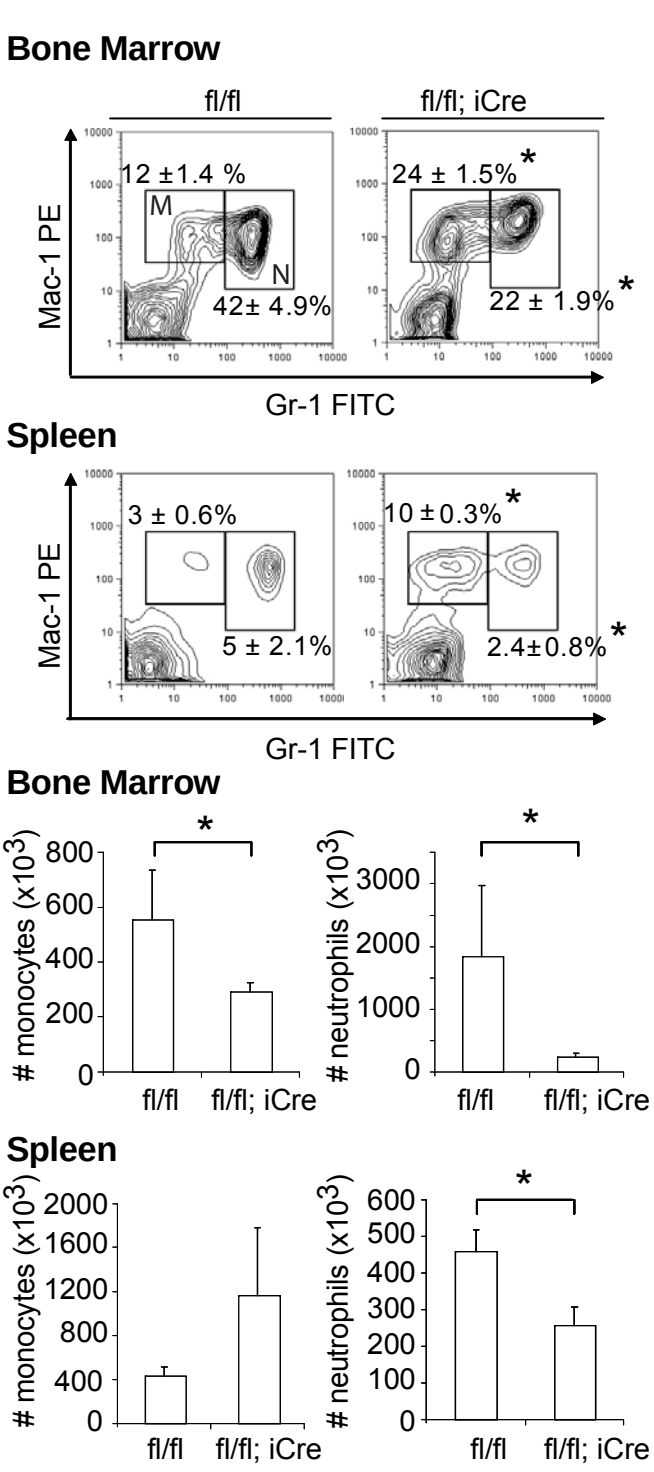
Bone Marrow
fl/fl
fl/fl; iCre
12 ±1.4 %
M
N
42± 4.9%
24 ± 1.5%*
22 ± 1.9%*
Mac-1 PE
Gr-1 FITC
Spleen
3 ± 0.6%
5 ± 2.1%
10 ± 0.3%*
2.4±0.8%*
Mac-1 PE
Gr-1 FITC
Bone Marrow
monocytes (x10^3)
800
600
400
200
0
fl/fl
fl/fl; iCre
*
neutrophils (x10^3)
3000
2000
1000
0
fl/fl
fl/fl; iCre
*
Spleen
monocytes (x10^3)
2000
1600
1200
800
400
0
fl/fl
fl/fl; iCre
neutrophils (x10^3)
600
500
400
300
200
100
0
fl/fl
fl/fl; iCre
*

B

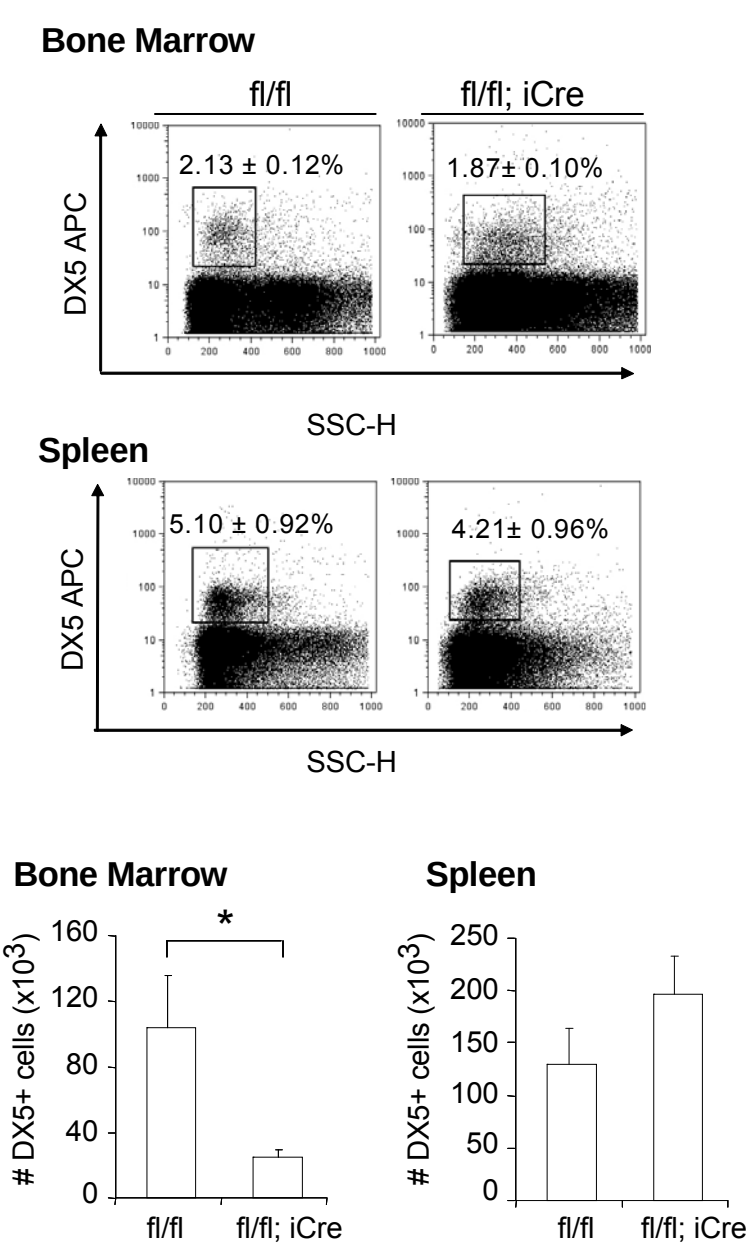
Bone Marrow
fl/fl
fl/fl; iCre
2.13 ± 0.12%
1.87± 0.10%
DX5 APC
SSC-H
Spleen
5.10 ± 0.92%
4.21± 0.96%
DX5 APC
SSC-H

Bone Marrow
*
DX5+ cells (x10^3)
160
120
80
40
0
fl/fl
fl/fl; iCre
Spleen
DX5+ cells (x10^3)
250
200
150
100
50
0
fl/fl
fl/fl; iCre

C

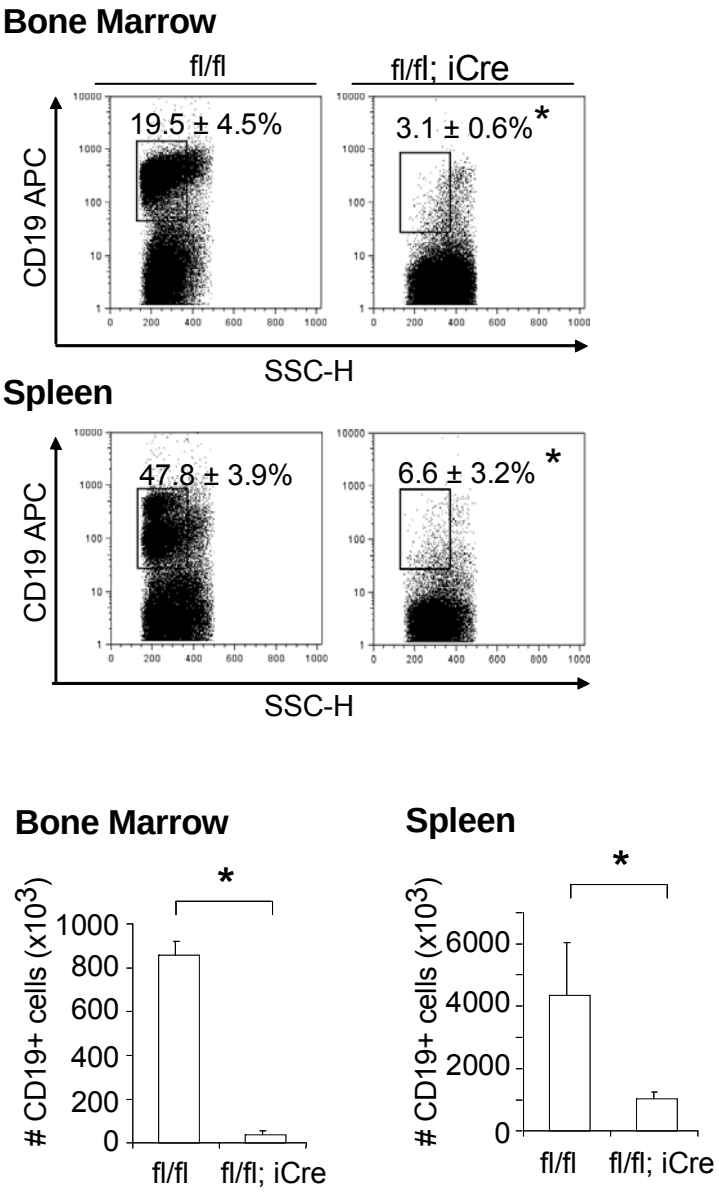
Bone Marrow
fl/fl
fl/fl; iCre
19.5 ± 4.5%
3.1 ± 0.6%*
CD19 APC
SSC-H
Spleen
47.8 ± 3.9%
6.6 ± 3.2%*
CD19 APC
SSC-H
Bone Marrow
CD19+ cells (x10^3)
1000
800
600
400
200
0
*
fl/fl
fl/fl; iCre
Spleen
CD19+ cells (x10^3)
6000
4000
2000
0
*
fl/fl
fl/fl; iCre

D

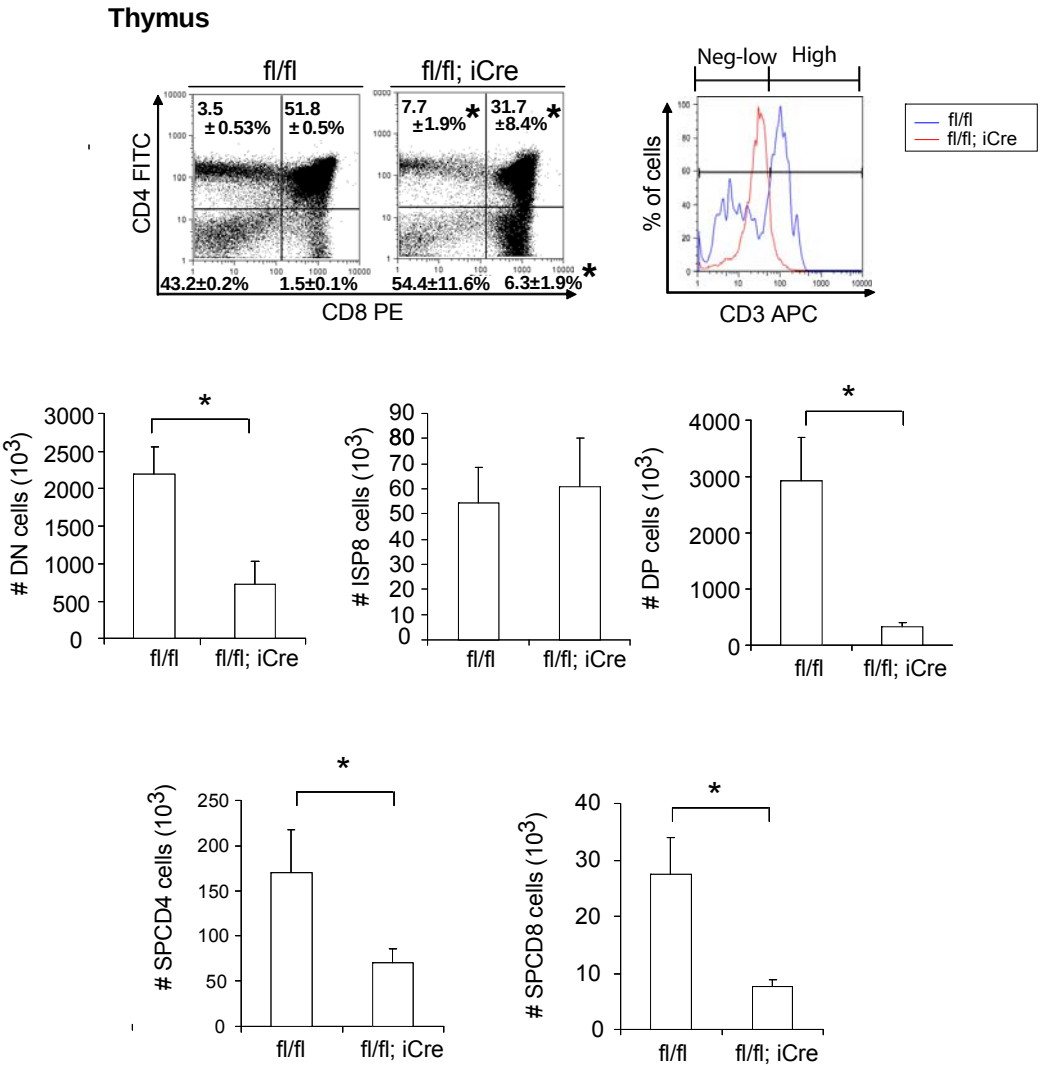

Figure 3.7. Organ-specific effects of RHAU ablation on different hematopoietic cell lineages. (A) Effect of RHAU ablation on monocytes and neutrophils. Monocytes and neutrophils were identified as Gr-1-/lowMac-1high (left area) and Gr-1highMac-1high (right area), respectively. The mean percentages with standard errors (n=4) are shown at the top of the boxes in dot plot graphs. The bar charts below show the absolute numbers of monocytes and neurtophils recovered from the mice. *P<0.05, n=4. (B) Effect of RHAU ablation on NK cells. NK cells were identified as low side-scattering and DX5+ cells. The mean percentages with standard errors (n=5 for bone marrow; n=4 for spleen) are shown at the top of the boxes in dot plot graphs. The bar charts show the absolute number of NK cells. *P<0.05, n=4. (C) Effect of RHAU ablation on B cells. B cells were identified by low SSC-H and CD19+ cells. The mean percentages with standard errors (n=4) are shown at the top of the boxes in dot plot graphs. The bar charts below show the absolute number of B cells. *P<0.05; n=4. (D) Effect of RHAU ablation on T cells. T-cell progenitors at different stages of differentiation were first monitored by CD4 and CD8 expressions. The means proportions percentages with standard errors (n=4) are shown in corresponding sections of dot plot graphs. Single CD8+ cells were further characterized for CD3 expression to distinguish between immature (ISP8) and mature single CD8+ cells (histogram). The bar charts show absolute numbers of different T-cell progenitors. *P<0.05, n=4.

3.7.3 Characterization of hematopoietic progenitors in RHAU-ablation mice showed a shift of progenitor and stem cell populations

Previous FACS analysis showed that loss of RHAU led to differentiation defects in both myeloid and lymphoid lineages. We speculated that RHAU ablation affected differentiation at its early stage before cells committed to any specific lineage. By FACS analysis, we examined whether RHAU ablation affected progenitor cells, including megakaryocyte/erythroid progenitor (MEP), granulocyte/macrophage progenitor (GMP), common myeloid progenitor (CMP), common lymphoid progenitor (CLP), lymphoid primed multipotent progenitor (LMPP), short-term repopulating HSC (ST-HSC) and long-term repopulating HSC (LT-HSC). Of these, we first examined the CMP, GMP, MEP and CLP cell populations. CMP, GMP and MEP were examined simultaneously. RHAU ablation significantly enhanced the MEP fraction but reduced GMP and CMP cells, both in bone marrow and spleen (Figure 3.8A). However, RHAU ablation had no effect on total CMP cell number either in bone marrow or spleen, but significantly decreased GMP cell number in bone marrow and increased MEP cell number in spleen (Figure 3.8C). Interestingly, RHAU ablation led to elevated levels of CLPs in percentage as well as in total cell number (Figure 3.8B, C).

The LT-HSC, ST-HSC and LMPP populations were examined simultaneously. As shown in Figure 3.8D, the percentage of LT-HSC cells increased in response to RHAU ablation whereas that of ST-HSC and LMPP cells decreased. In terms of absolute cell number, both LT-HSC and ST-HSC cells increased and LMPP did not change (Figure 3.8D). In RHAU-ablated bone marrow, LT-HSC cell numbers were elevated 5.8-fold. The elevation of ST-HSC cells, which are derived from LT-HSC, was only 2.8-fold and, finally, the elevation of downstream MEP and LMPP cells was negligible (Figure 3.8E).

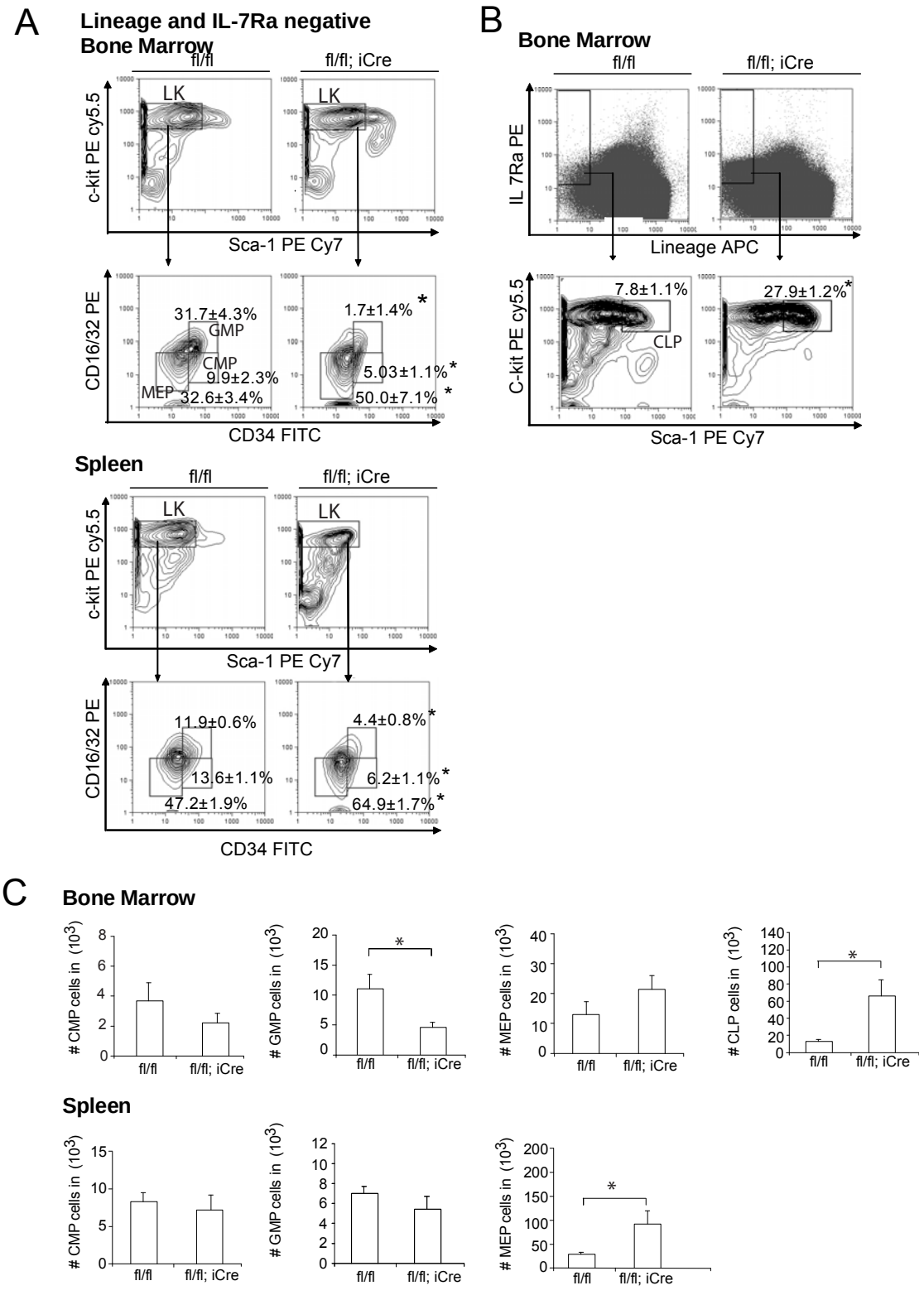
A
Lineage and IL-7Ra negative
Bone Marrow
fl/fl
fl/fl; iCre
LK
c-kit PE cy5.5
Sca-1 PE Cy7
CD16/32 PE
31.7±4.3%
GMP
CMP
9.9±2.3%
MEP
32.6±3.4%
1.7±1.4%
5.03±1.1%
50.0±7.1%
CD34 FITC
Spleen
11.9±0.6%
13.6±1.1%
47.2±1.9%
4.4±0.8%
6.2±1.1%
64.9±1.7%
B
Bone Marrow
IL 7Ra PE
Lineage APC
C-kit PE cy5.5
7.8±1.1%
CLP
27.9±1.2%
Sca-1 PE Cy7
C
Bone Marrow
CMP cells in (10^3)
GMP cells in (10^3)
MEP cells in (10^3)
CLP cells in (10^3)
Spleen

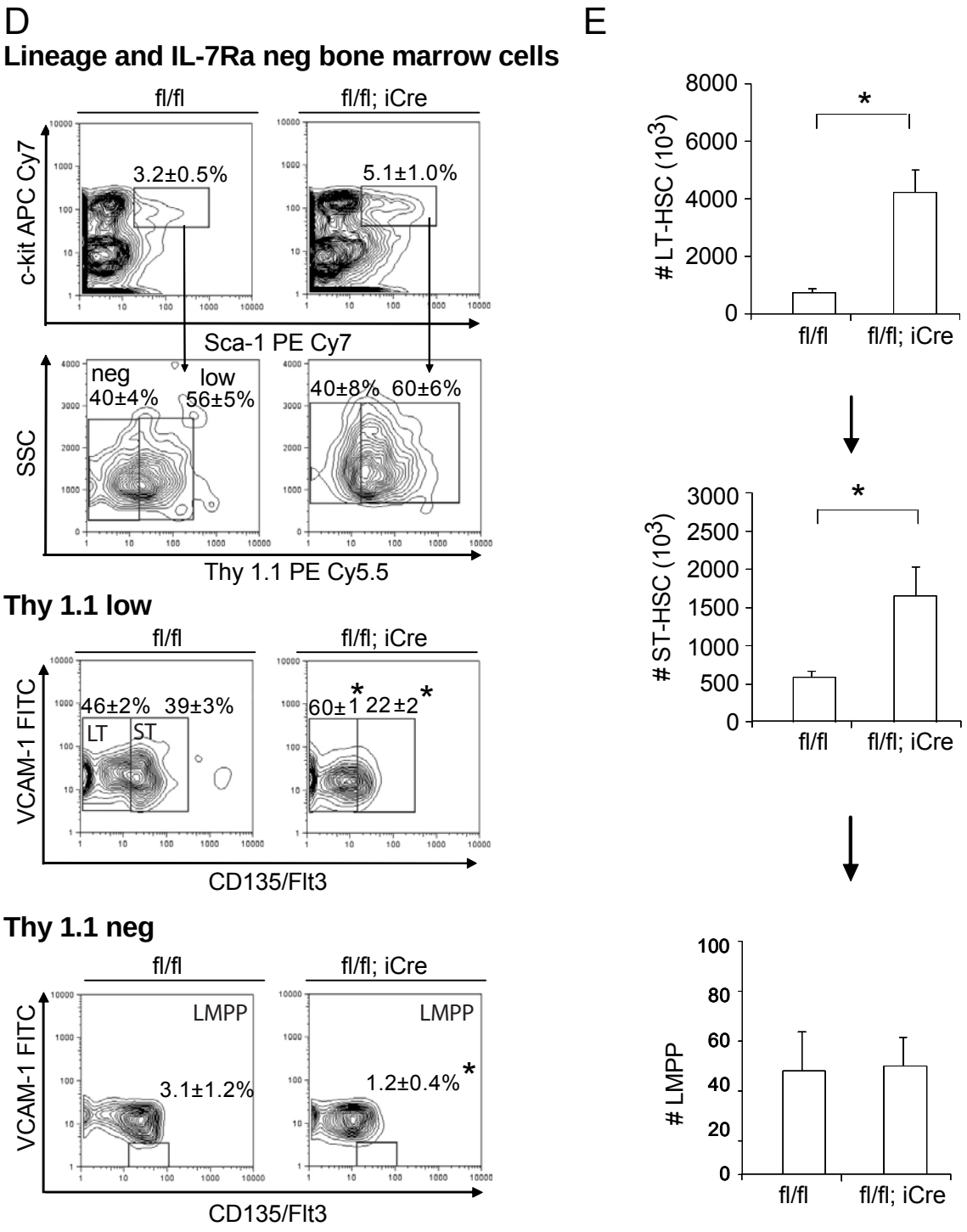

Figure 3.8. Effects of RHAU ablation on progenitors and stem cells. (A) FACS analysis of MEP, GMP and CMP cells in bone marrow and spleen. The lineage-negative, CD127Ra-negative living cells were gated and analyzed for c-kit positive and Sca-1 negative populations (LK). The LK subgroup was further gated for CD34 and CD16/32 (FcγR). CMP, GMP and MEP were were identified as FcγRlowCD34+, FcγRhighCD34+ and FcγRlowCD34-, respectively. The mean proportions of CMP, GMP and MEP cells with standard errors are indicated in the graphs. * P<0.05, n = 6. (B) FACS analysis of CLP cells in bone marrow and spleen. Cells were first gated for lineage-negative and CD127Ra positive living cells. This population was further probed for f c-kit and Sca-1. CLP cells were defined as C-kit+Sca-1+ double-positive populations. The mean proportions of CLP cells with standard errors are indicated in the graphs. *P<0.05, n

= 6. (C) Absolute numbers of progenitor cells in bone marrow and spleen. * P<0.05, n=6. (D) FACS analysis of LT-HST, ST-HST and LMPP cells in bone marrow. Lineage negative bone marrow cells were first gated to obtain IL-7Ra-Sca-1+c-Kit+ cells, which were further gated into two populations Thy1.1low (Thy1.1+) and Thy1.1neg (Thy1.1-) (upper panel). These were further probed for VCAM-1 and Flt3 (CD135) expression (lower panel). LT-HSC, ST-HSC and LMPP were defined as Thy1.1+ VCAM-1+ Flt3-, Thy1.1+ VCAM-1+ Flt3+ and Thy1.1-VCAM-1-Flt3+, respectively. The mean proportions of different populations with standard errors are indicated in the graphs. *P<0.05, n=6. (E) Effect of RHAU ablation on the numbers of stem cells. The mean numbers of each cell type with standard errors are shown as bar charts. *P<0.05, n=6.

3.7.4 Loss of RHAU leads to progressive reduction of population expansion ability in hematopoietic stem cells and erythroblasts

When we were calculating the absolute numbers of LT-HSCs, ST-HSCs and LMPPs, we found that there was a progressive decrease in the ratio of cell number in RHAU-ablated mice over that in control mice through differentiation (Figure 3.9A). It suggests that RHAU ablation suppresses population expansion and reduces differentiation potential of hematopoietic stem cells.

We also observed a similar tendency in the erythrocyte differentiation in bone marrow and spleen. MEPs have the potential to differentiate into either megakaryocytes or erythrocytes. Once MEPs have differentiated to ProEs they are fully committed to the erythrocytic lineage. When RHAU was knockout, MEPs in bone marrow did not change in number significantly and increased by 3.2-fold in spleen. ProE cells increased in number 3.6- and 74-fold in bone marrow and spleen, respectively. Elevation of the numbers of the subsequent Ery.A cells declined to 1.1- and 14-fold in bone marrow and spleen, respectively. Finally, changes in Ery.B and Ery.C cells were 0.4-fold in bone marrow and 5.7- and 3.2-fold, respectively, in the spleen (Figure 3.9B). Although the Ery.C number increased in the RHAU-ablated spleen and decreased in the RHAU-ablated bone marrows, the progressive reduction in population expansion ability was consistent in the two organs.

To confirm that decrease in population expansion and differentiation potential of hematopoietic stem cells were caused by RHAU ablation in these cells, we performed competitive bone marrow transplantation experiments. Lethally irradiated BL6.CD45.1 mice were used as recipients and transplanted with mixtures of bone marrow cells. The cell mixtures were either composed of (i) UBC-GFP and RHAUfl/fl in a 1 to 10 ratio, or (ii) UBC-GFP and $RHAU^{fl/fl}$; $MxCre^{tg}$ in a 1 to 10 ratio. The mice were then divided into three groups. In Group 1, three recipient mice were transplanted with UBC-GFP and $RHAU^{fl/fl}$ cells. In Group 2, four recipient mice were transplanted with UBC-GFP and $RHAU^{fl/fl}$; $MxCre^{tg}$ cells. In Group 3, four recipient mice were transplanted with UBC-GFP and $RHAU^{fl/fl}$; $MxCre^{tg}$ cells. Mice from group 1 and 2 were treated with polyI:C after five weeks of transplantation (described in Materials and Methods) and group 3 were not treated. We used anti-CD45.1 and anti-CD45.2 to distinguish between leukocyte sources: recipients and donors. The UBC-GFP donor cells were positive for GFP expression. CD45.2+GFP- leukocytes were

considered to be derived from $RHAU^{fl/fl}$ or $RHAU^{fl/fl}$; $MxCre^{tg}$ donors. Before polyI:C treatment, there were 90.7%, 90.3% and 91.3% CD45.2+ leukocytes in Group 1, 2 and 3, respectively. This indicates that the majority of cells were derived from donors. Amongst CD45.2+ leukocytes, 88.7%, 80.7% and 84.0% of them were GFP- in Group 1, 2 and 3, respectively (Figure 3.9C, Leukocytes, time=0). By treating the mice with polyI:C, RHAU was ablated in the hematopoietic cells of the genotype $RHAU^{fl/fl}$; $MxCre^{tg}$ (Group 2). The ratio CD45.2+GFP- cells over total CD45.2+ cells [CD45.2+GFP- / (CD45.2+GFP- + CD45.2+GFP+)] was monitored after one week of polyI:C treatment. The changes of the ratio were recorded every two weeks. As expected, only Group 2 RHAU-ablated hematopoietic cells showed progressive reduction in population (Figure 3.9C). The reduction became significant after three weeks of the treatment. The reduction of leukocytes in RHAU-ablated conditions could be explained by depletion of B cells because there was a dramatic decrease of B cells in the $RHAU^{fl/fl}$; $iCre^{tg}$ mice. On the other hand, the reduction of erythrocytes was faster than leukocytes and reached the steady state after seven weeks of the treatment. This was due to the shorter half lives of erythrocytes compare to leukocytes. These results suggest that GFP+ leukocytes and erythrocytes out-grow RHAU-ablated cells (Group 2: $RHAU^{fl/fl}$; $MxCre^{tg}$ + polyI:C) but not RHAU-expressing cells ($RHAU^{fl/fl}$ + polyI:C or $RHAU^{fl/fl}$;$MxCre^{tg}$ without polyI:C). These results support the idea that the decrease in population expansion and differentiation potential was caused specifically by RHAU-ablation and was cell autonomous.

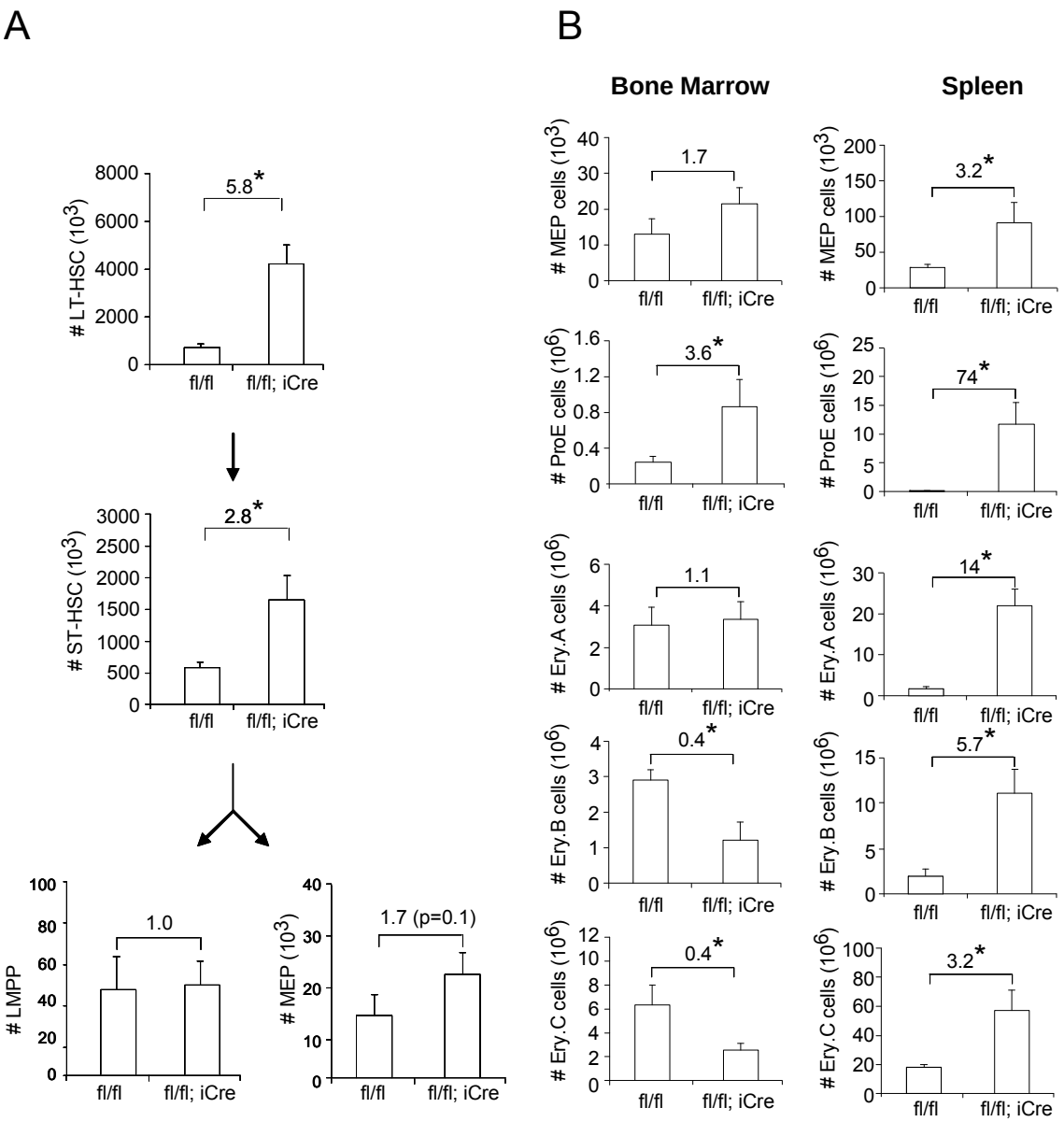
A
B
Bone Marrow
Spleen
LT-HSC (10^3)
5.8*
ST-HSC (10^3)
2.8*
LMPP
1.0
MEP (10^3)
1.7 (p=0.1)
MEP cells (10^3)
1.7
3.2*
ProE cells (10^6)
3.6*
74*
Ery.A cells (10^6)
1.1
14*
Ery.B cells (10^6)
0.4*
5.7*
Ery.C cells (10^6)
0.4*
3.2*
fl/fl
fl/fl; iCre

C

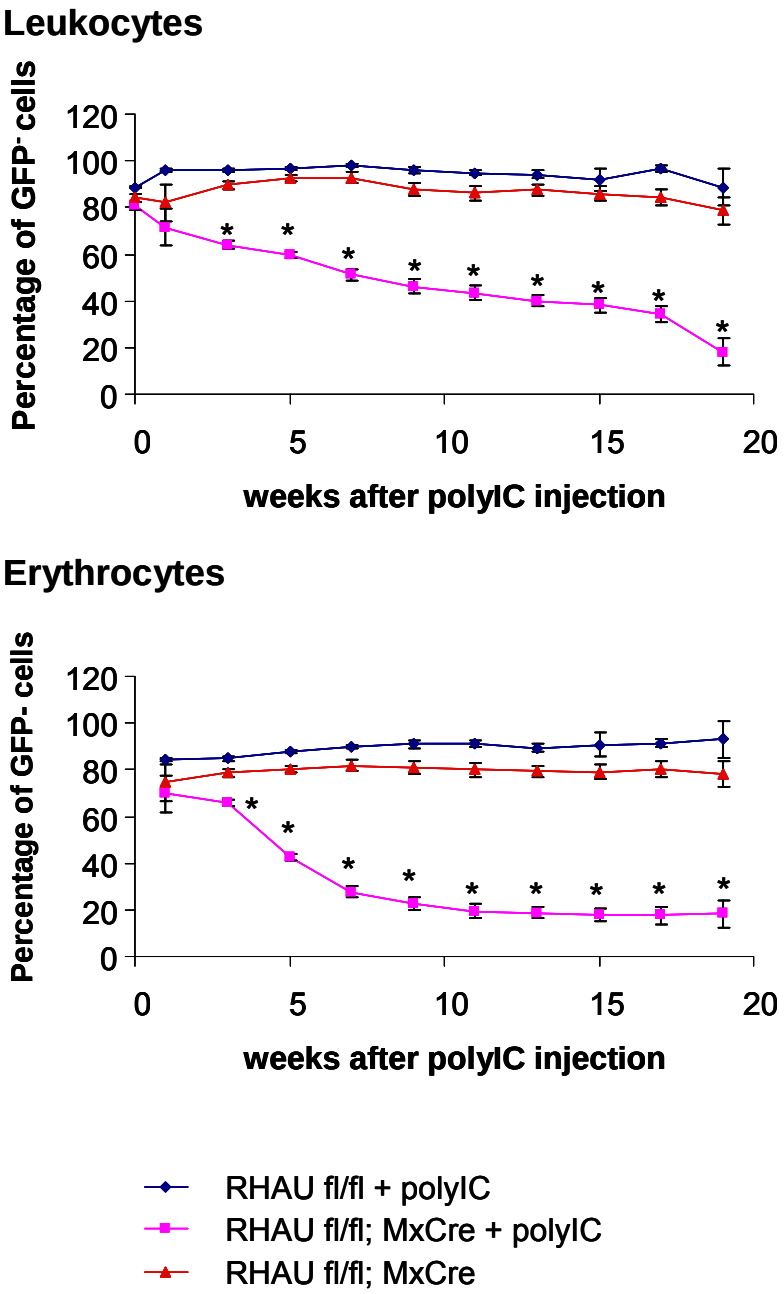

Figure 3.9. Loss of RHAU leads to progressive reduction of population expansion ability in the hematopoietic cells. (A) Effect of RHAU ablation on the number of stem cells. The mean numbers of different cell types with standard errors are shown as bar charts. The number at the top of two bars in each graph indicates the fold change after RHAU ablation. Arrows indicate the path of early hematopoiesis. *P<0.05, n=6. The numbers of stem cells presented in this figure are the same as those presented in Figure 3.9E. (B)The numbers of MEP, ProE, Ery.A, Ery.B and Ery.C cells in bone marrow (left panel) and spleen (right panel) are shown. The number at the top of two bars in each graph indicates the fold increase after RHAU ablation. The order of cell differentiation in the erythrocytic lineage is MEP → ProE → Ery.A → Ery.B → Ery.C. *P<0.05; n=6 for MEP and n=4 for other cell types. (C) Progressive reduction of RHAU-ablated hematopoietic cells in population expansion ability was demonstrated in competitive repopulation assay. Two different combinations of bone marrow cells, (i) UBC-GFP and $RHAU^{fl/fl}$ in a 1 to 10 ratio and (ii) UBC-GFP and $RHAU^{fl/fl}$; $MxCre^{tg}$ in a 1 to 10 ratio, were transplanted into three and eight BL6.CD45.1 mice, respectively. The mice were divided into three groups. Group 1, recipient mice were transplanted with UBC-GFP and $RHAU^{fl/fl}$ cells (n=3) Group 2, recipient mice were transplanted with UBC-GFP and $RHAU^{fl/fl}$; $MxCre^{tg}$ cells (n=4). Group 3, recipient mice were transplanted with UBC-GFP and $RHAU^{fl/fl}$; $MxCre^{tg}$ cells

(n=4). Mice from Groups 1 and 2 were treated with polyI:C after five weeks of bone marrow transplantation (described in Materials and Methods) and Group 3 were not treated with polyI:C. *P<0.05

3.7.5 In vitro colony forming assay

FACS analysis showed changes in cell number distribution among monocytes, neutriphils and erythroblasts. In vitro colony forming assay supported our observation. Equal number of bone marrow cells and splenocytes isolated from either $RHAU^{fl/fl}$ or $RHAU^{fl/fl}$; $iCre^{tg}$ mice were plated in 1 mL MethoCult® Methylcellulose-Based Medium in 35 mm dish. Colonies were counted after twelve days. The number of colonies formed can reflect the differentiation potential of the precursor cells. When RHAU was ablated, the BFU-E count deceased in bone marrow culture but increased in splenocyte culture. This result corroborates the result of FACS analysis that the erythroblast numbers were decreased in the bone marrow but increased in the spleen. At the same time, CFU-M, CFU-GM and CFU-GEMM cells were increased in splenocyte cultures (Figure 3.10). CFU-GEMM cells are derived from the progenitors that have potential to differentiate into erythrocytes, megakaryocyte, monocyte and granulocyte. CFU-GM cells are derived from more lineage committed progenitors that can differentiate into granulocyte and monocytes. CFU-G and CFU-M derived from the progenitors that can differentiate into granulocytes and monocytes, respectively. The differentiation pathway can be expressed as CFU-GEMM → CFU-GM→ CFU-G or CFU-M. Since there was no change of CFU-G counts but increase of CFU-M counts, it is concluded that RHAU ablation enhanced differentiation potential of monocytes in the spleen. Also, CFU-M counts increased in bone marrow cell culture. These results support the FACS data that monocytes percentage was increased in the bone marrow and the spleen.

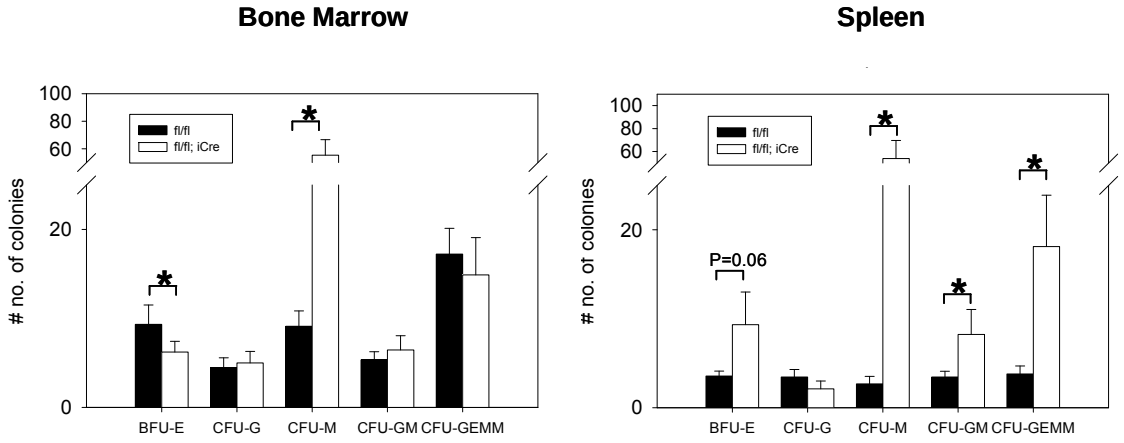

.
Figure 10. Loss of RHAU resulted in higher CFU-M counts both in the bone marrow and spleen, higher BFU-E, CFU-GM and CFU-GEMM counts in the spleen and lower BFU-E count in the bone marrow. Unfractionated $2x10^4$ cells bone marrow or 10^5 splenocytes excluding the red cells were plated in 1mL methylcellulose-base media supplied. Colonies were counts after 12 days of seedling. This figure is a representative result, *p< 0.05, student's t-test, n = 3, experiment was repeated in triplicates and similar results were obtained.

From complete blood counting and FACS analysis, it was found that the loss of RHAU led to decreased differentiation potential of the erythrocyteand lymphoid cell lineages but to increased differentiation potential of the monocyte lineage. Next, we further characterized the anemic phenotype of $RHAU^{fl/fl}$; $iCre^{tg}$ mice.

3.7.6 Quantization of plasma concentrations of erythropoietin

Since RHAU-ablated mice were anemic, we wanted to know whether the animals produced appropriate amount of erythropoietin to respond to anemia. As shown in Fig. 3.11, $RHAU^{fl/fl}$; $iCre^{tg}$ mice showed 800 times higher erythropoietin concentration in blood than $RHAU^{fl/fl}$ control mice (Figure 3.11). This implies that $RHAU^{fl/fl}$; $iCre^{tg}$ mice responded to anemia by enhancing erythropoietin levels in blood in order to promote erythrocytosis. According to the results of complete blood counting, RHAU-ablated mice developed reticulocytosis. This indicates that RHAU-ablated mice responded to enhanced Epo.

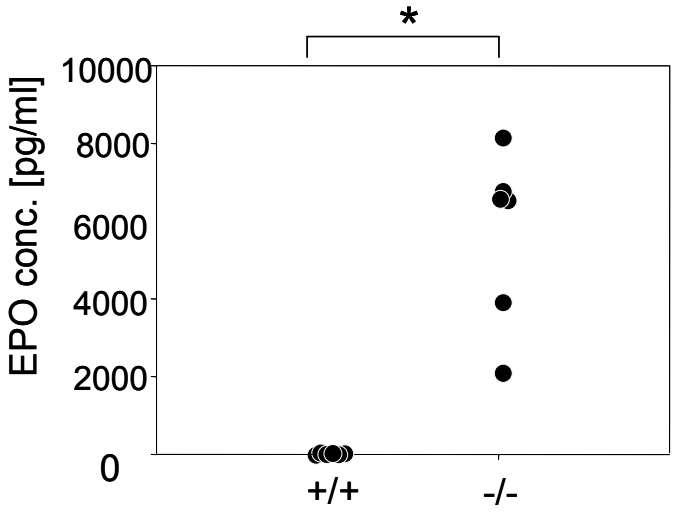

Figure 3.11 Increased erythropoietin level in blood plasma of $RHAU^{fl/fl}$; $iCre^{tg}$ mice. *$p<0.05$, n=6 for each group.

3.7.7 Blood smear examination showed spherocytosis in the RHAU$^{fl/fl}$; iCre^{tg} mice

Spherocytes could be detected in the blood of RHAU$^{fl/fl}$; iCre^{tg} mice suggesting the possibility of hemolytic anemia (Figure 3.12).

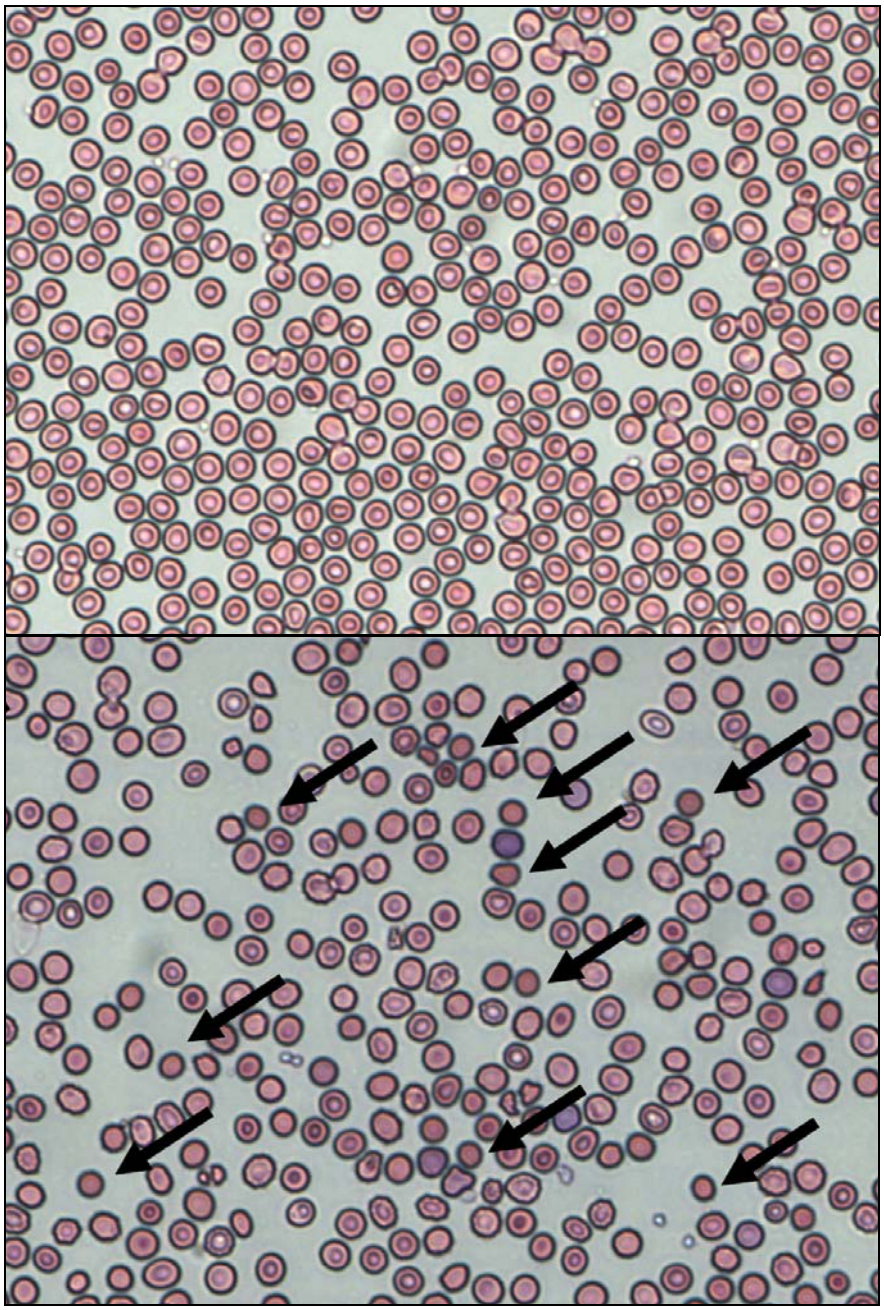

Figure 3.12 Blood smear examination showed spherocytes were present (pointed with arrows) in RHAU$^{fl/fl}$; iCre^{tg} mice. *Top*. RHAU$^{fl/fl}$. *Bottom*. RHAU$^{fl/fl}$ iCre^{tg}

3.7.8 Determination of the osmotic resistance

Since the blood smear test showed that the mice might have developed hemolytic anemia through genetic defects of some skeleton membrane protein, we tested the fragility of the erythrocytes. We placed the blood cells of these mice in aqueous solutions of different NaCl concentrations ranging from 0% (pure water) to 1% w/v. All erythrocytes are disrupted in pure water and we set this as the reference point. The calculation of percentages of disrupted cells was described in the Materials and Methods. Surprisingly, between 0.35 and 0.65% w/v of NaCl, more $RHAU^{fl/fl}$ erythrocytes were disrupted than $RHAU^{fl/fl}$; $iCre^{tg}$ erythrocytes. The osmotic resistance curve of $RHAU^{fl/fl}$; $iCre^{tg}$ erythrocytes shifted to the left of the curve of $RHAU^{fl/fl}$ control erythrocytes (Figure 3.11A). This implies that erythrocytes of $RHAU^{fl/fl}$; $iCre^{tg}$ mice are more resistant to osmotic shock compared to control erythrocytes. Since there were more reticulocytes present in the blood of $RHAU^{fl/fl}$; $iCre^{tg}$ than $RHAU^{fl/fl}$ mice, which might have interfered with the sensitivity of the cells to low osmolarity, we isolated mature erythrocytes excluding cells that carried nucleic acid by cell sorting (Materials and Methods). Consistently, the erythrocytes from $RHAU^{fl/fl}$; $iCre^{tg}$ mice showed higher osmotic resistance at 0.55% of NaCl (Figure 3.11B) in both sorted and unsorted cells, indicating that erythrocytes from $RHAU^{fl/fl}$; $iCre^{tg}$ mice were indeed more resistant to low osmolarity.

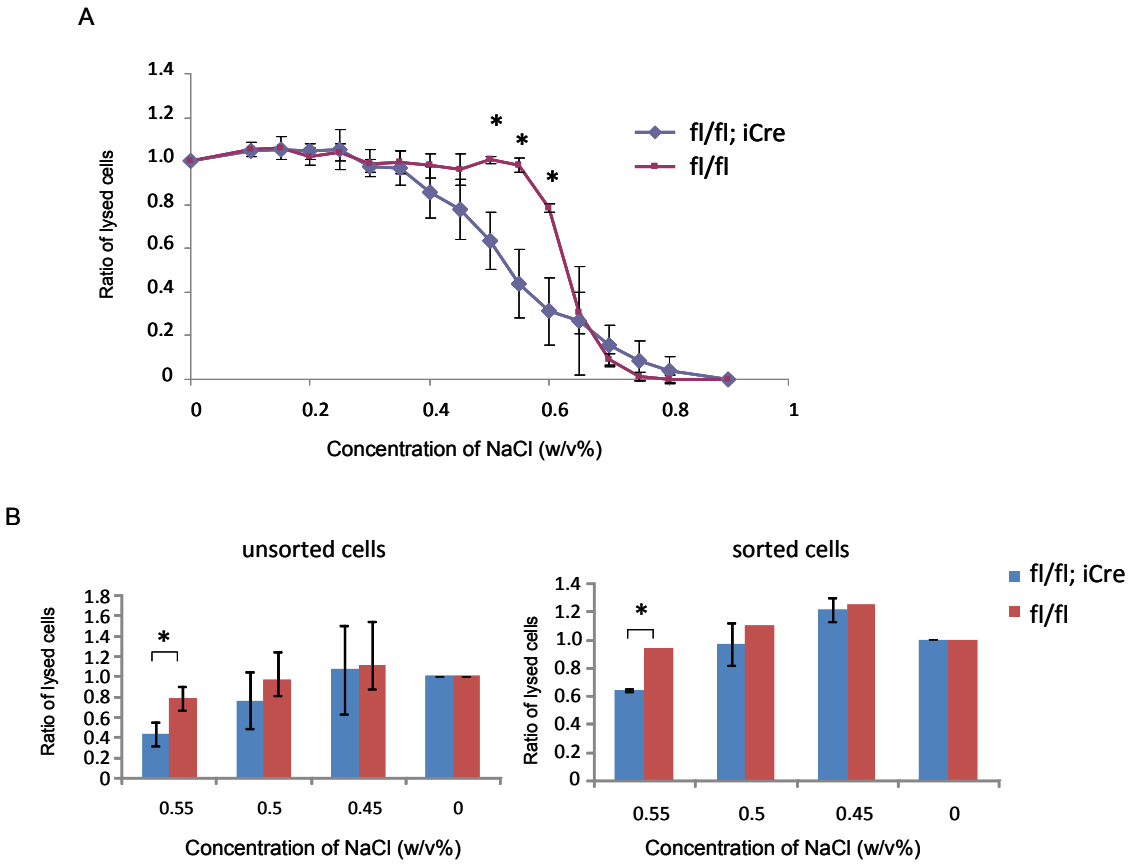

Figure 3.11. Enhanced osmotic resistance in RHAU$^{fl/fl}$; iCre^{tg} erythrocytes. (A) Blood cells from RHAU$^{fl/fl}$ and RHAU$^{fl/fl}$; iCre^{tg} mice were plated in different concentration of NaCl from 0% w/v (pure water) to maximum 0.9% w/v. This figure represents one representative experimental result, n=3 for each group. Experiment was repeated and similar results were obtained. (B) Both unsorted blood cells and sorted enucleated erythrocytes from either RHAU$^{fl/fl}$ or RHAU$^{fl/fl}$; iCre^{tg} mice consistently showed significantly enhanced osmotic resistance.

3.7.9 Chasing of biotinylated erythrocytes revealed shortening of half lives of erythrocytes in RHAU knockout condition

From the results of complete blood cell counts, we know that RHAU-ablated mice are anemic. At the same time, there was a higher number of reticulocytes in the RHAU-ablated mice including those mice that received bone marrow transplantation. The reticulocytes are immature erythrocytes released from hematopoietic organs. Reticulocytes continue to develop into mature erythrocytes and circulate in the peripheral blood until the end of their lives. The higher number of immature reticulocytes and the lower number of total erythrocytes suggested a higher turn over rate of erythrocytes in $RHAU^{fl/fl}$; $iCre^{tg}$ mice. Therefore, we measured the half lives of erythrocytes in control $RHAU^{fl/fl}$ and $RHAU^{fl/fl}$; $iCre^{tg}$ mice. Firstly, we labeled the erythrocytes by injecting biotin-x-HNS directly into the blood circulation. The half life of erythrocytes in each mouse was calculated as described in the Materials and Methods. We found that the half lives of erythrocyte of $RHAU^{fl/fl}$ and $RHAU^{fl/fl}$; $iCre^{tg}$ were 22 days and 11 days, respectively (Figure 3.12A). From this result, we conclude that RHAU ablation leads to shortening the half life of erythrocytes.

Next, we repeated to measure the half lives of erythrocytes. This time, we first labeled the erythrocytes from $RHAU^{fl/fl}$ or $RHAU^{fl/fl}$; $iCre^{tg}$ ex vivo (as described in the Materials and Method) and then transfused into $RHAU^{fl/fl}$ or $RHAU^{fl/fl}$; $iCre^{tg}$ mice. We found that the half life of erythrocyte from $RHAU^{fl/fl}$ mice was 22 days from this experiment. This result was similar to that obtained from in vivo biotin labeling experiment. Surprisingly, when the erythrocytes from $RHAU^{fl/fl}$; $iCre^{tg}$ mice were transfused to $RHAU^{fl/fl}$ mice, the average half life was 20 days and showed no significant difference from that of $RHAU^{fl/fl}$ erythrocyte. On the other hand, we found that the average half life of erythrocytes from $RHAU^{fl/fl}$; $iCre^{tg}$ mice decreased to 15 days when transfused into $RHAU^{fl/fl}$; $iCre^{tg}$ mice (Figure 3.12B). The decrease was significant. Therefore, the shortening of the half life of erythrocytes in $RHAU^{fl/fl}$; $iCre^{tg}$ mice was due to “extrinsic” effect.

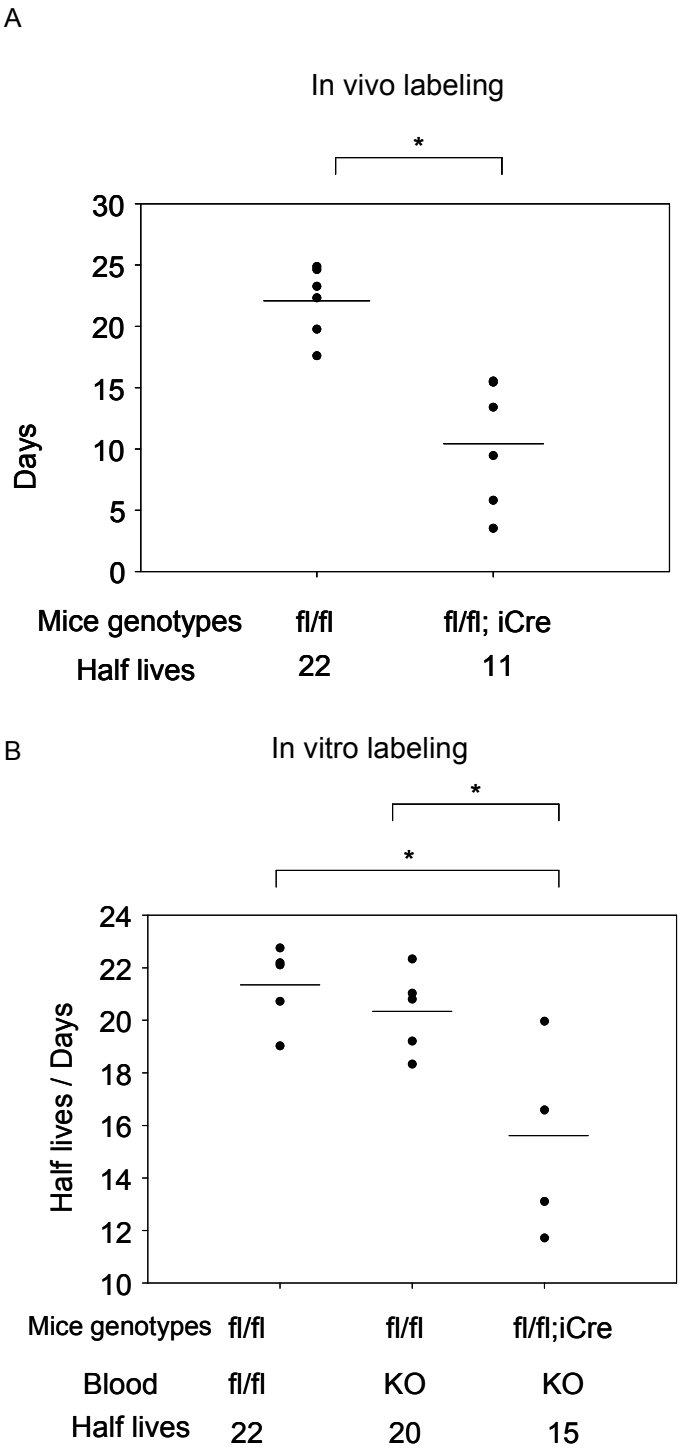

Figure 3.12. Half lives of erythrocyte from RHAU$^{fl/lf}$; iCre^{tg} mice specifically reduced in RHAU$^{fl/fl}$; iCre^{tg} mice but not in RHAU$^{fl/fl}$ mice. (A) Shortened life-span of erythrocytes in RHAU$^{fl/fl}$; iCre^{tg} mice.The half life of erythrocytes was determined by chasing biotinylated cells in vivo. Each dot represents a half life value of erythrocytes from each mouse. (B) Shortened life-span of RHAU$^{fl/fl}$; iCre^{tg} erythrocytes in RHAU$^{fl/fl}$; iCre^{tg} mice and RHAU$^{fl/fl}$ mice. The horizontal lines show the average values and presented at the bottom of the graph. *P<0.05, n=6 for RHAUfl/fl and n=5 for RHAU$^{fl/fl}$.

3.7.10 Comparison of ProE transcriptomes of RHAU$^{fl/fl}$ control mice and RHAU$^{fl/fl}$; iCre^{tg} mice revealed an enrichment of genes with G-quadruplexe motifs at their promoters

Since we observed a defective expansion of cells in erythrocyte lineages, we speculated the effect of RHAU on the gene expression in ProEs. ProE is a stage of erythroblast which proliferates extensively during population expansion. In order to compare the transcriptome of ProEs from control RHAU$^{fl/fl}$ mice and RHAU$^{fl/fl}$; iCre^{tg} mice, 1 x 10^7 bone marrow cells were labeled with FITC anti-Ter119 and PE anti-CD71 antibodies. ProEs (Ter119medCD71hi) were sorted with MoFlo (DakoCytomation) operated with the software Summit (DakoCytomation). Two control and two target mice were used and ProEs collected from one mouse were treated as one sample. RNA samples were submitted for transcriptome analyses using Affeymetrix microarray chip as described in Materials and Methods. A list of genes that were deregulated in RHAU-ablated ProEs was made by program written in R with a two-fold change cutoff and p value < 0.01 (Appendix). The gene list was imported to Ingenuity Pathways Analysis (Ingenuity system) and genes were grouped according to biological pathways (Table 3.3A). Since we were interested in the genes that regulated cell death and proliferation that lead to the phenotype of the RHAU$^{fl/fl}$; iCre^{tg} mice, the genes that were involved in cell death and cell cycle regulation pathways were listed and grouped according to the localization of the gene products. Furthermore, we also searched for genes which contain potential G-quadruplex motifs in the promoter regions, genes contain G-quadruplex motifs in the RNAs and genes that contains AU-rich element in the 3'UTR of mRNA. The databases used for motif search were listed in the Materials and Methods.

According to the Greglist databse (Zhang et al., 2008), there were 31.57% of genes containing promoters with putative G-quadruplex motifs in the whole mouse genome. When we look at the complete list of genes that were deregulated by RHAU-ablation (2-fold, p value < 0.05), we found that there were 83 out of 377 genes (35.4%) containing G-quadruplex motifs at their promoters. There was no obvious enrichment of gene in numbers. However, when we group the genes according to their functions and localization, the result was interesting. We found that there were around 42% and 50% of the genes which involved in cell death pathway and cell cycle regulation, respectively, were containing putative G-quadruplex motifs in their promoters (Table 3.3B).

On another hand, there were 24 out of 377 genes (6.3%) that are deregulated by RHAU knockout are containing G-quadruplex motifs in their RNAs (Kikin et al., 2008). Amongst them, 8% (11/136) of genes were downregulated and 5.4% (13/241) of genes were upregulated.

In mouse genome, there is at least ~5% of genes contain ARE in the 3'UTR. Amongst the genes that were deregulated by RHAU knockout, there were 8 out of 377 genes contain ARE in their 3'UTR. Amongst these genes, 3 out of 136 (2%) were downregulated, and 5 out of 241 (2%) were upregulated. Therefore, in the

RHAU knockout ProEs, there were no obvious enrichement of gene in numbers that contain ARE in the 3'UTR of mRNA (Halees et al., 2008).

Genes associate with cell death pathway

Extracellular Space

Probe ID	logFC	Gene_symbol	Description	Type(s)	G4 promoter	G4 RNA	ARE
10364535	-3.730	ELA2	elastase, neutrophil expressed	peptidase			
10364529	-2.960	PRTN3	proteinase 3	peptidase	yes		
10481627	-1.583	LCN2	lipocalin 2	transporter	yes		
10452316	-1.550	C3	complement component 3	peptidase			
10408693	-1.429	F13A1	coagulation factor XIII, A1 polypeptide	enzyme	yes		
10389214	-1.237	CCL9	chemokine (C-C motif) ligand 9	cytokine	yes	yes	
10478633	-1.219	MMP9	matrix metallopeptidase 9 (gelatinase B, 92kDa gelatinase, 92kDa type IV collagenase)	peptidase	yes		yes
10415052	-1.031	MMP14	matrix metallopeptidase 14 (membrane-inserted)	peptidase			
10563116	1.006	FLT3LG	fms-related tyrosine kinase 3 ligand	cytokine			
10373912	1.068	OSM	oncostatin M	cytokine	yes		yes
10425161	1.184	LGALS1	lectin, galactoside-binding, soluble, 1	other	yes	yes	
10569962	1.839	CCL25	chemokine (C-C motif) ligand 25	cytokine			

Plasma Membrane

Probe ID	logFC	Gene_symbol	Description	Type(s)	G4 promoter	G4 RNA	ARE
10478048	-1.731	LBP	lipopolysaccharide binding protein	transporter	yes		
10550509	-1.561	PGLYRP1	peptidoglycan recognition protein 1	transmembrane receptor			
10501608	-1.435	VCAM1	vascular cell adhesion molecule 1	other			yes
10561008	-1.172	CEACAM1	carcinoembryonic antigen-related cell adhesion molecule 1 (biliary glycoprotein)	transmembrane receptor		yes	
10466172	-1.160	MS4A1	membrane-spanning 4-domains, subfamily A, member 1	other			
10502224	-1.126	SGMS2	sphingomyelin synthase 2	enzyme			
10557862	-1.065	ITGAM	integrin, alpha M (complement component 3 receptor 3 subunit)	other			
10363173	-1.033	GJA1	gap junction protein, alpha 1, 43kDa	transporter			
10559486	-1.014	LAIR1	leukocyte-associated immunoglobulin-like receptor 1	transmembrane receptor			
10546024	1.109	PROKR1	prokineticin receptor 1	G-protein coupled receptor	yes		
10476314	1.227	PRNP	prion protein	other	yes		
10438530	1.247	CLCN2	chloride channel 2	ion channel	yes		
10497079	1.421	PTGER3	prostaglandin E receptor 3 (subtype EP3)	G-protein coupled receptor		yes	
10507594	2.927	SLC2A1	solute carrier family 2 (facilitated glucose transporter), member 1	transporter	yes		

Cytoplasm

Probe ID	logFC	Gene_symbol	Description	Type(s)	G4 promoter	G4 RNA	ARE
10420261	-3.566	CTSG	cathepsin G	peptidase			
10380174	-3.147	MPO	myeloperoxidase	enzyme			
10499861	-1.988	S100A9	S100 calcium binding protein A9	other	yes		
10493831	-1.835	S100A8	S100 calcium binding protein A8	other			
10603551	-1.565	CYBB (includes EG:1536	cytochrome b-245, beta polypeptide	enzyme			
10597098	-1.534	CAMP	cathelicidin antimicrobial peptide	other	yes		
10411235	-1.313	IQGAP2	IQ motif containing GTPase activating protein 2	other			
10501229	-1.292	GSTM5	glutathione S-transferase mu 5	enzyme			
10534202	-1.268	NCF1	neutrophil cytosolic factor 1	enzyme			
10523595	-1.263	PTPN13	protein tyrosine phosphatase, non-receptor type 13 (APO-1/CD95 (Fas) associated phosphatase)	phosphatase			yes
10461979	-1.056	ALDH1A1	aldehyde dehydrogenase 1 family, member A1	enzyme			
10476301	1.043	SMOX	spermine oxidase	enzyme			yes
10488655	1.220	BCL2L1	BCL2-like 1	other			
10430956	1.280	CYB5R3	cytochrome b5 reductase 3	enzyme			
10563338	1.334	PPP1R15A (includes EG:23645)	protein phosphatase 1, regulatory (inhibitor) subunit 15A	other			
10389654	1.363	EPX	eosinophil peroxidase	enzyme			yes
10443527	1.424	PIM1	pim-1 oncogene	kinase	yes		
10469255	1.536	PRKCQ	protein kinase C, theta	kinase			
10425410	2.133	GRAP2	GRB2-related adaptor protein 2	other			

Nucleus

Probe ID	logFC	Gene_symbol	Description	Type(s)	G4 promoter	G4 RNA	ARE
10531724	-1.924	PLAC8	placenta-specific 8	other	yes		
10541260	-1.286	CECR2	cat eye syndrome chromosome region, candidate 2	other			
10366266	-1.181	PAWR	PRKC, apoptosis, WT1, regulator	transcription regulator	yes		
10473809	-1.138	SPI1	spleen focus forming virus (SFFV) proviral integration oncogene spi1	transcription regulator	yes		
10542317	1.019	CDKN1B	cyclin-dependent kinase inhibitor 1B (p27, Kip1)	other	yes		
10545921	1.244	MXD1	MAX dimerization protein 1	transcription regulator	yes		
10545130	1.397	GADD45A	growth arrest and DNA-damage-inducible, alpha	other			
10449284	1.501	DUSP1	dual specificity phosphatase 1	phosphatase	yes		
10443463	1.581	CDKN1A	cyclin-dependent kinase inhibitor 1A (p21, Cip1)	kinase			
10404059	1.600	HIST1H1C	histone cluster 1, H1c	other			
10476252	1.725	CDC25B	cell division cycle 25 homolog B (S. pombe)	phosphatase	yes		
10505512	1.893	TRIM32	tripartite motif-containing 32	transcription regulator			
10357875	1.973	BTG2	BTG family, member 2	transcription regulator	yes	yes	
10405211	2.271	GADD45G	growth arrest and DNA-damage-inducible, gamma	other	yes		

Genes associate with cell cycle regulation pathway

Extracellular Space

Probe ID	logFC	Gene_symbol	Description	Type(s)	G4 promoter	G4 RNA	ARE
10478633	-1.219	MMP9	matrix metallopeptidase 9 (gelatinase B, 92kDa gelatinase, 92kDa type IV collagenase)	peptidase	Yes		yes
10563116	1.006	FLT3LG	fms-related tyrosine kinase 3 ligand	cytokine			
10373912	1.068	OSM	oncostatin M	cytokine	yes		yes
10425161	1.184	LGALS1	lectin, galactoside-binding, soluble, 1	other	yes	yes	

Plasma Membrane

Probe ID	logFC	Gene_symbol	Description	Type(s)	G4 promoter	G4 RNA	ARE
10466224	-2.256	MS4A3	membrane-spanning 4-domains, subfamily A, member 3 (hematopoietic cell-specific)	other			
10561008	-1.172	CEACAM1	carcinoembryonic antigen-related cell adhesion molecule 1 (biliary glycoprotein)	transmembrane receptor		yes	
10363173	-1.033	GJA1	gap junction protein, alpha 1, 43kDa	transporter			
10559486	-1.014	LAIR1	leukocyte-associated immunoglobulin-like receptor 1	transmembrane receptor			
10476314	1.227	PRNP	prion protein	other			
10438530	1.247	CLCN2	chloride channel 2	ion channel			

Cytoplasm

Probe ID	logFC	Gene_symbol	Description	Type(s)	G4 promoter	G4 RNA	ARE
10488655	1.220	BCL2L1	BCL2-like 1	other			
10456254	1.282	NEDD4L	neural precursor cell expressed, developmentally down-regulated 4-like	enzyme			
10563338	1.334	P1R15A (includes EG:23	protein phosphatase 1, regulatory (inhibitor) subunit 15A	other			
10443527	1.424	PIM1	pim-1 oncogene	kinase	yes		
10469255	1.536	PRKCQ	protein kinase C, theta	kinase			

Nucleus

Probe ID	logFC	Gene_symbol	Description	Type(s)	G4 promoter	G4 RNA	ARE
10531724	-1.924	PLAC8	placenta-specific 8	other	yes		
10366266	-1.181	PAWR	PRKC, apoptosis, WT1, regulator	transcription regulator	yes		
10473809	-1.138	SPI1	spleen focus forming virus (SFFV) proviral integration oncogene spi1	transcription regulator	yes		
10362811	1.001	SESN1	sestrin 1	other	Yes		
10542317	1.019	CDKN1B	cyclin-dependent kinase inhibitor 1B (p27, Kip1)	other	yes		
10569102	1.05	IRF7	interferon regulatory factor 7	transcription regulator	yes		
10545921	1.244	MXD1	MAX dimerization protein 1	transcription regulator	yes		
10545130	1.397	GADD45A	growth arrest and DNA-damage-inducible, alpha	other			
10449284	1.501	DUSP1	dual specificity phosphatase 1	phosphatase	yes		
10523297	1.566	CCNG2	cyclin G2	other			
10443463	1.581	CDKN1A	cyclin-dependent kinase inhibitor 1A (p21, Cip1)	kinase			
10425207	1.678	H1F0	H1 histone family, member 0	other			
10476252	1.725	CDC25B	cell division cycle 25 homolog B (S. pombe)	phosphatase	yes		
10357875	1.973	BTG2	BTG family, member 2	transcription regulator	yes	yes	
10405211	2.271	GADD45G	growth arrest and DNA-damage-inducible, gamma	other	yes		

Localization of the protein	No. of genes with putative G4-promoter	Total no of genes	Percentage of gene with putative G4- promoter
Extracellular Space	7	12	58.33
Plasma Membrane	5	14	35.71
Cytoplasm	3	19	15.79
Nucleus	10	14	71.43
Overall	25	59	42.37

Genes involve in cell cycle regulation

Localization of the protein	No. of genes with putative G4-promoter	Total no of genes	Percentage of gene with putative G4- promoter
Extracellular Space	3	4	75.00
Plasma Membrane	0	6	0.00
Cytoplasm	1	5	20.00
Nucleus	11	15	73.33
Overall	15	30	50.00

Table 3.3 Genes deregulated in ProE when RHAU was knockout out. (A) Genes that involve in cell death pathway and cell cycle regulation were listed in separated table analyzed by Ingenuity Pathways Analysis (Ingenuity system) software. (B) Summary of gene numbers that contain putative G-quadruplex motif (G4) in their promoters.

4 DISCUSSION

We suggested previously that RHAU is a multi-functional protein after showing that (1) it enhances urokinase mRNA decay by recruiting poly(A) ribonuclease and exosomes to the AU-rich element in the message (Tran et al., 2004), (2) it translocates to cytoplasmic stress granules upon various stresses in a manner dependent on its RNA binding (Chalupnikova et al., 2008) and is co-localized in nuclear speckles with DEAD-box helicases p68 and p72 (Iwamoto et al., 2008) that are involved in transcriptional regulation, (3) it influences the transcription of various genes both positively and negatively, as revealed by RNAi-mediated knockdown in HeLa cells (Iwamoto et al., 2008), and (4) it displays and is a major source of tetramolecular quadruplex G4-DNA and G4-RNA resolvase activity in HeLa cell lysates (Vaughn et al., 2005) (Creacy et al., 2008), which depends on a evolution conserved RHAU-specific-motif (RSM) domain (Lattmann et al., 2010), in an ATP-dependent manner. Though there were biochemistry assays showing the interesting properties of RHAU, biological information is still missing. Here, we show the first RHAU knockout animal model which revealed RHAU is essential for embryogenesis and hematopoiesis.

4.1 RHAU is required for mouse early embryogenesis

During embryogenesis, embryo implantation occurs at 4.5 dpc and gastrulation starts at around 6 dpc. During gastrulation, three embryonic germ layers are formed by massive cell migration accompanied by a burst of the transcription of key genes important for organogenesis (Pfister et al., 2007; Tam and Loebel, 2007). We found that RHAU knockout embryos degenerated before 7.5 dpc. RHAU appears to become indispensable for gastrulation. We also found that there was no difference in embryo implantation rates between two different breeding: $RHAU^{\Delta/+} \times RHAU^{\Delta/+}$ and $RHAU^{+/+} \times RHAU^{\Delta/+}$, the former of which should give rise to embryos of $RHAU^{\Delta/\Delta}$ genotype. This resuts suggests that RHAU ablation does not affect implantation. However, we cannot exclude the possibility that other helicases compensate the loss of RHAU at this stage. Interestingly, embryos with the ablation of DHX9, another DEAH helicase, knockout embryos also degenerated at similar time point during gastrulation. It would be interesting to understand why DEAH helicase be important for gastrulation (Lee et al., 1998).

4.2 RNA helicases in hematopoiesis

Haematopoiesis involves qualitatively asymmetric cell divisions followed by propagation to establish progenitor cells at several steps. The asymmetric cell division should involve alteration of gene expression, whether its regulation is at the step of template DNA modification, transcription, mRNA maturation or translation, in some of which RNA molecules are necessarily engaged. Thus, the involvement of specific RNA helicases in this process is expected. However, so

far only one member of the DEAH RNA helicase family has been suggested to play a role in the hematopoiesis. It was found that ubiquitously expressed DHX32 was specifically down-regulated in acute lymphoblastic leukemia (Abdelhaleem, 2002), possibly through suppressing apoptosis (Alli et al., 2007). Causal role of this helicase in leukemia development, however, has not yet been addressed. In the present work by ablating RHAU specifically in the hematopoietic system, we have shown an essential role of RHAU in the hematopoiesis acting in a stage- and lineage-specific manner. As the hematopoiesis involves many discrete steps in which various RNA molecules should be modified both covalently and non-covalently, it would not be surprising to find in future more RNA helicases playing important roles in the process. The application of the same strategy employed in this work to other RNA helicases may unravel interesting roles of them in the hematopoiesis and the potential therapeutic target for hematopoietic system disorder.

4.3 Loss of RHAU causes anemia, low blood platelet counts and leucopenia

Complete blood counting consistently showed decrease of RBC, PLT and WBC cells in RHAU ablated conditions brought about by different systems: (1) $RHAU^{fl/fl}$; $iCre^{tg}$ mice, (2) recipient mice transplanted with $RHAU^{fl/fl}$; $iCre^{tg}$ bone marrow, and (3) recipient mice transplanted with $RHAU^{fl/fl}$; $MxCre^{tg}$ bone marrow and treated with polyI:C treatments (Table 3.2). The effects of RHAU knockout on low red blood cell counts, low blood platelet counts and leucopenia were cell autonomous. RHAU-ablation mice developed anemia and reticulocytosis. Increased MCV was due to increased reticulocytes counts because reticulocytes are generally larger than mature red blood cells. Erythrocytosis is promoted by Epo signaling. It is common amongst mammals that anemia induces Epo production in order to compensate the anemic condition. In fact, we also found that the plasma Epo was 800 times higher in the $RHAU^{fl/fl}$; $iCre^{tg}$ mice than the control $RHAU^{fl/fl}$ mice (Figure 3.11). Therefore, reticulocytosis was not directly due to RHAU-ablation. A more detailed discussion on anemia in $RHAU^{fl/fl}$; $iCre^{tg}$ mice will be presented later (see below).

Amongst the WBC, the neutrophil and lymphocytes were decreased in number in the RHAU-ablated mice of all groups. However, basophils and esinophils counts were not affected by RHAU-ablation in mice that received bone marrow transplantation but increased in number in $RHAU^{fl/fl}$; $iCre^{tg}$ mice (which did not receive bone marrow transplantation). We do not know what causes the discrepancy of basophils and esinophils counts between the two systems. One possible cause of this discrepancy is the different housing environment of the two groups of mice. The $RHAU^{fl/fl}$; $iCre^{tg}$ mice and their control siblings were housed in open cages while the recipient mice were housed in sterilized filter-top cages. An increase in number of basophils and esinophils in the $RHAU^{fl/fl}$; $iCre^{tg}$ mice might be the consequence of exposure to air borne pathogens.

Since RHAU-ablation in mice with the vav-iCre system or in recipient mice that received RHAU-ablated bone marrow cells showed similar phenotypes in the peripheral blood, it is suggested that the observation obtained in mice with the vav-iCre system was not caused by non-specific Cre activity in non-hematopoietic systems. Therefore, we decided to study the effect of RHAU ablation in hematopoiesis in a more detail manner using this $RHAU^{fl/fl}$;$iCre^{tg}$ mice.

RHAU ablation specifically in the hematopoietic system causes a defect in hematopoiesis in the bone marrow and extramedullary hematopoiesis

We found that there was a reduction in bone marrow cellularity in $RHAU^{fl/fl}$; $iCre^{tg}$ because the number of cells recovered from RHAUfl/fl; iCretg mice was always lower than that from control sibling mice. Morphological examination by hematoxylin and eosin staining revealed thickening of femur and tibia bones in $RHAU^{fl/fl}$; $iCre^{tg}$ mice. At the same time, the spleen of $RHAU^{fl/fl}$; $iCre^{tg}$ mice was enlarged. Though the RHAU-ablated mice were anemic, complete blood count showed the $RHAU^{fl/fl}$; $iCre^{tg}$ mice developed reticulocytosis induced by high serum Epo level, In vitro colony forming assay showed BFU-E decreased in bone marrow but increased in the spleen of $RHAU^{fl/fl}$; $iCre^{tg}$ mice. Parallel to the in vitro studies, FACS analysis showed no change of MEP and decreased of total erythroblast counts in the bone marrow of $RHAU^{fl/fl}$; $iCre^{tg}$ mice. However, MEP and total erythroblast counts increased in the spleen of $RHAU^{fl/fl}$; $iCre^{tg}$ mice. Therefore, the spleen became a major source of erythroblasts in $RHAU^{fl/fl}$; $iCre^{tg}$ mice.

4.4 Lineage-specific effect of RHAU ablation on lymphoid cell differentiation

RHAU appears to play an essential but differential role in the development of myeloid and lymphoid lineages. In the myeloid lineage, RHAU ablation hinders progression of erythroblast cells at the ProE-to-Ery.A stage. RHAU-ablated erythroblasts, however, still develop to mature red blood cells. In the lymphoid lineage, CLPs can develop into T cells, B cells or natural killer cells. In $RHAU^{fl/fl}$; $iCre^{tg}$ mice, the number of CLPs increased in bone marrow but not in the spleen. In these mice, however, the number of CD19+ cells was very low both in bone marrow and spleen. Expression of CD19 begins in ProB cells, the earliest stage in the B lymphoid lineage (Cobaleda and Sanchez-Garcia, 2009). This indicates that RHAU ablation blocks the CLP-to-B cell branch of lymphoid cell differentiation in the bone marrow. On the other hand, while the differentiation process of the T cell lineage was not completely arrested, ISP8 cells accumulated in the thymus of RHAU-ablated mice. Thus, in both B and T cell lineages, RHAU ablation caused developmental defects at stages during which DNA rearrangements occurred. In the B cell lineage, DH–JH rearrangements are initiated at a low level at the earliest lymphoid progenitor stage and are completed as the cells progress to the CLP and pre-pro-B cell stages (Ceredig and Rolink, 2002; Fuxa and Skok, 2007).

In the T cell lineage, during progression from ISP8 cells to DP cells, Vα→Jα arrangements at the TCRα locus occur (Okamura et al., 1998) (Ceredig and Rolink, 2002). Thus, the accumulation of CLP and ISP8 cells in RHAU-ablated mice implies that RHAU might play a role in DNA rearrangements during B and T lymphoid cell differentiation.

Dramatic decrease of B and T cells in the hematopoietic tissues may account for decreased counts of lymphocytes in the peripheral blood.

4.5 Specific potentiation of monocytes differentiation by RHAU ablation

According to the Akashi-Kondo-Weissman scheme of hematopoietic differentiation, HSCs give rise to CMPs, CMPs to more lineage-restricted GMPs, and finally GMPs to monocytes, neutrophils, basophils and eosinophils (Laiosa et al., 2006). In the colony forming assay, colonies formed reflect the state of differentiation of the pathway CFU-GEMM → CFU-GM → CFU-M or CFU-G. The result of colony forming assays suggests monocyte differentiation potential specifically enhanced both in the bone marrow and spleen of $RHAU^{fl/fl}$; $iCre^{tg}$ mice. FACS analysis also showed an increase monocyte counts but a decrease in neutrophil counts in the spleen. These observations suggest that RHAU ablation potentiates GMPs and CMPs to differentiate into monocytes.

4.6 Study of transcriptome in RHAU knockout ProE showed enrichment of genes that contained putative G-quadruplex (G4) motifs in their promoters

G4-DNA and G4-RNA are highly stable structures that are formed in guanine-rich motifs of DNA or RNA under physiological conditions. It was previously reported that RHAU was the major source of G4-DNA resolvase in HeLa cells. Depletion of RHAU protein either by a monoclonal antibody or shRNA dramatically reduced G4-DNA and G4-RNA resolving activities in these cells (Creacy et al., 2008; Vaughn et al., 2005). Interestingly, we observed among deregulated genes in ProE cells an increased number of genes that harbored G4 motifs at their promoters and were involved in cell death and cell cycle regulation. This enrichment of genes with G4-DNA motif at the promoter can be detected only when genes are categorized according to their functions. Otherwise, there was no observable enrichment. In addition, the genes that code for nuclear proteins occupy the highest fraction of these selected genes. According to the biochemical feature of RHAU, it may resolve G4-DNA in vivo. G4-DNA motifs in the promoter are expected to be inhibitory for transcription and, if so, resolving this stable structure would derepress transcription. However, amongst the genes with G4 motifs in their promoters, not all genes were up-regulated when RHAU was ablated. Among deregulated genes that were involved in cell death, eleven genes were downregulated and thirteen genes were upregulated. Among the genes

that were involved in cell cycle regulation, four genes were downregulated and eleven genes were upregulated. Thus, RHAU ablation preferentially affects some genes of specific functions. We do not know yet whether RHAU directly binds G4 motifs of these genes in vivo. This question should be addressed by chromatin immunoprecipitation experiments in the future.

Though RHAU was originally identified as a protein associating with the ARE in the 3'UTR of urokinase mRNA and decreasing its stabilty, we found no enrichment of ARE-containing mRNAs among deregulated genes in RHAU-ablated ProEs. It may be possible that RHAU specifically regulate the stability of uPA mRNA or of limited number of mRNAs through AREs in the 3'UTR of these mRNA. It would be interesting to search for the genes that can be bound by RHAU and associated with the mouse phenotypes induced by RHAU ablation.

4.7 Hemolytic anemia in $RHAU^{fl/fl}$; $iCre^{tg}$ mice

One of prominent phenotypes exhibited in $RHAU^{fl/fl}$; $iCre^{tg}$ mice are anemia. $RHAU^{fl/fl}$; $iCre^{tg}$ pups were born with the appearance of less redness compared to normal pups. By complete blood counting, we found that the $RHAU^{fl/fl}$; $iCre^{tg}$ mice developed reticulocytosis. Although we already showed that there was a defect in erythropoiesis at the ProE to Ery.A step in the bone marrow and spleen, reticulocytes ratios were higher in $RHAU^{fl/fl}$; $iCre^{tg}$ mice than $RHAU^{fl/fl}$ mice and serum Epo levels were enhanced in $RHAU^{fl/fl}$; $iCre^{tg}$ mice. These results suggest that the anemic phenotype of $RHAU^{fl/fl}$; $iCre^{tg}$ mice is due to decreased life span of erythrocytes rather than the insufficient supply of of newly maturated erythrocytes from from hematopoietic organs.

Blood smear examination showed the presence of spherocytes in the blood of $RHAU^{fl/fl}$; $iCre^{tg}$ mice. In addition, the color of the liver and kidney of these mice were jaundice. This is a sign of hemolytic anemia. The spherocytes observed were erythrocytes that lose the biconcave disk shape and had smaller diameters. Spherocytes are derived from erythrocytes through partially phagocytoization by macrophages in the reticuloendothelial system in liver, spleen and bone marrow (Jain, 1993). The function of the reticuloendothelial system is to filter for antigens and aged erythrocytes with externalized phosphatidylserine (PS) and removes them by phagocytosis. When the destruction rate is higher than production rate of erythrocytes, hemolytic anemia is resulted. There are two types of hemolytic anemia, immunologically-mediated hemolytic anemias and hereditary spherocytosis. Immunologically-mediate hemolytic anemia is induced when erythrocytes bound by complements or autoantibodies and recognized by macrophages for phgocytosis. Hereditary spherocytosis is resulted from genetic defects of proteins involved in cytoskeletal structure (Salomao et al., 2008) (Webb, 2005). Deficiency of any cytoskeletal protein leads to decrease of deformability and special cell shape that can be recognized by macrophages in the reticuloendothelial system. Spherocytes of hemolytic anemias suffer enhanced osmotic fragility. In order to test the osmotic fragility of erythrocytes, blood

samples were put in solutions of various NaCl concentraions ranging from 0% to 0.9% w/v. Erythrocytes are very stable in isotonic 0.9% NaCl solution. In solution below this concentration of NaCl, erythrocytes take up water by osmosis and burst. We expected that sphere-shaped erythrocytes would have less capacity to take up water and be prone to burst in less hypotonic solution than disc-shaped control erythrocytes. Surprisingly, against our expectation, the sphere-shaped erythrocytes were more resistance to osmotic shock than control erythrocytes. In order to explain this phenomenon, we examined levels of several mRNAs encoding membrane proteins of ProE cells. Interestingly, we found that the mRNAs encoding five membrane proteins were up-regulated in $RHAU^{fl/fl}$; $iCre^{tg}$ mice. It was reported that lack of any of these proteins would lead to abnormal cytoskeleton structure in erythrocytes and causes spherocytosis (Salomao et al., 2008) (Webb, 2005). However, in the erythrocytes of $RHAU^{fl/fl}$; $iCre^{tg}$ mice, these proteins were overexpressed (Table 4.1 and Figure 4.1). So, the spherical shape of erythrocytes might be induced not only by downregulation but also by overexpression of these membrane proteins. However, sensitivity to osmotic stress may be different between the two cases. We still do not have an answer to the question why the half lives of erythrocytes were shorter in RHAU-ablated mice.

To know whether the abnormal protein arrangement in the cytoskeleton of erythrocytes was solely responsible for their shorter half lives in RHAU-ablated mice, in other words whether their shorter half lives were cell autonomous, we performed transfusion experiments. Blood cells of $RHAU^{fl/fl}$; $iCre^{tg}$ were biotin-labeled in vitro and then transfused to either $RHAU^{fl/fl}$; $iCre^{tg}$ mice or $RHAU^{fl/fl}$ mice (see Figure 3.12). When transfused into $RHAU^{fl/fl}$ mice, the half lives of erythrocytes were similarly long irrespective of whether labeled erythrocytes were originally derived from $RHAU^{fl/fl}$ or $RHAU^{fl/fl}$; $iCre^{tg}$ mice. On the other hand, erythrocytes from $RHAU^{fl/fl}$; $iCre^{tg}$ mice showed significantly shorter half lives when they were transfused into $RHAU^{fl/fl}$; $iCre^{tg}$ mice than when they were transfused into $RHAU^{fl/fl}$ mice. These results clearly indicate that the shortened half lives of $RHAU^{fl/fl}$; $iCre^{tg}$ erythrocytes were due to an “extrinsic” effect. However, this “extrinsic” effect still is within the hematopoietic system as we still see anemic effect in the bone marrow transplantation models. Whether the “extrinsic” effects reflect immunological response of erythrocytes or activated macrophages in the reticuloendothelial system needs to be further investigated.

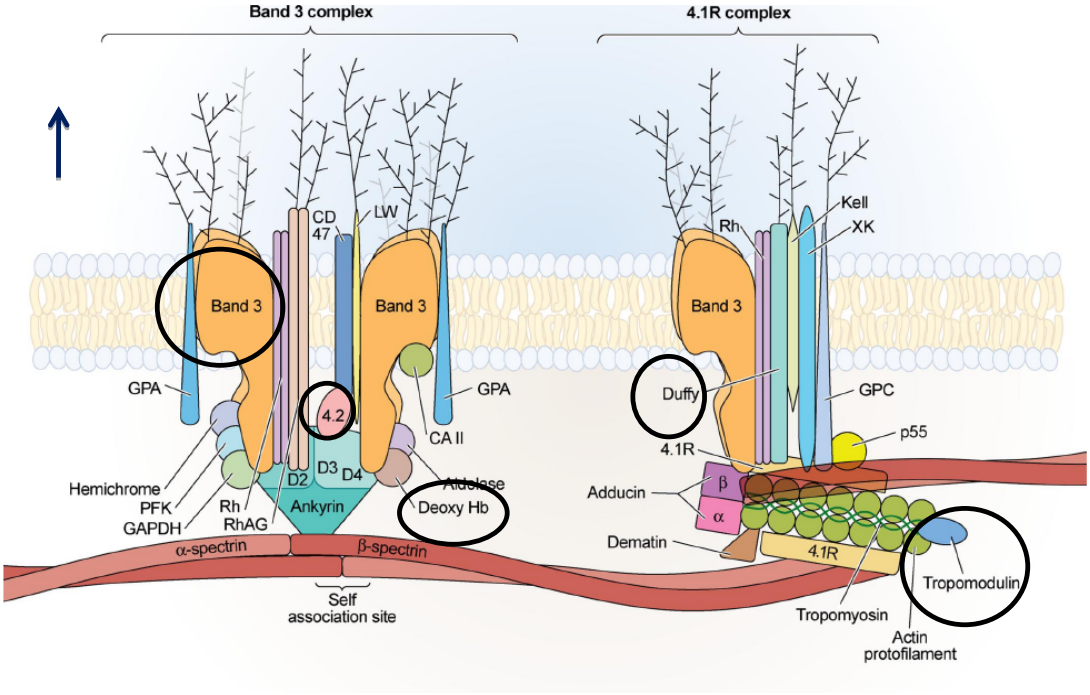

Salomao, *et al.* 2008, PNAS

Figure 4.1. Schematic representation of two types of multiprotein complexes in the red cell membrane. (Left) Protein complex attached to spectrin near the center of the tetramer (dimer–dimer interaction site). Tetrameric band 3 is bound to ankyrin, which is bound to spectrin. The membrane skeletal protein 4.2 has binding sites for band 3 and for ankyrin. Transmembrane glycoproteins GPA, Rh, and RhAG bind to band 3, and CD47 and LWassociate with Rh/RhAG. The two cytoplasmic domains of band3 contain binding sites for soluble proteins, the short C-terminal domain for CAII, the large N-terminal domain for deoxyhemoglobin and for glycolytic enzymes, aldolase, phosphofructokinase (PFK), and glyceraldehyde 3-phosphate dehydrogenase (GAPDH). (Right) Protein complex at membrane skeletal junctions. The junctions contain the ternary complex of spectrin, F-actin, and 4.1R, actin-binding proteins tropomyosin, tropomodulin, adducin,anddematin. 4.1R enters into an additional ternary interaction with the transmembrane protein GPC and p55 and is taken also to bind to band 3, in the form of a dimer, which also carries GPA. Rh, Kell, and XK also have binding sites on 4.1R. Note, however, that the copy numbers of all transmembrane proteins except GPA and GPC are low and therefore will not be present on all complexes (This figure is adopted from Salmona et al., 2008). The highlighted proteins were deregulated in RHAU-ablated ProE transcriptome.

Table 4.1 Fold changes of mRNA expression in RHAU$^{fl/fl}$; iCre^{tg} mice compare to control RHAU$^{fl/fl}$ mice analyzed from microarray data.

Genes	Fold changes
erythrocytes protein band 4.2	2.21
Band 3	3.71
Duffy	2.07
hemoglobin alpha,adult chain 1/2	2.25
tropomodulin 1	5.09

4.8 Potential target against leukemia

FACS analysis showed that the number of CD19+ or B220+ B cells in bone marrow and spleen was drastically reduced in RHAU-ablated mice. As for T cell

differentiation, RHAU ablation retarded progression from ISP8 to DP cells. The fact that RHAU ablation suppresses lymphoid cell differentiation at relatively early stages suggests RHAU as a target for therapy of acute lymphocytic leukemia in which a transforming mutation occurs at an early stage of differentiation (Bernt and Armstrong, 2009) (Passegue et al., 2003). As global gene expression analysis showed extremely high expression of RHAU in mature B and T cells (Su et al., 2004), a role for RHAU in the survival of these cells cannot be excluded. The indispensability of RHAU at an early stage of differentiation may have concealed its requirement in mature B and T cells. If this is the case, RHAU could also be an interesting target in chronic lymphocytic leukemia.

5 Reference

Abbrecht, P.H., and Littell, J.K. (1972). Erythrocyte life-span in mice acclimatized to different degrees of hypoxia. Journal of applied physiology *32*, 443-445.

Abdelhaleem, M. (2002). The novel helicase homologue DDX32 is down-regulated in acute lymphoblastic leukemia. Leuk Res *26*, 945-954.

Abdelhaleem, M. (2004). Do human RNA helicases have a role in cancer? Biochimica et biophysica acta *1704*, 37-46.

Abdelhaleem, M., Maltais, L., and Wain, H. (2003). The human DDX and DHX gene families of putative RNA helicases. Genomics *81*, 618-622.

Adams, B.K., and Smuts, N.A. (1989). The detection of extramedullary hematopoiesis in a patient with osteopetrosis. European journal of nuclear medicine *15*, 803-804.

Akashi, K., Traver, D., Miyamoto, T., and Weissman, I.L. (2000). A clonogenic common myeloid progenitor that gives rise to all myeloid lineages. Nature *404*, 193-197.

Alli, Z., Chen, Y., Abdul Wajid, S., Al-Saud, B., and Abdelhaleem, M. (2007). A role for DHX32 in regulating T-cell apoptosis. Anticancer Res *27*, 373-377.

Almarza, E., Segovia, J.C., Guenechea, G., Gomez, S.G., Ramirez, A., and Bueren, J.A. (2004). Regulatory elements of the vav gene drive transgene expression in hematopoietic stem cells from adult mice. Exp Hematol *32*, 360-364.

Alvarez, B.V., Kieller, D.M., Quon, A.L., Robertson, M., and Casey, J.R. (2007). Cardiac hypertrophy in anion exchanger 1-null mutant mice with severe hemolytic anemia. Am J Physiol Heart Circ Physiol *292*, H1301-1312.

Anantharaman, V., Koonin, E.V., and Aravind, L. (2002). Comparative genomics and evolution of proteins involved in RNA metabolism. Nucleic acids research *30*, 1427-1464.

Andersen, C.B., Ballut, L., Johansen, J.S., Chamieh, H., Nielsen, K.H., Oliveira, C.L., Pedersen, J.S., Seraphin, B., Le Hir, H., and Andersen, G.R. (2006). Structure of the exon junction core complex with a trapped DEAD-box ATPase bound to RNA. Science (New York, NY *313*, 1968-1972.

Anderson, S.F., Schlegel, B.P., Nakajima, T., Wolpin, E.S., and Parvin, J.D. (1998). BRCA1 protein is linked to the RNA polymerase II holoenzyme complex via RNA helicase A. Nature genetics *19*, 254-256.

Aratani, S., Fujii, R., Fujita, H., Fukamizu, A., and Nakajima, T. (2003). Aromatic residues are required for RNA helicase A mediated transactivation. International journal of molecular medicine *12*, 175-180.

Aratani, S., Fujii, R., Oishi, T., Fujita, H., Amano, T., Ohshima, T., Hagiwara, M., Fukamizu, A., and Nakajima, T. (2001). Dual roles of RNA helicase A in CREB-dependent transcription. Molecular and cellular biology *21*, 4460-4469.

Arinobu, Y., Iwasaki, H., and Akashi, K. (2009). Origin of basophils and mast cells. Allergol Int *58*, 21-28.

Arinobu, Y., Iwasaki, H., Gurish, M.F., Mizuno, S., Shigematsu, H., Ozawa, H., Tenen, D.G., Austen, K.F., and Akashi, K. (2005). Developmental checkpoints of the basophil/mast cell lineages in adult murine hematopoiesis. Proceedings of the National Academy of Sciences of the United States of America *102*, 18105-18110.

Baim, S.B., and Sherman, F. (1988). mRNA structures influencing translation in the yeast Saccharomyces cerevisiae. Molecular and cellular biology *8*, 1591-1601.

Bates, G.J., Nicol, S.M., Wilson, B.J., Jacobs, A.M., Bourdon, J.C., Wardrop, J., Gregory, D.J., Lane, D.P., Perkins, N.D., and Fuller-Pace, F.V. (2005). The DEAD box protein p68: a novel transcriptional coactivator of the p53 tumour suppressor. The EMBO journal *24*, 543-553.

Behrens, A., Sibilia, M., David, J.P., Mohle-Steinlein, U., Tronche, F., Schutz, G., and Wagner, E.F. (2002). Impaired postnatal hepatocyte proliferation and liver regeneration in mice lacking c-jun in the liver. The EMBO journal *21*, 1782-1790.

Benoist, C., and Mathis, D. (2002). Mast cells in autoimmune disease. Nature *420*, 875-878.

Beran, R.K., Bruno, M.M., Bowers, H.A., Jankowsky, E., and Pyle, A.M. (2006). Robust translocation along a molecular monorail: the NS3 helicase from hepatitis C virus traverses unusually large disruptions in its track. Journal of molecular biology *358*, 974-982.

Bernt, K.M., and Armstrong, S.A. (2009). Leukemia stem cells and human acute lymphoblastic leukemia. Semin Hematol *46*, 33-38.

Bleichert, F., and Baserga, S.J. (2007). The long unwinding road of RNA helicases. Molecular cell *27*, 339-352.

Bleoo, S., Sun, X., Hendzel, M.J., Rowe, J.M., Packer, M., and Godbout, R. (2001). Association of human DEAD box protein DDX1 with a cleavage stimulation factor involved in 3'-end processing of pre-MRNA. Molecular biology of the cell *12*, 3046-3059.

Bolinger, C., Sharma, A., Singh, D., Yu, L., and Boris-Lawrie, K. (2010). RNA helicase A modulates translation of HIV-1 and infectivity of progeny virions. Nucleic acids research *38*, 1686-1696.

Bono, F., Ebert, J., Lorentzen, E., and Conti, E. (2006). The crystal structure of the exon junction complex reveals how it maintains a stable grip on mRNA. Cell *126*, 713-725.

Bosch, F.H., Werre, J.M., Schipper, L., Roerdinkholder-Stoelwinder, B., Huls, T., Willekens, F.L., Wichers, G., and Halie, M.R. (1994). Determinants of red blood cell deformability in relation to cell age. Eur J Haematol *52*, 35-41.

Bosman, G.J., Werre, J.M., Willekens, F.L., and Novotny, V.M. (2008). Erythrocyte ageing in vivo and in vitro: structural aspects and implications for transfusion. Transfus Med *18*, 335-347.

Burtrum, D.B., Kim, S., Dudley, E.C., Hayday, A.C., and Petrie, H.T. (1996). TCR gene recombination and alpha beta-gamma delta lineage divergence: productive TCR-beta rearrangement is neither exclusive nor preclusive of gamma delta cell development. J Immunol *157*, 4293-4296.

Caretti, G., Schiltz, R.L., Dilworth, F.J., Di Padova, M., Zhao, P., Ogryzko, V., Fuller-Pace, F.V., Hoffman, E.P., Tapscott, S.J., and Sartorelli, V. (2006). The RNA helicases p68/p72 and the noncoding RNA SRA are coregulators of MyoD and skeletal muscle differentiation. Developmental cell *11*, 547-560.

Caruthers, J.M., and McKay, D.B. (2002). Helicase structure and mechanism. Current opinion in structural biology *12*, 123-133.

Causevic, M., Hislop, R.G., Kernohan, N.M., Carey, F.A., Kay, R.A., Steele, R.J., and Fuller-Pace, F.V. (2001). Overexpression and poly-ubiquitylation of the DEAD-box RNA helicase p68 in colorectal tumours. Oncogene *20*, 7734-7743.

Ceredig, R., and Rolink, T. (2002). A positive look at double-negative thymocytes. Nat Rev Immunol *2*, 888-897.

Chalupnikova, K., Lattmann, S., Selak, N., Iwamoto, F., Fujiki, Y., and Nagamine, Y. (2008). Recruitment of the RNA helicase RHAU to stress granules via a unique RNA-binding domain. The Journal of biological chemistry.

Chen, C.F., Jia, H.Y., Ma, H.W., Wang, D.Y., Guo, S.S., and Qu, S. (1999). Rheologic determinant changes of erythrocytes in Binswanger's disease. Zhonghua Yi Xue Za Zhi (Taipei) *62*, 76-85.

Cherukuri, S., Tripoulas, N.A., Nurko, S., and Fox, P.L. (2004). Anemia and impaired stress-induced erythropoiesis in aceruloplasminemic mice. Blood Cells Mol Dis *33*, 346-355.

Christensen, J.L., and Weissman, I.L. (2001). Flk-2 is a marker in hematopoietic stem cell differentiation: a simple method to isolate long-term stem cells. Proceedings of the National Academy of Sciences of the United States of America *98*, 14541-14546.

Cobaleda, C., and Sanchez-Garcia, I. (2009). B-cell acute lymphoblastic leukaemia: towards understanding its cellular origin. Bioessays *31*, 600-609.

Cobaleda, C., Schebesta, A., Delogu, A., and Busslinger, M. (2007). Pax5: the guardian of B cell identity and function. Nature immunology *8*, 463-470.

Coller, J., and Parker, R. (2004). Eukaryotic mRNA decapping. Annual review of biochemistry *73*, 861-890.

Creacy, S.D., Routh, E.D., Iwamoto, F., Nagamine, Y., Akman, S.A., and Vaughn, J.P. (2008). G4 resolvase-1 binds both DNA and RNA tetramolecular quadruplex with high affinity and is the major source of tetramolecular quadruplex G4-DNA and G4-RNA resolving activity in HeLa cell lysates. The Journal of biological chemistry.

Cumano, A., and Godin, I. (2007). Ontogeny of the hematopoietic system. Annual review of immunology *25*, 745-785.

Curry, J.L., and Trentin, J.J. (1967). Hemopoietic spleen colony studies. I. Growth and differentiation. Developmental biology *15*, 395-413.

Das, R., Dufu, K., Romney, B., Feldt, M., Elenko, M., and Reed, R. (2006). Functional coupling of RNAP II transcription to spliceosome assembly. Genes & development *20*, 1100-1109.

Davis, B.N., Hilyard, A.C., Lagna, G., and Hata, A. (2008). SMAD proteins control DROSHA-mediated microRNA maturation. Nature *454*, 56-61.

de Boer, J., Williams, A., Skavdis, G., Harker, N., Coles, M., Tolaini, M., Norton, T., Williams, K., Roderick, K., Potocnik, A.J., *et al.* (2003). Transgenic mice with hematopoietic and lymphoid specific expression of Cre. European journal of immunology *33*, 314-325.

de Franceschi, L., Turrini, F., Honczarenko, M., Ayi, K., Rivera, A., Fleming, M.D., Law, T., Mannu, F., Kuypers, F.A., Bast, A., *et al.* (2004). In vivo reduction of erythrocyte oxidant stress in a murine model of beta-thalassemia. Haematologica *89*, 1287-1298.

Doolittle, W.F. (2000). The nature of the universal ancestor and the evolution of the proteome. Current opinion in structural biology *10*, 355-358.

Fairman, M.E., Maroney, P.A., Wang, W., Bowers, H.A., Gollnick, P., Nilsen, T.W., and Jankowsky, E. (2004). Protein displacement by DExH/D "RNA helicases" without duplex unwinding. Science (New York, NY *304*, 730-734.

Ferreira, R., Ohneda, K., Yamamoto, M., and Philipsen, S. (2005). GATA1 function, a paradigm for transcription factors in hematopoiesis. Molecular and cellular biology *25*, 1215-1227.

Fischer, A., and Malissen, B. (1998). Natural and engineered disorders of lymphocyte development. Science (New York, NY *280*, 237-243.

Foller, M., Sopjani, M., Koka, S., Gu, S., Mahmud, H., Wang, K., Floride, E., Schleicher, E., Schulz, E., Munzel, T., *et al.* (2009). Regulation of erythrocyte survival by AMP-activated protein kinase. Faseb J *23*, 1072-1080.

Ford, M.J., Anton, I.A., and Lane, D.P. (1988). Nuclear protein with sequence homology to translation initiation factor eIF-4A. Nature *332*, 736-738.

Forsberg, E.C., Serwold, T., Kogan, S., Weissman, I.L., and Passegue, E. (2006). New evidence supporting megakaryocyte-erythrocyte potential of flk2/flt3+ multipotent hematopoietic progenitors. Cell *126*, 415-426.

Frischmeyer, P.A., van Hoof, A., O'Donnell, K., Guerrerio, A.L., Parker, R., and Dietz, H.C. (2002). An mRNA surveillance mechanism that eliminates transcripts lacking termination codons. Science (New York, NY *295*, 2258-2261.

Fukuda, T., Yamagata, K., Fujiyama, S., Matsumoto, T., Koshida, I., Yoshimura, K., Mihara, M., Naitou, M., Endoh, H., Nakamura, T., *et al.* (2007). DEAD-box RNA helicase subunits of the Drosha complex are required for processing of rRNA and a subset of microRNAs. Nat Cell Biol.

Fuller-Pace, F.V. (2006). DExD/H box RNA helicases: multifunctional proteins with important roles in transcriptional regulation. Nucleic acids research *34*, 4206-4215.

Fuxa, M., and Skok, J.A. (2007). Transcriptional regulation in early B cell development. Current opinion in immunology *19*, 129-136.

Glansdorff, N., Xu, Y., and Labedan, B. (2008). The last universal common ancestor: emergence, constitution and genetic legacy of an elusive forerunner. Biology direct *3*, 29.

Godbout, R., Packer, M., and Bie, W. (1998). Overexpression of a DEAD box protein (DDX1) in neuroblastoma and retinoblastoma cell lines. The Journal of biological chemistry *273*, 21161-21168.

Gorbalenya, A.E., and Koonin, E.V. (1993). Helicases: amino acid sequence comparisons and structure-function relationships. Current opinion in structural biology *3*, 419-429.

Graf, T., and Trumpp, A. (2007). Haematopoietic stem cells, niches and differentiation pathways (Nature Reviews Immunology), pp. Poster.

Gregory, T., Yu, C., Ma, A., Orkin, S.H., Blobel, G.A., and Weiss, M.J. (1999). GATA-1 and erythropoietin cooperate to promote erythroid cell survival by regulating bcl-xL expression. Blood *94*, 87-96.

Hagman, J., Gutch, M.J., Lin, H., and Grosschedl, R. (1995). EBF contains a novel zinc coordination motif and multiple dimerization and transcriptional activation domains. The EMBO journal *14*, 2907-2916.

Halees, A.S., El-Badrawi, R., and Khabar, K.S. (2008). ARED Organism: expansion of ARED reveals AU-rich element cluster variations between human and mouse. Nucleic acids research *36*, D137-140.

Hartman, T.R., Qian, S., Bolinger, C., Fernandez, S., Schoenberg, D.R., and Boris-Lawrie, K. (2006). RNA helicase A is necessary for translation of selected messenger RNAs. Nature structural & molecular biology *13*, 509-516.

He, Y., Andersen, G.R., and Nielsen, K.H. (2010). Structural basis for the function of DEAH helicases. EMBO reports *11*, 180-186.

Hebbel, R.P. (1991). Beyond hemoglobin polymerization: the red blood cell membrane and sickle disease pathophysiology. Blood *77*, 214-237.

Herschlag, D. (1995). RNA chaperones and the RNA folding problem. The Journal of biological chemistry *270*, 20871-20874.

Hilbert, M., Karow, A.R., and Klostermeier, D. (2009). The mechanism of ATP-dependent RNA unwinding by DEAD box proteins. Biological chemistry *390*, 1237-1250.

Hoek, K.L., Antony, P., Lowe, J., Shinners, N., Sarmah, B., Wente, S.R., Wang, D., Gerstein, R.M., and Khan, W.N. (2006). Transitional B cell fate is associated with developmental stage-specific regulation of diacylglycerol and calcium signaling upon B cell receptor engagement. J Immunol *177*, 5405-5413.

Hoffbrand, A.V., Moss, P.A.H., and Pettit, J.E. (2006a). Erythropoiesis and general aspects of anaemia. In Essential Haematology (Blackwell publising), pp. 108-112.

Hoffbrand, A.V., Moss, P.A.H., and Pettit, J.E. (2006b). Haemolytic anaemias. In Essential Haematology (Blackwell publising), pp. 58-71.

Hoffbrand, A.V., Moss, P.A.H., and Pettit, J.E. (2006c). The spleen. In Essential Haematology (Blackwell publising), pp. 123-128.

Hoffbrand, A.V., Moss, P.A.H., and Pettit, J.E. (2006d). The white cells 2: lymphocytes and their benign disorders. In Essential Haematology (Blackwell publising), pp. 108-112.

Hoffmann-Fezer, G., Trastl, C., Beisker, W., Berg, D., Obermaier, J., Kessler, W., Mysliwietz, J., Schumm, M., Filser, J., and Thierfelder, S. (1997). Preclinical evaluation of biotin labeling for red cell survival testing. Annals of hematology *74*, 231-238.

Iost, I., Dreyfus, M., and Linder, P. (1999). Ded1p, a DEAD-box protein required for translation initiation in Saccharomyces cerevisiae, is an RNA helicase. The Journal of biological chemistry *274*, 17677-17683.

Iwamoto, F. (2007). Biological roles of DExH RNA helicase, RHAU. In Friedrich Miescher Institute for Biomedical Research, of the Novartis Research Foundation (Basel, University of Basel), pp. 85.

Iwamoto, F., Stadler, M., Chalupnikova, K., Oakeley, E., and Nagamine, Y. (2008). Transcription-dependent nucleolar cap localization and possible nuclear function of DExH RNA helicase RHAU. Exp Cell Res *314*, 1378-1391.

Iwasaki, H., Mizuno, S., Mayfield, R., Shigematsu, H., Arinobu, Y., Seed, B., Gurish, M.F., Takatsu, K., and Akashi, K. (2005). Identification of eosinophil lineage-committed progenitors in the murine bone marrow. The Journal of experimental medicine *201*, 1891-1897.

Jain, N. (1993). Erythrocyte physiology and changes in disease (Philadelphia, Lea & Febiger).

Jankowsky, E., and Fairman, M.E. (2007). RNA helicases - one fold for many functions. Current opinion in structural biology.

Jankowsky, E., Gross, C.H., Shuman, S., and Pyle, A.M. (2001). Active disruption of an RNA-protein interaction by a DExH/D RNA helicase. Science (New York, NY *291*, 121-125.

Kaneko, H., Shimizu, R., and Yamamoto, M. (2010). GATA factor switching during erythroid differentiation. Current opinion in hematology.

Katoh, K., and Toh, H. (2008). Recent developments in the MAFFT multiple sequence alignment program. Briefings in bioinformatics *9*, 286-298.

Kawaoka, J., Jankowsky, E., and Pyle, A.M. (2004). Backbone tracking by the SF2 helicase NPH-II. Nature structural & molecular biology *11*, 526-530.

Kedersha, N., Stoecklin, G., Ayodele, M., Yacono, P., Lykke-Andersen, J., Fritzler, M.J., Scheuner, D., Kaufman, R.J., Golan, D.E., and Anderson, P. (2005). Stress granules and processing bodies are dynamically linked sites of mRNP remodeling. J Cell Biol *169*, 871-884.

Kikin, O., Zappala, Z., D'Antonio, L., and Bagga, P.S. (2008). GRSDB2 and GRS_UTRdb: databases of quadruplex forming G-rich sequences in pre-mRNAs and mRNAs. Nucleic acids research *36*, D141-148.

Kim, J.L., Morgenstern, K.A., Griffith, J.P., Dwyer, M.D., Thomson, J.A., Murcko, M.A., Lin, C., and Caron, P.R. (1998). Hepatitis C virus NS3 RNA helicase domain with a bound oligonucleotide: the crystal structure provides insights into the mode of unwinding. Structure *6*, 89-100.

Kitamura, A., Nishizuka, M., Tominaga, K., Tsuchiya, T., Nishihara, T., and Imagawa, M. (2001). Expression of p68 RNA helicase is closely related to the early stage of adipocyte differentiation of mouse 3T3-L1 cells. Biochemical and biophysical research communications *287*, 435-439.

Kondo, M., Weissman, I.L., and Akashi, K. (1997). Identification of clonogenic common lymphoid progenitors in mouse bone marrow. Cell *91*, 661-672.

Kostadinov, R., Malhotra, N., Viotti, M., Shine, R., D'Antonio, L., and Bagga, P. (2006). GRSDB: a database of quadruplex forming G-rich sequences in alternatively processed mammalian pre-mRNA sequences. Nucleic acids research *34*, D119-124.

Kotlikova, I.V., Demakova, O.V., Semeshin, V.F., Shloma, V.V., Boldyreva, L.V., Kuroda, M.I., and Zhimulev, I.F. (2006). The Drosophila dosage compensation complex binds to polytene chromosomes independently of developmental changes in transcription. Genetics *172*, 963-974.

Kumari, S., Bugaut, A., Huppert, J.L., and Balasubramanian, S. (2007). An RNA G-quadruplex in the 5' UTR of the NRAS proto-oncogene modulates translation. Nature chemical biology *3*, 218-221.

Kuroda, M.I., Kernan, M.J., Kreber, R., Ganetzky, B., and Baker, B.S. (1991). The maleless protein associates with the X chromosome to regulate dosage compensation in Drosophila. Cell *66*, 935-947.

Lagasse, E., and Weissman, I.L. (1996). Flow cytometric identification of murine neutrophils and monocytes. J Immunol Methods *197*, 139-150.

Laiosa, C.V., Stadtfeld, M., and Graf, T. (2006). Determinants of lymphoid-myeloid lineage diversification. Annual review of immunology *24*, 705-738.

Lattmann, S., Giri, B., Vaughn, J., Akman, S.A., and Nagamine, Y. (2010). Role of the amino terminal RHAU-specific motif domain in the recognition and resolution of guanine quadruplex-RNA by the DEAH-box RNA helicase RHAU. Nucleic acids research.

Lee, C.G. (2002). RH70, a bidirectional RNA helicase, co-purifies with U1snRNP. The Journal of biological chemistry *277*, 39679-39683.

Lee, C.G., Chang, K.A., Kuroda, M.I., and Hurwitz, J. (1997). The NTPase/helicase activities of Drosophila maleless, an essential factor in dosage compensation. The EMBO journal *16*, 2671-2681.

Lee, C.G., da Costa Soares, V., Newberger, C., Manova, K., Lacy, E., and Hurwitz, J. (1998). RNA helicase A is essential for normal gastrulation. Proceedings of the National Academy of Sciences of the United States of America *95*, 13709-13713.

Lee, C.G., and Hurwitz, J. (1992). A new RNA helicase isolated from HeLa cells that catalytically translocates in the 3' to 5' direction. The Journal of biological chemistry *267*, 4398-4407.

Levine, R.F., Shoff, P., Han, Z.C., and Eldor, A. (1990). Circulating megakaryocytes and platelet production in the lungs. Progress in clinical and biological research *356*, 41-52.

Lind, E.F., Prockop, S.E., Porritt, H.E., and Petrie, H.T. (2001). Mapping precursor movement through the postnatal thymus reveals specific microenvironments supporting defined stages of early lymphoid development. The Journal of experimental medicine *194*, 127-134.

Linder, P. (2003). Yeast RNA helicases of the DEAD-box family involved in translation initiation. Biology of the cell / under the auspices of the European Cell Biology Organization *95*, 157-167.

Liu, Y., Pop, R., Sadegh, C., Brugnara, C., Haase, V.H., and Socolovsky, M. (2006). Suppression of Fas-FasL coexpression by erythropoietin mediates erythroblast expansion during the erythropoietic stress response in vivo. Blood *108*, 123-133.

Liu, Z.R. (2002). p68 RNA helicase is an essential human splicing factor that acts at the U1 snRNA-5' splice site duplex. Molecular and cellular biology *22*, 5443-5450.

Lok, C.N., and Ponka, P. (1999). Identification of a hypoxia response element in the transferrin receptor gene. The Journal of biological chemistry *274*, 24147-24152.

Longman, D., Plasterk, R.H., Johnstone, I.L., and Caceres, J.F. (2007). Mechanistic insights and identification of two novel factors in the C. elegans NMD pathway. Genes & development *21*, 1075-1085.

Lorenz, M., Slaughter, H.S., Wescott, D.M., Carter, S.I., Schnyder, B., Dinchuk, J.E., and Car, B.D. (1999). Cyclooxygenase-2 is essential for normal recovery from 5-fluorouracil-induced myelotoxicity in mice. Exp Hematol *27*, 1494-1502.

Lorsch, J.R., and Herschlag, D. (1998). The DEAD box protein eIF4A. 1. A minimal kinetic and thermodynamic framework reveals coupled binding of RNA and nucleotide. Biochemistry *37*, 2180-2193.

MacDonald, H.R., Budd, R.C., and Howe, R.C. (1988). A CD3- subset of CD4-8+ thymocytes: a rapidly cycling intermediate in the generation of CD4+8+ cells. European journal of immunology *18*, 519-523.

Mackintosh, S.G., Lu, J.Z., Jordan, J.B., Harrison, M.K., Sikora, B., Sharma, S.D., Cameron, C.E., Raney, K.D., and Sakon, J. (2006). Structural and biological identification of residues on the surface of NS3 helicase required for optimal replication of the hepatitis C virus. The Journal of biological chemistry *281*, 3528-3535.

Manohar, C.F., Salwen, H.R., Brodeur, G.M., and Cohn, S.L. (1995). Co-amplification and concomitant high levels of expression of a DEAD box gene with MYCN in human neuroblastoma. Genes, chromosomes & cancer *14*, 196-203.

Matthias, P., and Rolink, A.G. (2005). Transcriptional networks in developing and mature B cells. Nat Rev Immunol *5*, 497-508.

McGrath, K.E., Koniski, A.D., Malik, J., and Palis, J. (2003). Circulation is established in a stepwise pattern in the mammalian embryo. Blood *101*, 1669-1676.

Medina, K.L., Garrett, K.P., Thompson, L.F., Rossi, M.I., Payne, K.J., and Kincade, P.W. (2001). Identification of very early lymphoid precursors in bone marrow and their regulation by estrogen. Nature immunology *2*, 718-724.

Mertsching, E., Wilson, A., MacDonald, H.R., and Ceredig, R. (1997). T cell receptor alpha gene rearrangement and transcription in adult thymic gamma delta cells. European journal of immunology *27*, 389-396.

Meyer, S., Temme, C., and Wahle, E. (2004). Messenger RNA turnover in eukaryotes: pathways and enzymes. Crit Rev Biochem Mol Biol *39*, 197-216.

Mikkola, H.K., and Orkin, S.H. (2006). The journey of developing hematopoietic stem cells. Development *133*, 3733-3744.

Morrison, S.J., Uchida, N., and Weissman, I.L. (1995). The biology of hematopoietic stem cells. Annual review of cell and developmental biology *11*, 35-71.

Myohanen, S., and Baylin, S.B. (2001). Sequence-specific DNA binding activity of RNA helicase A to the p16INK4a promoter. The Journal of biological chemistry *276*, 1634-1642.

Nakajima, T., Uchida, C., Anderson, S.F., Lee, C.G., Hurwitz, J., Parvin, J.D., and Montminy, M. (1997). RNA helicase A mediates association of CBP with RNA polymerase II. Cell *90*, 1107-1112.

Nakorn, T.N., Miyamoto, T., and Weissman, I.L. (2003). Characterization of mouse clonogenic megakaryocyte progenitors. Proceedings of the National Academy of Sciences of the United States of America *100*, 205-210.

Natarajan, A., Wagner, B., and Sibilia, M. (2007). The EGF receptor is required for efficient liver regeneration. Proceedings of the National Academy of Sciences of the United States of America *104*, 17081-17086.

Neidle, S., and Balasubramanian, S. (2006). Quadruplex Nucleic Acids, 1 edn (RSC Publishing).

Neubauer, G., King, A., Rappsilber, J., Calvio, C., Watson, M., Ajuh, P., Sleeman, J., Lamond, A., and Mann, M. (1998). Mass spectrometry and EST-database searching allows characterization of the multi-protein spliceosome complex. Nature genetics *20*, 46-50.

Nicholas, K.B., Nicholas H.B. Jr., and Deerfield, D.W.I. (1997). GeneDoc: Analysis and Visualization of Genetic Variation. EMBNEWNEWS *4*.

Nicholson, P., Yepiskoposyan, H., Metze, S., Zamudio Orozco, R., Kleinschmidt, N., and Muhlemann, O. Nonsense-mediated mRNA decay in human cells: mechanistic insights, functions beyond quality control and the double-life of NMD factors. Cell Mol Life Sci *67*, 677-700.

Okamura, R.M., Sigvardsson, M., Galceran, J., Verbeek, S., Clevers, H., and Grosschedl, R. (1998). Redundant regulation of T cell differentiation and TCRalpha gene expression by the transcription factors LEF-1 and TCF-1. Immunity *8*, 11-20.

Pan, D., Schomber, T., Kalberer, C.P., Terracciano, L.M., Hafen, K., Krenger, W., Hao-Shen, H., Deng, C., and Skoda, R.C. (2007). Normal erythropoiesis but severe polyposis and bleeding anemia in Smad4-deficient mice. Blood *110*, 3049-3055.

Pandita, A., Godbout, R., Zielenska, M., Thorner, P., Bayani, J., and Squire, J.A. (1997). Relational mapping of MYCN and DDXI in band 2p24 and analysis of amplicon arrays in double minute chromosomes and homogeneously staining regions by use of free chromatin FISH. Genes, chromosomes & cancer *20*, 243-252.

Parsyan, A., Shahbazian, D., Martineau, Y., Petroulakis, E., Alain, T., Larsson, O., Mathonnet, G., Tettweiler, G., Hellen, C.U., Pestova, T.V., *et al.* (2009). The helicase protein DHX29 promotes translation initiation, cell proliferation, and tumorigenesis. Proceedings of the National Academy of Sciences of the United States of America *106*, 22217-22222.

Passegue, E., Jamieson, C.H., Ailles, L.E., and Weissman, I.L. (2003). Normal and leukemic hematopoiesis: are leukemias a stem cell disorder or a reacquisition of stem cell characteristics? Proceedings of the National Academy of Sciences of the United States of America *100 Suppl 1*, 11842-11849.

Patel, S.S., and Donmez, I. (2006). Mechanisms of helicases. The Journal of biological chemistry *281*, 18265-18268.

Pelletier, J., and Sonenberg, N. (1985). Insertion mutagenesis to increase secondary structure within the 5' noncoding region of a eukaryotic mRNA reduces translational efficiency. Cell *40*, 515-526.

Pellizzoni, L., Charroux, B., Rappsilber, J., Mann, M., and Dreyfuss, G. (2001). A functional interaction between the survival motor neuron complex and RNA polymerase II. J Cell Biol *152*, 75-85.

Pena, V., Jovin, S.M., Fabrizio, P., Orlowski, J., Bujnicki, J.M., Luhrmann, R., and Wahl, M.C. (2009). Common design principles in the spliceosomal RNA helicase Brr2 and in the Hel308 DNA helicase. Molecular cell *35*, 454-466.

Pfister, S., Steiner, K.A., and Tam, P.P. (2007). Gene expression pattern and progression of embryogenesis in the immediate post-implantation period of mouse development. Gene Expr Patterns *7*, 558-573.

Polach, K.J., and Uhlenbeck, O.C. (2002). Cooperative binding of ATP and RNA substrates to the DEAD/H protein DbpA. Biochemistry *41*, 3693-3702.

Reenan, R.A., Hanrahan, C.J., and Ganetzky, B. (2000). The mle(napts) RNA helicase mutation in drosophila results in a splicing catastrophe of the para Na+ channel transcript in a region of RNA editing. Neuron *25*, 139-149.

Reya, T., O'Riordan, M., Okamura, R., Devaney, E., Willert, K., Nusse, R., and Grosschedl, R. (2000). Wnt signaling regulates B lymphocyte proliferation through a LEF-1 dependent mechanism. Immunity *13*, 15-24.

Richter, L., Bone, J.R., and Kuroda, M.I. (1996). RNA-dependent association of the Drosophila maleless protein with the male X chromosome. Genes Cells *1*, 325-336.

Rivera, A., De Franceschi, L., Peters, L.L., Gascard, P., Mohandas, N., and Brugnara, C. (2006). Effect of complete protein 4.1R deficiency on ion transport properties of murine erythrocytes. Am J Physiol Cell Physiol *291*, C880-886.

Roitt, I., Brostoff, J., and Male, D. (2001). Immunology, Vol Edinburgh, sixth edn (Elsevier Science Limited).

Rossow, K.L., and Janknecht, R. (2003). Synergism between p68 RNA helicase and the transcriptional coactivators CBP and p300. Oncogene *22*, 151-156.

Rothenberg, E.V., Moore, J.E., and Yui, M.A. (2008). Launching the T-cell-lineage developmental programme. Nat Rev Immunol *8*, 9-21.

Salomao, M., Zhang, X., Yang, Y., Lee, S., Hartwig, J.H., Chasis, J.A., Mohandas, N., and An, X. (2008). Protein 4.1R-dependent multiprotein complex: new insights into the structural organization of the red blood cell membrane. Proceedings of the National Academy of Sciences of the United States of America *105*, 8026-8031.

Sambrook, J. (2001). Molecular Cloning: A Laboratory Manual, Third Edition (3 Volume Set), Vol 3, 3 edn (New York, Cold Spring Harbor).

Samokhvalov, I.M., Samokhvalova, N.I., and Nishikawa, S. (2007). Cell tracing shows the contribution of the yolk sac to adult haematopoiesis. Nature *446*, 1056-1061.

Schilham, M.W., Moerer, P., Cumano, A., and Clevers, H.C. (1997). Sox-4 facilitates thymocyte differentiation. European journal of immunology *27*, 1292-1295.

Schmidt, M.L., Salwen, H.R., Manohar, C.F., Ikegaki, N., and Cohn, S.L. (1994). The biological effects of antisense N-myc expression in human neuroblastoma. Cell Growth Differ *5*, 171-178.

Schwarz, B.A., and Bhandoola, A. (2004). Circulating hematopoietic progenitors with T lineage potential. Nature immunology *5*, 953-960.

Scott, D.K., Board, J.R., Lu, X., Pearson, A.D., Kenyon, R.M., and Lunec, J. (2003). The neuroblastoma amplified gene, NAG: genomic structure and characterisation of the 7.3 kb transcript predominantly expressed in neuroblastoma. Gene *307*, 1-11.

Sen, D., and Gilbert, W. (1988). Formation of parallel four-stranded complexes by guanine-rich motifs in DNA and its implications for meiosis. Nature *334*, 364-366.

Sengoku, T., Nureki, O., Nakamura, A., Kobayashi, S., and Yokoyama, S. (2006). Structural basis for RNA unwinding by the DEAD-box protein Drosophila Vasa. Cell *125*, 287-300.

Shams, I., Nevo, E., and Avivi, A. (2005). Ontogenetic expression of erythropoietin and hypoxia-inducible factor-1 alpha genes in subterranean blind mole rats. Faseb J *19*, 307-309.

Shemin, D., and Rittenberg, D. (1946). The life span of the human red blood cell. The Journal of biological chemistry *166*, 627-636.

Short, J.D., and Pfarr, C.M. (2002). Translational regulation of the JunD messenger RNA. The Journal of biological chemistry *277*, 32697-32705.

Shyu, A.B., Greenberg, M.E., and Belasco, J.G. (1989). The c-fos transcript is targeted for rapid decay by two distinct mRNA degradation pathways. Genes & development *3*, 60-72.

Siddiqui-Jain, A., Grand, C.L., Bearss, D.J., and Hurley, L.H. (2002). Direct evidence for a G-quadruplex in a promoter region and its targeting with a small molecule to repress c-MYC transcription. Proceedings of the National Academy of Sciences of the United States of America *99*, 11593-11598.

Simonsson, T., Pecinka, P., and Kubista, M. (1998). DNA tetraplex formation in the control region of c-myc. Nucleic acids research *26*, 1167-1172.

Singh, P., Marikkannu, R., Bitomsky, N., and Klempnauer, K.H. (2009). Disruption of the Pdcd4 tumor suppressor gene in chicken DT40 cells reveals its role in the DNA-damage response. Oncogene *28*, 3758-3764.

Slayton, W.B., Georgelas, A., Pierce, L.J., Elenitoba-Johnson, K.S., Perry, S.S., Marx, M., and Spangrude, G.J. (2002). The spleen is a major site of megakaryopoiesis following transplantation of murine hematopoietic stem cells. Blood *100*, 3975-3982.

Spanopoulou, E., Zaitseva, F., Wang, F.H., Santagata, S., Baltimore, D., and Panayotou, G. (1996). The homeodomain region of Rag-1 reveals the parallel mechanisms of bacterial and V(D)J recombination. Cell *87*, 263-276.

Squire, J.A., Thorner, P.S., Weitzman, S., Maggi, J.D., Dirks, P., Doyle, J., Hale, M., and Godbout, R. (1995). Co-amplification of MYCN and a DEAD box gene (DDX1) in primary neuroblastoma. Oncogene *10*, 1417-1422.

Staley, J.P., and Guthrie, C. (1998). Mechanical devices of the spliceosome: motors, clocks, springs, and things. Cell *92*, 315-326.

Stevenson, R.J., Hamilton, S.J., MacCallum, D.E., Hall, P.A., and Fuller-Pace, F.V. (1998). Expression of the 'dead box' RNA helicase p68 is developmentally and growth regulated and correlates with organ differentiation/maturation in the fetus. The Journal of pathology *184*, 351-359.

Stolle, C.A., and Benz, E.J., Jr. (1988). Cellular factor affecting the stability of beta-globin mRNA. Gene *62*, 65-74.

Su, A.I., Wiltshire, T., Batalov, S., Lapp, H., Ching, K.A., Block, D., Zhang, J., Soden, R., Hayakawa, M., Kreiman, G.*, et al.* (2004). A gene atlas of the mouse and human protein-encoding transcriptomes. Proceedings of the National Academy of Sciences of the United States of America *101*, 6062-6067.

Talavera, M.A., and De La Cruz, E.M. (2005). Equilibrium and kinetic analysis of nucleotide binding to the DEAD-box RNA helicase DbpA. Biochemistry *44*, 959-970.

Tallquist, M.D., and Soriano, P. (2000). Epiblast-restricted Cre expression in MORE mice: a tool to distinguish embryonic vs. extra-embryonic gene function. Genesis *26*, 113-115.

Tam, P.P., and Loebel, D.A. (2007). Gene function in mouse embryogenesis: get set for gastrulation. Nat Rev Genet *8*, 368-381.

Tanaka, N., Aronova, A., and Schwer, B. (2007). Ntr1 activates the Prp43 helicase to trigger release of lariat-intron from the spliceosome. Genes & development *21*, 2312-2325.

Tanner, N.K., and Linder, P. (2001). DExD/H box RNA helicases: from generic motors to specific dissociation functions. Molecular cell *8*, 251-262.

Tetsuka, T., Uranishi, H., Sanda, T., Asamitsu, K., Yang, J.P., Wong-Staal, F., and Okamoto, T. (2004). RNA helicase A interacts with nuclear factor kappaB p65 and functions as a transcriptional coactivator. Eur J Biochem *271*, 3741-3751.

Tonegawa, S. (1983). Somatic generation of antibody diversity. Nature *302*, 575-581.

Tran, H., Schilling, M., Wirbelauer, C., Hess, D., and Nagamine, Y. (2004). Facilitation of mRNA deadenylation and decay by the exosome-bound, DExH protein RHAU. Molecular cell *13*, 101-111.

Trentin, L., Pizzolo, G., Feruglio, C., Zambello, R., Masciarelli, M., Bulian, P., Agostini, C., Vinante, F., Zanotti, R., and Semenzato, G. (1989). Functional analysis of cytotoxic cells in patients with acute nonlymphoblastic leukemia in complete remission. Cancer *64*, 667-672.

Ueno, H., and Weissman, I.L. (2006). Clonal analysis of mouse development reveals a polyclonal origin for yolk sac blood islands. Developmental cell *11*, 519-533.

Uhlmann-Schiffler, H., Jalal, C., and Stahl, H. (2006). Ddx42p--a human DEAD box protein with RNA chaperone activities. Nucleic acids research *34*, 10-22.

Van Hoof, J. (2001). Manufacturing issues related to combining different antigens: an industry perspective. Clin Infect Dis *33 Suppl 4*, S346-350.

Vaughn, J.P., Creacy, S.D., Routh, E.D., Joyner-Butt, C., Jenkins, G.S., Pauli, S., Nagamine, Y., and Akman, S.A. (2005). The DEXH protein product of the DHX36 gene is the major source of tetramolecular quadruplex G4-DNA resolving activity in HeLa cell lysates. The Journal of biological chemistry *280*, 38117-38120.

Verma, A., Yadav, V.K., Basundra, R., Kumar, A., and Chowdhury, S. (2009). Evidence of genome-wide G4 DNA-mediated gene expression in human cancer cells. Nucleic acids research *37*, 4194-4204.

Wallis, V.J., Leuchars, E., Chwalinski, S., and Davies, A.J. (1975). On the sparse seeding of bone marrow and thymus in radiation chimaeras. Transplantation *19*, 2-11.

Webb, D. (2005). Disorders of the red cell membrane. Current Paediatrics *15*, 40-43.

Wei, X., Pacyna-Gengelbach, M., Schluns, K., An, Q., Gao, Y., Cheng, S., and Petersen, I. (2004). Analysis of the RNA helicase A gene in human lung cancer. Oncology reports *11*, 253-258.

Wimmer, K., Zhu, X.X., Lamb, B.J., Kuick, R., Ambros, P.F., Kovar, H., Thoraval, D., Motyka, S., Alberts, J.R., and Hanash, S.M. (1999). Co-amplification of a novel gene, NAG, with the N-myc gene in neuroblastoma. Oncogene *18*, 233-238.

Yang, L., Lin, C., and Liu, Z.R. (2005). Phosphorylations of DEAD box p68 RNA helicase are associated with cancer development and cell proliferation. Mol Cancer Res *3*, 355-363.

Zhang, L., Xu, T., Maeder, C., Bud, L.O., Shanks, J., Nix, J., Guthrie, C., Pleiss, J.A., and Zhao, R. (2009). Structural evidence for consecutive Hel308-like modules in the spliceosomal ATPase Brr2. Nature structural & molecular biology *16*, 731-739.

Zhang, R., Lin, Y., and Zhang, C.T. (2008). Greglist: a database listing potential G-quadruplex regulated genes. Nucleic acids research *36*, D372-376.

Zhang, S., Herrmann, C., and Grosse, F. (1999). Pre-mRNA and mRNA binding of human nuclear DNA helicase II (RNA helicase A). Journal of cell science *112 (Pt 7)*, 1055-1064.

Zhang, S., Maacke, H., and Grosse, F. (1995). Molecular cloning of the gene encoding nuclear DNA helicase II. A bovine homologue of human RNA helicase A and Drosophila Mle protein. The Journal of biological chemistry *270*, 16422-16427.

Zhao, C., Blum, J., Chen, A., Kwon, H.Y., Jung, S.H., Cook, J.M., Lagoo, A., and Reya, T. (2007). Loss of beta-catenin impairs the renewal of normal and CML stem cells in vivo. Cancer Cell *12*, 528-541.

Zhuang, Y., Cheng, P., and Weintraub, H. (1996). B-lymphocyte development is regulated by the combined dosage of three basic helix-loop-helix genes, E2A, E2-2, and HEB. Molecular and cellular biology *16*, 2898-2905.

APPENDIX I: Antibody list for FACS analysis

	Populations	Markers	Antibodies
Bone Marrow	LT-HSC	Lin- IL-7Ra- c-Kit+ Sca-1+ Thy-1.1+ Flt3- VCAM-1+	APC anti-lineage markers include: APC anti-B220 [RA3-6B2] (BD Pharmingen), APC anti-Mac-1 [M1/70] (BD Pharmingen), APC anti-Gr-1[RB6-8C5] (BD Pharmingen), APC anti-TER119 [TER119] (BD Pharmingen), APC anti-CD3ε [145-2C11] (BD Pharmingen), APC anti-IgM [II/41] (BD Pharmingen), APC DX5[HM α 2], (BD Pharmingen), APC anti-CD4 [PJP6] (ImmunoTools), and APC anti-CD8α [YTS 169,4]) (ImmunoTools). APC anti-IL7aR [A7R34] (e-Bioscience), APC/Cy7 anti-c-Kit [2B8] (BioLegend), PE/Cy7 anti-Sca-1 [D7](BD Pharmingen), biotin conjugated anti–Thy-1.1 (HIS51) (e-Bioscience), PE/Cy5.5 conjugated streptavidin (e-Bioscience), FITC-anti-VCAM-1 [429(MVCAM.A)] (BD Pharmingen) and PE-anti- Flt3 [A2F10.1] (BD Pharmingen).
	ST-HSC	Lin- IL-7Ra- c-Kit+ Sca-1+ Thy-1.1+ Flt3+ VCAM-1+	
	MPP	Lin- IL-7Ra- c-Kit+ Sca-1+ Thy-1.1-	
	LMPP	Lin- IL-7Ra- c-Kit+ Sca-1+ Thy-1.1- Flt3+ VCAM-1-	

Bone Marrow and spleen	CMP	Lin- IL-7Ra- c-Kit+ Sca-1- FcgRII/III (CD16/32)low CD34+	APC anti-lineage markers include: APC anti-B220 APC anti-Mac-1 APC anti-Gr-1 APC anti-TER119 APC anti-CD3ε APC anti-IgM APC DX5 APC anti-CD4 and APC anti-CD8α APC anti-IL7Ra[A7R34] (e-Bioscience), PE/Cy5.5 anti-c-Kit [2B8] (eBioscience), PE/Cy7 anti-Sca-1 [D7](BD Pharmingen), PE anti-CD16/32 [2.4G2] (BD Pharmingen) and FITC-CD34 [RAM34] (BD Pharmingen).
	MEP	Lin- IL-7Ra- c-Kit+ Sca-1- FcgRII/III (CD16/32)low CD34-	
	GMP	Lin- IL-7Ra- c-Kit+ Sca-1- FcgRII/III (CD16/32)hi CD34+	
	CLP	Lin- IL-7Ra+ c-Kitlow Sca-1low	APC anti-lineage markers include: APC anti-B220 APC anti-Mac-1 APC anti-Gr-1 APC anti-TER119 APC anti-CD3ε. Biotin conjugated anti-IL-7Ra (BD Pharmingen) PE conjugated streptavidin (BD Pharmingen), PE/Cy5.5-anti-c-Kit PE/Cy7-anti-Sca-1.
	B cell	B220	APC anti-B220
	NK cells	DX5	APC DX5
	Monocytes	Mac-1+ Gr-1low	FITC anti-Gr-1[RB6-8C5] (BD Pharmingen) PE anti-Mac-1 [M1/70.15](ImmunoTools)
	Neutrophils	Mac-1+ Gr-1hi	

Thymus	DN	CD3- CD4- CD8-	APC anti-CD3ε [145-2C11] (BD Pharmingen) FITC anti-CD4 [Clone GK1.5] (Southern Biothech) PE anti-CD8 [53-6.7] (BD Pharmingen)
	ISP8	CD3neg-low (CD3-) CD4- CD8+	
	DP	CD4+ CD8+	
	SPCD4	CD4+ CD8-	
	SPCD8	CD3+ CD4- CD8+	

Supplementary Table 1.Staining and enrichment procedures for different population were achieved by different combination of specific markers as reported previously (Forsberg et al., 2006) (Akashi et al., 2000) (Christensen and Weissman, 2001; Nakorn et al., 2003). Except for MEP, CMP and GMP analysis, non-antigen-specific binding of immunoglobulins to the Fc γ were firstly blocked with anti- Fc γ (CD16/32) [2.4G2] (BD Pharmingen) before the addition of other antibodies. Antibodies for different markers were showed in the table with the clone identity enclosed with [ ]. The suppliers of the antibodies were indicated for once only when it was firstly mentioned.

APPENDIX II:

List of genes that are down-regulated in ProE when RHAU was knockout

	Probe ID	logFC	Gene_symbol	Accession	Description	P.Value	adj.P.Val	B value	G4 promoter	G4 RNA	ARE
1	10364535	-3.730	Ela2	NM_015779	elastase 2, neutrophil	0.000	0.010	4.668			
2	10420261	-3.566	Ctsg	NM_007800	cathepsin G	0.000	0.011	4.457			
3	10380174	-3.147	Mpo	NM_010824	myeloperoxidase	0.000	0.016	3.520			
4	10364529	-2.960	Prtn3	NM_011178	proteinase 3	0.000	0.011	4.292	Yes		
5	10552406	-2.525	Nkg7	NM_024253	natural killer cell group 7 sequence	0.000	0.009	5.067	Yes		
6	10408557	-2.425	Serpinb1a	NM_025429	serine (or cysteine) peptidase inhibitor, clade B, member 1a	0.000	0.066	0.516			
7	10544273	-2.324	Clec5a	NM_001038604	C-type lectin domain family 5, member a	0.000	0.029	1.987			
8	10466224	-2.256	Ms4a3	NM_133246	membrane-spanning 4-domains, subfamily A, member 3	0.000	0.046	1.233			
9	10588243	-2.192	Ryk	NM_013649	receptor-like tyrosine kinase	0.000	0.025	2.331	Yes	Yes	
10	10429568	-2.185	Ly6c1	NM_010741	lymphocyte antigen 6 complex, locus C1	0.000	0.050	1.093			
11	10567580	-2.153	Igsf6	NM_030691	immunoglobulin superfamily, member 6	0.000	0.021	2.524			
12	10429573	-2.143	Ly6c1	NM_010741	lymphocyte antigen 6 complex, locus C1	0.000	0.034	1.756			
13	10556528	-2.134	Pde3b	NM_011055	phosphodiesterase 3B, cGMP-inhibited	0.000	0.041	1.450		Yes	
14	10542164	-2.070	Clec12a	NM_177686	C-type lectin domain family 12, member a	0.000	0.059	0.792			
15	10501020	-1.988	Chi3l3	NM_009892	chitinase 3-like 3	0.002	0.181	-1.120			
16	10499861	-1.988	S100a9	NM_009114	S100 calcium binding protein A9 (calgranulin B)	0.001	0.082	0.169	Yes		
17	10531724	-1.924	Plac8	NM_139198	placenta-specific 8	0.000	0.044	1.337	Yes		
18	10487208	-1.907	Atp8b4	NM_001080944	ATPase, class I, type 8B, member 4	0.001	0.121	-0.437			
19	10589535	-1.904	Ngp	NM_008694	neutrophilic granule protein	0.002	0.187	-1.193			
20	10481262	-1.855	Fcnb	NM_010190	ficolin B	0.000	0.027	2.131			
21	10493831	-1.835	S100a8	NM_013650	S100 calcium binding protein A8 (calgranulin A)	0.000	0.062	0.659			
22	10440002	-1.827	Gpr128	NM_172825	G protein-coupled receptor 128	0.000	0.016	3.344	Yes		
23	10498415	-1.767	Dhx36	NM_028136	DEAH (Asp-Glu-Ala-His) box polypeptide 36	0.000	0.062	0.693			
24	10581605	-1.755	Hp	NM_017370	haptoglobin	0.000	0.075	0.328			
25	10563927	-1.737		---		0.001	0.127	-0.533			
26	10478048	-1.731	Lbp	NM_008489	lipopolysaccharide binding protein	0.000	0.042	1.435	Yes		
27	10442932	-1.712	Tmem8	NM_021793	transmembrane protein 8 (five membrane-spanning domains)	0.000	0.014	3.821			
28	10604564	-1.682	Gpc4	NM_008150	glypican 4	0.001	0.090	0.027	Yes		
29	10589647	-1.671	Tsp50	NM_146227	testes-specific protease 50	0.000	0.017	2.910			
30	10600852	-1.664		---		0.004	0.260	-1.829			
31	10495659	-1.629	Cnn3	NM_028044	calponin 3, acidic	0.000	0.016	3.424	Yes		
32	10589087	-1.628	Prkar2a	NM_008924	protein kinase, cAMP dependent regulatory, type II alpha	0.000	0.062	0.625			
33	10481627	-1.583	Lcn2	NM_008491	lipocalin 2	0.004	0.250	-1.743	Yes		
34	10603551	-1.565	Cybb	NM_007807	cytochrome b-245, beta polypeptide	0.003	0.217	-1.446			
35	10550509	-1.561	Pglyrp1	NM_009402	peptidoglycan recognition protein 1	0.001	0.077	0.251			
36	10452316	-1.550	C3	NM_009778	complement component 3	0.001	0.122	-0.448			
37	10366645	-1.535	1700006J14Rik	ENSMUST00000041178	RIKEN cDNA 1700006J14 gene	0.000	0.017	3.081			
38	10597098	-1.534	Camp	NM_009921	cathelicidin antimicrobial peptide	0.003	0.218	-1.475	Yes		
39	10596053	-1.529	Pccb	NM_025835	propionyl Coenzyme A carboxylase, beta polypeptide	0.000	0.017	2.967			
40	10523451	-1.528	Anxa3	NM_013470	annexin A3	0.001	0.126	-0.509			
41	10457733	-1.513	B4galt6	NM_019737	UDP-Gal:betaGlcNAc beta 1,4-galactosyltransferase, polypeptide 6	0.000	0.052	1.006	Yes		
42	10406852	-1.487	Cnn3	ENSMUST00000029773	calponin 3, acidic	0.000	0.073	0.364	Yes		
43	10376096	-1.482	Acsl6	NM_001033598	acyl-CoA synthetase long-chain family member 6	0.000	0.011	4.183	Yes	Yes	
44	10341801	-1.478		---		0.009	0.369	-2.521			
45	10594798	-1.449		---		0.008	0.357	-2.448			
46	10501608	-1.435	Vcam1	NM_011693	vascular cell adhesion molecule 1	0.000	0.035	1.696			Yes
47	10408693	-1.429	F13a1	NM_028784	coagulation factor XIII, A1 subunit	0.000	0.051	1.080	Yes		
48	10338819	-1.424		---		0.007	0.338	-2.339			
49	10358928	-1.408	Cacna1e	NM_009782	calcium channel, voltage-dependent, R type, alpha 1E subunit	0.000	0.033	1.811		Yes	
50	10432652	-1.404	Ela1	NM_033612	elastase 1, pancreatic	0.000	0.034	1.736			

List of genes that are down-regulated in ProE when RHAU was knockout (continue)

	Probe ID	logFC	Gene_symbol	Accession	Description	P.Value	adj.P.Val	B value	G4 promoter	G4 RNA	ARE
51	10559467	-1.398	Pira11	NM_011088	paired-Ig-like receptor A11	0.000	0.069	0.443	Yes		
52	10348432	-1.363	Centg2	NM_178119	centaurin, gamma 2	0.000	0.062	0.651	Yes	Yes	
53	10472350	-1.351	Gca	NM_145523	grancalcin	0.004	0.242	-1.672			
54	10603346	-1.349	Plp2	NM_019755	proteolipid protein 2	0.000	0.030	1.961			
55	10499045	-1.327	Trim2	NM_030706	tripartite motif-containing 2	0.000	0.044	1.313			
56	10424559	-1.324	Khdrbs3	NM_010158	KH domain containing, RNA binding, signal transduction associated 3	0.001	0.104	-0.183	Yes		
57	10554574	-1.319	Tm6sf1	NM_145375	transmembrane 6 superfamily member 1	0.005	0.280	-1.953	Yes		
58	10411235	-1.313	Iqgap2	NM_027711	IQ motif containing GTPase activating protein 2	0.000	0.077	0.280			
59	10356020	-1.304	Dock10	NM_175291	dedicator of cytokinesis 10	0.000	0.016	3.372			
60	10501229	-1.292	Gstm1	NM_010358	glutathione S-transferase, mu 1	0.005	0.289	-2.028			
61	10571325	-1.290	Mfhas1	NM_001081279	malignant fibrous histiocytoma amplified sequence 1	0.000	0.018	2.801			
62	10541260	-1.286	Cecr2	NM_001128151	cat eye syndrome chromosome region, candidate 2 homolog (human)	0.000	0.042	1.425			
63	10550217	-1.285	Crxos1	NM_001033638	Crx opposite strand transcript 1	0.006	0.318	-2.197			
64	10409376	-1.278	Hk3	NM_001033245	hexokinase 3	0.000	0.077	0.283			
65	10534202	-1.268	Ncf1	NM_010876	neutrophil cytosolic factor 1	0.004	0.247	-1.713			
66	10523595	-1.263	Ptpn13	NM_011204	protein tyrosine phosphatase, non-receptor type 13	0.000	0.058	0.875			Yes
67	10466624	-1.256	Aldh1a7	NM_011921	aldehyde dehydrogenase family 1, subfamily A7	0.001	0.083	0.138			
68	10506004	-1.248	Hook1	NM_030014	hook homolog 1 (Drosophila)	0.006	0.309	-2.151			
69	10367154	-1.240	Gls2	NM_001033264	glutaminase 2 (liver, mitochondrial)	0.001	0.124	-0.485	Yes		
70	10389214	-1.237	Ccl9	NM_011338	chemokine (C-C motif) ligand 9	0.003	0.201	-1.306	Yes	Yes	
71	10425053	-1.222	Ncf4	NM_008677	neutrophil cytosolic factor 4	0.003	0.203	-1.321			
72	10445753	-1.219	Trem3	NM_021407	triggering receptor expressed on myeloid cells 3	0.003	0.221	-1.507			
73	10478633	-1.219	Mmp9	NM_013599	matrix metallopeptidase 9	0.006	0.313	-2.176	Yes		Yes
74	10362111	-1.210		---		0.000	0.059	0.804			
75	10378781	-1.210		---		0.000	0.059	0.804			
76	10381681	-1.210		---		0.000	0.059	0.804			
77	10396110	-1.210		---		0.000	0.059	0.804			
78	10480273	-1.210		---		0.000	0.059	0.804			
79	10496917	-1.210		---		0.000	0.059	0.804			
80	10521600	-1.210		---		0.000	0.059	0.804			
81	10394990	-1.201	Mboat2	NM_026037	membrane bound O-acyltransferase domain containing 2	0.004	0.236	-1.628			
82	10473022	-1.200	Plp2	NM_019755	proteolipid protein 2	0.000	0.062	0.706			
83	10379987	-1.195		---		0.000	0.066	0.511			
84	10553859	-1.195		---		0.000	0.066	0.511			
85	10495830	-1.192	Sec24d	NM_027135	Sec24 related gene family, member D (S. cerevisiae)	0.001	0.115	-0.371	Yes	Yes	
86	10411359	-1.190	Plp2	NM_019755	proteolipid protein 2	0.000	0.041	1.458			
87	10366266	-1.181	Pawr	NM_054056	PRKC, apoptosis, WT1, regulator	0.000	0.036	1.647	Yes		
88	10561008	-1.172	Ceacam1	NM_001039185	carcinoembryonic antigen-related cell adhesion molecule 1	0.006	0.295	-2.065		Yes	
89	10529824	-1.171	Prom1	NM_008935	prominin 1	0.000	0.062	0.618			
90	10563712	-1.169	Mrgpra2	NM_153101	MAS-related GPR, member A2	0.003	0.214	-1.413			
91	10343194	-1.164		---		0.005	0.279	-1.941			
92	10466172	-1.160	Ms4a1	NM_007641	membrane-spanning 4-domains, subfamily A, member 1	0.002	0.153	-0.864			
93	10503174	-1.144	Chd7	NM_001081417	chromodomain helicase DNA binding protein 7	0.003	0.213	-1.398			
94	10362162	-1.139	Taar7d	NM_001010838	trace amine-associated receptor 7D	0.007	0.334	-2.314			
95	10473809	-1.138	Sfpi1	NM_011355	SFFV proviral integration 1	0.010	0.383	-2.589	Yes		
96	10420338	-1.136	Pspc1	NM_025682	paraspeckle protein 1	0.000	0.059	0.851			
97	10543239	-1.126	Tcfec	NM_031198	transcription factor EC	0.001	0.143	-0.717			
98	10502224	-1.126	Sgms2	NM_028943	sphingomyelin synthase 2	0.001	0.129	-0.560			
99	10431697	-1.123	Abcd2	NM_011994	ATP-binding cassette, sub-family D (ALD), member 2	0.004	0.243	-1.681	Yes	Yes	
100	10338090	-1.119		---		0.009	0.365	-2.491			

List of genes that are down-regulated in ProE when RHAU was knockout (continue)

	Probe ID	logFC	Gene_symbol	Accession	Description	P.Value	adj.P.Val	B value	G4 promoter	G4 RNA	ARE
101	10549635	-1.115	EG232801	NM_001081239	predicted gene, EG232801	0.005	0.282	-1.968			
102	10525365	-1.112	Hvcn1	NM_001042489	hydrogen voltage-gated channel 1	0.001	0.099	-0.116		Yes	
103	10574276	-1.105	Gpr97	NM_173036	G protein-coupled receptor 97	0.006	0.301	-2.103	Yes		
104	10589329	-1.104	Pfkfb4	NM_173019	6-phosphofructo-2-kinase	0.000	0.043	1.386	Yes	Yes	
105	10581772	-1.102	Glg1	NM_009149	golgi apparatus protein 1	0.000	0.046	1.258			
106	10540523	-1.097	Lmcd1	NM_144799	LIM and cysteine-rich domains 1	0.000	0.047	1.190			
107	10341621	-1.093		---		0.007	0.334	-2.312			
108	10555762	-1.090	Olfr584	NM_147054	olfactory receptor 584	0.003	0.231	-1.580			
109	10563715	-1.086	Mrgpra2	NM_153101	MAS-related GPR, member A2	0.002	0.181	-1.126			
110	10362294	-1.085	Arhgap18	NM_176837	Rho GTPase activating protein 18	0.006	0.301	-2.108			
111	10412345	-1.077	Parp8	NM_001081009	poly (ADP-ribose) polymerase family, member 8	0.001	0.119	-0.422	Yes		
112	10563170	-1.075	Dkkl1	NM_015789	dickkopf-like 1	0.001	0.142	-0.701			
113	10541599	-1.071	Clec4b2	NM_001004159	C-type lectin domain family 4, member b2	0.001	0.144	-0.737			
114	10466087	-1.069	Tmem109	NM_134142	transmembrane protein 109	0.002	0.185	-1.183			
115	10557862	-1.065	Itgam	NM_001082960	integrin alpha M	0.002	0.188	-1.205			
116	10343371	-1.058		---		0.006	0.309	-2.154			
117	10461979	-1.056	Aldh1a1	NM_013467	aldehyde dehydrogenase family 1, subfamily A1	0.008	0.348	-2.388			
118	10479159	-1.052	OTTMUSG00000017459	NM_001099328	predicted gene, OTTMUSG00000017459	0.001	0.106	-0.238			
119	10431872	-1.042	Slc38a1	ENSMUST00000100262	solute carrier family 38, member 1	0.008	0.346	-2.380	Yes		
120	10537828	-1.041	Olfr434	NM_146369	olfactory receptor 434	0.007	0.334	-2.296			
121	10581813	-1.040	Mlkl	NM_029005	mixed lineage kinase domain-like	0.000	0.062	0.674			
122	10519497	-1.040	Steap4	NM_054098	STEAP family member 4	0.003	0.219	-1.488			
123	10351197	-1.038	Sell	NM_011346	selectin, lymphocyte	0.001	0.104	-0.184			
124	10446376	-1.035	Man2a1	NM_008549	mannosidase 2, alpha 1	0.001	0.099	-0.123	Yes		
125	10406663	-1.035	Arsb	NM_009712	arylsulfatase B	0.007	0.334	-2.306	Yes		
126	10363173	-1.033	Gja1	NM_010288	gap junction protein, alpha 1	0.001	0.099	-0.119			
127	10415052	-1.031	Mmp14	NM_008608	matrix metallopeptidase 14 (membrane-inserted)	0.001	0.145	-0.751			
128	10400483	-1.031	Slc25a21	NM_172577	solute carrier family 25 (mitochondrial oxodicarboxylate carrier), member 21	0.002	0.165	-0.983			
129	10541587	-1.027	Clec4a2	NM_011999	C-type lectin domain family 4, member a2	0.009	0.368	-2.508			
130	10469322	-1.026	Vim	NM_011701	vimentin	0.004	0.237	-1.633	Yes		
131	10508074	-1.017	Csf3r	NM_007782	colony stimulating factor 3 receptor (granulocyte)	0.008	0.361	-2.470			
132	10559486	-1.014	Lair1	NM_001113474	leukocyte-associated Ig-like receptor 1	0.000	0.039	1.535			
133	10603708	-1.013	Cask	NM_009806	calcium	0.009	0.369	-2.510	Yes		
134	10343118	-1.013		---		0.008	0.349	-2.393			
135	10341657	-1.011		---		0.003	0.216	-1.426			
136	10341646	-1.008		---		0.009	0.378	-2.563			

List of genes that are up-regulated in ProE when RHAU was knockout

	Probe ID	logFC	Gene_symbol	Accession	Description	P.Value	adj.P.Val	B value	G4 promoter	G4 RNA	ARE
1	10543791	3.218	Podxl	NM_013723	podocalyxin-like	0.000	0.011	4.180			
2	10399710	2.936	Rsad2	NM_021384	radical S-adenosyl methionine domain containing 2	0.000	0.009	5.376	Yes		
3	10507594	2.927	Slc2a1	NM_011400	solute carrier family 2 (facilitated glucose transporter), member 1	0.000	0.014	3.654	Yes		
4	10343937	2.732		---		0.001	0.085	0.101			
5	10340051	2.624		---		0.000	0.018	2.770			
6	10533229	2.575	Oas1e	NM_145210	2'-5' oligoadenylate synthetase 1E	0.000	0.044	1.357			
7	10343514	2.516		---		0.001	0.140	-0.681			
8	10343538	2.459		---		0.000	0.041	1.472			
9	10338428	2.438		---		0.000	0.066	0.538			
10	10341603	2.436		---		0.000	0.059	0.803			
11	10403821	2.418	Tcrg-V3	ENSMUST00000103558	T-cell receptor gamma, variable 3	0.000	0.062	0.686			
12	10339563	2.371		---		0.000	0.017	2.944			
13	10504692	2.352	Tmod1	NM_021883	tropomodulin 1	0.000	0.003	7.320			
14	10341865	2.342		---		0.000	0.034	1.716			
15	10338686	2.328		---		0.000	0.027	2.120			
16	10341292	2.325		---		0.001	0.107	-0.260			
17	10340943	2.306		---		0.000	0.016	3.289			
18	10342380	2.303		---		0.000	0.010	4.541			
19	10338866	2.287		---		0.001	0.129	-0.558			
20	10405211	2.271	Gadd45g	NM_011817	growth arrest and DNA-damage-inducible 45 gamma	0.003	0.223	-1.525	Yes		
21	10407940	2.265	Naip3	ENSMUST00000103563	NLR family, apoptosis inhibitory protein 3	0.000	0.052	1.000			
22	10341023	2.257		---		0.000	0.017	2.911			
23	10338617	2.256		---		0.000	0.062	0.685			
24	10344016	2.243		---		0.000	0.062	0.676			
25	10342017	2.217		---		0.000	0.047	1.179			
26	10338654	2.192		---		0.000	0.016	3.291			
27	10425410	2.133	Grap2	NM_010815	GRB2-related adaptor protein 2	0.000	0.006	6.365			
28	10338772	2.125		---		0.000	0.009	5.126			
29	10341301	2.095		---		0.000	0.070	0.418			
30	10340679	2.092		---		0.000	0.077	0.255			
31	10338234	2.085		---		0.003	0.201	-1.308			
32	10602372	2.068	Alas2	NM_009653	aminolevulinic acid synthase 2, erythroid	0.000	0.010	4.548	Yes		
33	10339174	2.056		---		0.000	0.029	2.008			
34	10341384	2.053		---		0.004	0.238	-1.643			
35	10342241	2.052		---		0.001	0.088	0.056			
36	10343302	2.048		---		0.000	0.042	1.414			
37	10339296	2.038		---		0.000	0.017	2.918			
38	10344286	2.038		---		0.005	0.267	-1.863			
39	10339038	2.033		---		0.002	0.185	-1.179			
40	10340720	2.019		---		0.000	0.027	2.129			
41	10342410	1.994		---		0.001	0.145	-0.742			
42	10421456	1.986	Xpo7	NM_023045	exportin 7	0.000	0.016	3.500			
43	10338487	1.981		---		0.000	0.017	2.928			
44	10357875	1.973	Btg2	NM_007570	B-cell translocation gene 2, anti-proliferative	0.000	0.030	1.941	Yes	Yes	
45	10339823	1.959		---		0.000	0.033	1.790			
46	10343818	1.956		---		0.000	0.026	2.259			
47	10343957	1.929		---		0.001	0.098	-0.099			
48	10490838	1.921	Fabp5	NM_010634	fatty acid binding protein 5, epidermal	0.000	0.019	2.661			
49	10343768	1.918		---		0.000	0.066	0.538			
50	10342215	1.917		---		0.000	0.010	4.626			

List of genes that are up-regulated in ProE when RHAU was knockout (continue)

	Probe ID	logFC	Gene_symbol	Accession	Description	P.Value	adj.P.Val	B value	G4 promoter	G4 RNA	ARE
51	10342397	1.914		---		0.000	0.017	3.215			
52	10338101	1.909		---		0.005	0.286	-1.992			
53	10391649	1.893	Slc4a1	NM_011403	solute carrier family 4 (anion exchanger), member 1	0.000	0.009	5.153	Yes		
54	10505512	1.893	Trim32	NM_053084	tripartite motif-containing 32	0.000	0.034	1.719			
55	10338760	1.892		---		0.000	0.017	3.168			
56	10341547	1.875		---		0.006	0.294	-2.057			
57	10341062	1.873		---		0.000	0.017	2.923			
58	10343283	1.862		---		0.002	0.185	-1.174			
59	10340116	1.856		---		0.000	0.017	2.912			
60	10343402	1.851		---		0.000	0.026	2.222			
61	10507500	1.845	Slc6a9	NM_008135	solute carrier family 6 (neurotransmitter transporter, glycine), member 9	0.000	0.009	5.625		Yes	
62	10569962	1.839	Ccl25	NM_009138	chemokine (C-C motif) ligand 25	0.001	0.083	0.142			
63	10585699	1.833	Fabp5	ENSMUST00000029046	fatty acid binding protein 5, epidermal	0.000	0.017	3.030			
64	10344422	1.832		---		0.000	0.017	2.966			
65	10341472	1.802		---		0.000	0.051	1.059			
66	10338377	1.796		---		0.001	0.148	-0.783			
67	10341847	1.787		---		0.000	0.016	3.470			
68	10339089	1.785		---		0.002	0.197	-1.273			
69	10473349	1.780	Ypel4	NM_001005342	yippee-like 4 (Drosophila)	0.000	0.046	1.251	Yes		
70	10340287	1.772		---		0.000	0.032	1.852			
71	10369932	1.770	Susd2	NM_027890	sushi domain containing 2	0.005	0.277	-1.930			
72	10339249	1.760		---		0.000	0.027	2.141			
73	10338380	1.758		---		0.000	0.014	3.872			
74	10340920	1.752		---		0.000	0.014	3.705			
75	10344331	1.750		---		0.000	0.035	1.682			
76	10339224	1.743		---		0.000	0.028	2.072			
77	10338163	1.741		---		0.000	0.067	0.480			
78	10338674	1.740		---		0.000	0.011	4.252			
79	10339567	1.739		---		0.005	0.273	-1.899			
80	10339733	1.736		---		0.005	0.283	-1.975			
81	10340029	1.727		---		0.001	0.118	-0.411			
82	10476252	1.725	Cdc25b	NM_023117	cell division cycle 25 homolog B (S. pombe)	0.000	0.010	4.830	Yes		
83	10375002	1.708	Cpeb4	NM_026252	cytoplasmic polyadenylation element binding protein 4	0.000	0.010	4.788			
84	10343345	1.704		---		0.000	0.017	3.038			
85	10597279	1.697	Ccrl2	NM_017466	chemokine (C-C motif) receptor-like 2	0.000	0.045	1.284	Yes		Yes
86	10341667	1.687		---		0.005	0.279	-1.945			
87	10339885	1.682		---		0.000	0.034	1.723			
88	10376326	1.678	Igtp	NM_018738	interferon gamma induced GTPase	0.000	0.032	1.840	Yes		
89	10425207	1.678	H1f0	NM_008197	H1 histone family, member 0	0.000	0.051	1.056		Yes	
90	10339230	1.674		---		0.000	0.059	0.781			
91	10499062	1.672	Fhdc1	NM_001033301	FH2 domain containing 1	0.000	0.006	6.158			
92	10343840	1.660		---		0.002	0.149	-0.809			
93	10339594	1.660		---		0.002	0.165	-0.994			
94	10341388	1.658		---		0.000	0.059	0.836			
95	10344233	1.655		---		0.002	0.196	-1.258			
96	10357698	1.653	Tmcc2	NM_178874	transmembrane and coiled-coil domains 2	0.000	0.014	3.760	Yes		
97	10339510	1.649		---		0.000	0.024	2.364			
98	10342237	1.638		---		0.004	0.240	-1.659			
99	10365344	1.622	Tcp11l2	NM_146008	t-complex 11 (mouse) like 2	0.000	0.012	4.062			
100	10340688	1.604		---		0.001	0.115	-0.358			

List of genes that are up-regulated in ProE when RHAU was knockout (continue)

	Probe ID	logFC	Gene_symbol	Accession	Description	P.Value	adj.P.Val	B value	G4 promoter	G4 RNA	ARE
101	10343106	1.602		---		0.001	0.122	-0.460			
102	10404059	1.600	Hist1h1c	NM_015786	histone cluster 1, H1c	0.000	0.046	1.219			
103	10342272	1.598		---		0.001	0.098	-0.102			
104	10443463	1.581	Cdkn1a	NM_007669	cyclin-dependent kinase inhibitor 1A (P21)	0.002	0.190	-1.227			
105	10341538	1.581		---		0.000	0.014	3.803			
106	10537179	1.569	Bpgm	NM_007563	2,3-bisphosphoglycerate mutase	0.000	0.017	2.900			
107	10523297	1.566	Ccng2	NM_007635	cyclin G2	0.001	0.109	-0.290			
108	10369911	1.561	1110038D17Rik	BC024851	RIKEN cDNA 1110038D17 gene	0.000	0.026	2.276			
109	10541131	1.559	Dcp1b	NM_001033379	DCP1 decapping enzyme homolog b (S. cerevisiae)	0.000	0.017	2.973	Yes		
110	10404885	1.543	Gmpr	NM_025508	guanosine monophosphate reductase	0.000	0.031	1.896			
111	10341495	1.538		---		0.000	0.038	1.573			
112	10469255	1.536	Prkcq	NM_008859	protein kinase C, theta	0.000	0.014	3.701			
113	10381697	1.533	Hexim1	NM_138753	hexamethylene bis-acetamide inducible 1	0.000	0.021	2.486			
114	10339740	1.533		---		0.000	0.027	2.181			
115	10343874	1.530		---		0.002	0.198	-1.280			
116	10342475	1.529		---		0.006	0.309	-2.159			
117	10339749	1.516		---		0.000	0.047	1.199			
118	10563314	1.513	Dhdh	NM_027903	dihydrodiol dehydrogenase (dimeric)	0.001	0.148	-0.784	Yes		
119	10390299	1.507	Pnpo	NM_134021	pyridoxine 5'-phosphate oxidase	0.000	0.016	3.337	Yes		
120	10394674	1.505	ENSMUSG00000050974	ENSMUST00000052528	predicted gene, ENSMUSG00000050974	0.003	0.218	-1.479			
121	10339336	1.502		---		0.000	0.038	1.577			
122	10449284	1.501	Dusp1	NM_013642	dual specificity phosphatase 1	0.000	0.060	0.768	Yes		
123	10338896	1.497		---		0.010	0.384	-2.618			
124	10344528	1.494		---		0.000	0.047	1.178			
125	10500610	1.481	4930431B09Rik	BC120717	RIKEN cDNA 4930431B09 gene	0.000	0.014	3.684			
126	10341823	1.474		---		0.003	0.231	-1.578			
127	10344180	1.455		---		0.000	0.044	1.335			
128	10368289	1.448	Enpp1	NM_008813	ectonucleotide pyrophosphatase	0.000	0.062	0.619	Yes		
129	10343004	1.441		---		0.009	0.380	-2.572			
130	10339804	1.439		---		0.001	0.087	0.076			
131	10340741	1.425		---		0.003	0.209	-1.357			
132	10443527	1.424	Pim1	NM_008842	proviral integration site 1	0.000	0.020	2.555	Yes		
133	10497079	1.421	Ptger3	NM_011196	prostaglandin E receptor 3 (subtype EP3)	0.000	0.017	3.009		Yes	
134	10513061	1.415	Ctnnal1	NM_018761	catenin (cadherin associated protein), alpha-like 1	0.001	0.084	0.129	Yes		
135	10533213	1.398	Oas3	NM_145226	2'-5' oligoadenylate synthetase 3	0.001	0.107	-0.251			
136	10545130	1.397	Gadd45a	NM_007836	growth arrest and DNA-damage-inducible 45 alpha	0.000	0.017	2.913			
137	10344040	1.395		---		0.003	0.201	-1.300			
138	10344572	1.391		---		0.003	0.222	-1.518			
139	10557470	1.375	Gdpd3	NM_024228	glycerophosphodiester phosphodiesterase domain containing 3	0.000	0.032	1.875		Yes	
140	10338235	1.371		---		0.007	0.334	-2.284			
141	10592106	1.366	Tirap	NM_054096	toll-interleukin 1 receptor (TIR) domain-containing adaptor protein	0.000	0.030	1.944			
142	10389654	1.363	Epx	NM_007946	eosinophil peroxidase	0.010	0.383	-2.591			
143	10344238	1.352		---		0.007	0.325	-2.237			
144	10554789	1.337	Ctsc	NM_009982	cathepsin C	0.003	0.218	-1.467	Yes		
145	10490903	1.336	Car13	NM_024495	carbonic anhydrase 13	0.002	0.170	-1.033	Yes		
146	10557481	1.335	Ypel3	NM_026875	yippee-like 3 (Drosophila)	0.000	0.045	1.273			
147	10563338	1.334	Myd116	NM_008654	myeloid differentiation primary response gene 116	0.000	0.017	3.093			Yes
148	10341386	1.323		---		0.000	0.065	0.554			
149	10537292	1.319	1810058I24Rik	ENSMUST00000101536	RIKEN cDNA 1810058I24 gene	0.000	0.011	4.208			
150	10339904	1.308		---		0.007	0.338	-2.338			

List of genes that are up-regulated in ProE when RHAU was knockout (continue)

	Probe ID	logFC	Gene_symbol	Accession	Description	P.Value	adj.P.Val	B value	G4 promoter	G4 RNA	ARE
151	10404965	1.305	Rnf144b	NM_146042	ring finger protein 144B	0.002	0.172	-1.053			
152	10416950	1.299		---		0.000	0.028	2.068			
153	10446986	1.290	Crim1	NM_015800	cysteine rich transmembrane BMP regulator 1 (chordin like)	0.000	0.044	1.317	Yes		
154	10456254	1.282	Nedd4l	NM_001114386	neural precursor cell expressed, developmentally down-regulated gene 4-like	0.000	0.019	2.665			
155	10430956	1.280	Cyb5r3	NM_029787	cytochrome b5 reductase 3	0.001	0.126	-0.515			
156	10451287	1.276	Isg15	NM_015783	ISG15 ubiquitin-like modifier	0.001	0.090	0.029			
157	10342198	1.270		---		0.002	0.172	-1.049			
158	10342665	1.269		---		0.008	0.352	-2.406			
159	10418275	1.268	Ccdc66	NM_177111	coiled-coil domain containing 66	0.002	0.190	-1.220	Yes		
160	10344117	1.267		---		0.002	0.149	-0.817			
161	10543686	1.264	Ube2h	NM_009459	ubiquitin-conjugating enzyme E2H	0.000	0.014	3.672	Yes		
162	10397966	1.262	Otub2	NM_026580	OTU domain, ubiquitin aldehyde binding 2	0.001	0.127	-0.521			
163	10358978	1.260	Ier5	NM_010500	immediate early response 5	0.003	0.234	-1.602			
164	10473356	1.256	Ube2l6	NM_019949	ubiquitin-conjugating enzyme E2L 6	0.000	0.052	1.040			
165	10512451	1.256	B230312A22Rik	BC046771	RIKEN cDNA B230312A22 gene	0.000	0.026	2.238			
166	10375055	1.252	F830116E18Rik	NM_001033981	RIKEN cDNA F830116E18 gene	0.001	0.126	-0.507			
167	10438530	1.247	Clcn2	NM_009900	chloride channel 2	0.000	0.070	0.418	Yes		
168	10545921	1.244	Mxd1	NM_010751	MAX dimerization protein 1	0.000	0.020	2.605	Yes		
169	10470529	1.239	Olfm1	NM_019498	olfactomedin 1	0.000	0.018	2.785	Yes	Yes	
170	10471154	1.237	Ass1	NM_007494	argininosuccinate synthetase 1	0.000	0.054	0.967	Yes		
171	10577114	1.237	Grtp1	NM_025768	GH regulated TBC protein 1	0.000	0.033	1.789	Yes	Yes	
172	10338326	1.234		---		0.005	0.285	-1.985			
173	10552276	1.233	Ube2h	NM_009459	ubiquitin-conjugating enzyme E2H	0.000	0.016	3.309	Yes		
174	10476314	1.227	Prnp	NM_011170	prion protein	0.001	0.147	-0.763	Yes		
175	10400748	1.226	Cdkl1	NM_183294	cyclin-dependent kinase-like 1 (CDC2-related kinase)	0.001	0.106	-0.241			Yes
176	10488655	1.220	Bcl2l1	NM_009743	BCL2-like 1	0.000	0.027	2.123			
177	10393320	1.218	Ube2o	NM_173755	ubiquitin-conjugating enzyme E2O	0.000	0.027	2.204	Yes	Yes	
178	10379034	1.216	Tlcd1	NM_026708	TLC domain containing 1	0.002	0.178	-1.092	Yes		
179	10341480	1.214		---		0.003	0.218	-1.472			
180	10537227	1.210	Tmem140	NM_197986	transmembrane protein 140	0.002	0.182	-1.147			
181	10339251	1.208		---		0.005	0.289	-2.026			
182	10551355	1.206	Sertad3	NM_133210	SERTA domain containing 3	0.006	0.295	-2.067			
183	10339308	1.205		---		0.004	0.255	-1.799			
184	10445767	1.199	Treml2	NM_001033405	triggering receptor expressed on myeloid cells-like 2	0.002	0.170	-1.030	Yes		
185	10411464	1.197	Fcho2	NM_172591	FCH domain only 2	0.000	0.017	2.882			
186	10373902	1.191	2410008K03Rik	BC039988	RIKEN cDNA 2410008K03 gene	0.000	0.062	0.698			
187	10425161	1.184	Lgals1	NM_008495	lectin, galactose binding, soluble 1	0.001	0.143	-0.711	Yes	Yes	
188	10339381	1.180		---		0.001	0.088	0.052			
189	10375058	1.175	Hba-a2	NM_001083955	hemoglobin alpha, adult chain 2	0.001	0.091	0.001	Yes		
190	10363541	1.174	Ass1	NM_007494	argininosuccinate synthetase 1	0.001	0.096	-0.051	Yes		
191	10507137	1.173	Pdzk1ip1	NM_026018	PDZK1 interacting protein 1	0.000	0.065	0.575			
192	10547056	1.153	Tmem40	NM_144805	transmembrane protein 40	0.000	0.047	1.195			
193	10487945	1.151	Prei4	NM_028802	preimplantation protein 4	0.000	0.058	0.889		Yes	
194	10527229	1.149	2810453I06Rik	NM_026050	RIKEN cDNA 2810453I06 gene	0.000	0.077	0.259			
195	10486664	1.147	Epb4.2	NM_013513	erythrocyte protein band 4.2	0.001	0.109	-0.301	Yes		
196	10526564	1.143	Ufsp1	NM_027356	UFM1-specific peptidase 1	0.002	0.172	-1.053			
197	10596812	1.140	6230427J02Rik	BC115538	RIKEN cDNA 6230427J02 gene	0.001	0.090	0.026			
198	10424607	1.119	Ptp4a3	NM_008975	protein tyrosine phosphatase 4a3	0.000	0.019	2.667			
199	10339418	1.119		---		0.010	0.384	-2.609			
200	10528332	1.110	Napepld	NM_178728	N-acyl phosphatidylethanolamine phospholipase D	0.008	0.345	-2.373			

List of genes that are up-regulated in ProE when RHAU was knockout (continue)

	Probe ID	logFC	Gene_symbol	Accession	Description	P.Value	adj.P.Val	B value	G4 promoter	G4 RNA	ARE
201	10546024	1.109	Prokr1	NM_021381	prokineticin receptor 1	0.000	0.073	0.355	Yes		
202	10408935	1.107	ENSMUSG00000074917	ENSMUST00000099550	predicted gene, ENSMUSG00000074917	0.007	0.333	-2.277			
203	10575534	1.104	St3gal2	NM_009179	ST3 beta-galactoside alpha-2,3-sialyltransferase 2	0.000	0.021	2.531	Yes		
204	10446777	1.103	Ehd3	NM_020578	EH-domain containing 3	0.000	0.062	0.629			
205	10381528	1.102	Nags	NM_178053	N-acetylglutamate synthase	0.001	0.143	-0.713			
206	10406407	1.096	Arrdc3	NM_001042591	arrestin domain containing 3	0.003	0.232	-1.586	Yes		Yes
207	10339193	1.096		---		0.003	0.226	-1.547			
208	10346764	1.092	Abi2	NM_198127	abl-interactor 2	0.000	0.052	1.000	Yes		
209	10608716	1.083		---		0.001	0.106	-0.231			
210	10452151	1.076	Rfx2	NM_009056	regulatory factor X, 2 (influences HLA class II expression)	0.000	0.067	0.474	Yes		
211	10507726	1.076	Cited4	NM_019563	Cbp	0.001	0.108	-0.275			
212	10602827	1.075	A830080D01Rik	NM_001033472	RIKEN cDNA A830080D01 gene	0.002	0.149	-0.818			
213	10373912	1.068	Osm	NM_001013365	oncostatin M	0.001	0.144	-0.728	Yes		Yes
214	10488709	1.066	8430427H17Rik	BC075648	RIKEN cDNA 8430427H17 gene	0.000	0.044	1.315			
215	10569569	1.064	Cttn	NM_007803	cortactin	0.001	0.104	-0.191			
216	10466410	1.062	Psat1	NM_177420	phosphoserine aminotransferase 1	0.007	0.334	-2.289		Yes	
217	10342877	1.060		---		0.001	0.115	-0.372			
218	10459912	1.057	Adnp2	NM_175028	ADNP homeobox 2	0.001	0.106	-0.232			
219	10360344	1.056	Darc	NM_010045	Duffy blood group, chemokine receptor	0.000	0.067	0.490			
220	10391332	1.053	Ptrf	NM_008986	polymerase I and transcript release factor	0.001	0.122	-0.451	Yes	Yes	
221	10569102	1.050	Irf7	NM_016850	interferon regulatory factor 7	0.001	0.077	0.251	Yes		
222	10476270	1.047	2310035K24Rik	BC048399	RIKEN cDNA 2310035K24 gene	0.001	0.082	0.174			
223	10476301	1.043	Smox	NM_145533	spermine oxidase	0.000	0.070	0.428			
224	10342129	1.043		---		0.005	0.271	-1.890			
225	10511226	1.042	Centb5	NM_207223	centaurin, beta 5	0.000	0.075	0.319			
226	10588786	1.042	Ube1l	NM_023738	ubiquitin-activating enzyme E1-like	0.000	0.062	0.613			
227	10419073	1.039	Tspan14	NM_145928	tetraspanin 14	0.001	0.106	-0.233	Yes		
228	10455967	1.037	2610318N02Rik	ENSMUST00000093336	RIKEN cDNA 2610318N02 gene	0.007	0.334	-2.299			
229	10421172	1.028	Slc25a37	NM_026331	solute carrier family 25, member 37	0.000	0.062	0.640		Yes	
230	10376854	1.021	Pigl	NM_001039536	phosphatidylinositol glycan anchor biosynthesis, class L	0.008	0.343	-2.362			
231	10542317	1.019	Cdkn1b	NM_009875	cyclin-dependent kinase inhibitor 1B	0.001	0.083	0.145	Yes		
232	10389339	1.017	Usp32	NM_001029934	ubiquitin specific peptidase 32	0.000	0.019	2.663			
233	10542993	1.016	Pon3	NM_173006	paraoxonase 3	0.004	0.254	-1.782			
234	10339935	1.015		---		0.003	0.221	-1.509			
235	10508454	1.013	Bsdc1	NM_133889	BSD domain containing 1	0.000	0.028	2.073			
236	10528268	1.011	Ptpn12	NM_011203	protein tyrosine phosphatase, non-receptor type 12	0.002	0.160	-0.942	Yes		
237	10341218	1.009		---		0.010	0.384	-2.627			
238	10408113	1.007	Hist1h4i	NM_175656	histone cluster 1, H4i	0.001	0.131	-0.591			
239	10563116	1.006	Flt3l	NM_013520	FMS-like tyrosine kinase 3 ligand	0.000	0.060	0.740			
240	10478962	1.002	2010011I20Rik	BC016210	RIKEN cDNA 2010011I20 gene	0.001	0.096	-0.062			
241	10362811	1.001	Sesn1	NM_001013370	sestrin 1	0.007	0.334	-2.296	Yes		

Supplementary Table 2

Up- and down-regulated probe sets when comparing the transcriptome of ProE isolated from RHAU $^{fl/fl}$ and RHAU$^{fl/fl}$; iCre^{tg} mice. Fold change is expressed as $\log_2$ FC. Gene expression with more than 2-fold changes and t-test p-value < 0.01 were filtered.

Abbreviation

Baso	basophils
CMP	common myeloid progenitor
DC	dendritic cell
DN	double negative
DP	double positive
dpc	days postcoitus
Eosino	eosinophils
Ery.	erythroblast
ETP	early T cell precursors
G4	G-quadruplex
HB	hemoglobin
Hct	hematocrit
HSC	haematopoietic stem cell
ISP	immature single positive
LMPP	lymphoid primed multipotent progenitor
LT-HSC	long-term repopulating haematopoietic stem cell
Luc	large unstained cells
Lympho	lymphocytes
MCH	mean corpuscular hemoglobin
MCHC	mean corpuscular hemoglobin concentration
MCV	mean corpuscular volume
MEP	megakaryocyte/erythroid progenitor
Mono	monocytes
MPP	multipotent progenitor
MPV	mean platelet volume
Neutro	neutrophils
NK	cell natural killer cell
ProE	proerythroblast
RBC	red blood cell count
RDW	red blood cell distribution width
RET	reticulocyte count
RNP	ribonucleoprotein
SP	single positive
ST-HSC	short-term repopulating haematopoietic stem cell
WBC	white blood cell count
WHD	winged-helix domain

Acknowledgements

First of all, I would like to thank Dr. Yoshikuni Nagamine for giving me the valuable opportunity to work in his lab and providing such a nice working environment throughout these years. Dr. Nagamine was always supportive and encouraging throughout my studies. His advice always helped me to make the right decisions. He is not only a good mentor for scientific work, but also a good educator for philosophy. I believe the education I received in the last few years is very useful for my whole life.

I also give my thanks to all the members of my PhD thesis committee, Prof. Radek Skoda, Prof. Patrick Matthias, and Prof. Nancy Hynes, for their helpful suggestions and advice in the committee meetings. Thanks to Prof. Ruth Chiquet for being the chairman of my thesis examination. In addition, I would like to give my special thanks to Prof. Patrick Matthias for all his kindness guidance of my research and thanks for providing me with all the necessary materials and licenses for all the mouse work, and materials for FACS analysis.

Thank you to Dr. Dejing Pan for many fruitful discussions and guidance of my project and his technical help. I thank Svetlana Ponti, Jean-François Spetz, and Patrick Kopp for the preparation of the targeting vector, the ES cells work, and generating the valuable transgenic mice. Thank you to Hubertus Kohler from the FACS facility for his professional technical service in cell sorting. I also thank Chun Cao and Gabriele Matthias from Patrick Matthias' lab for their kindness and assistance. Thank you to all the great FMI members that contributed to my PhD work.

I want to thank all the former and current lab members who were always nice and had created such a happy and positive working environment. Thank you to Simon Lattmann for his excellent advice in the scientific work as well as computational assistance. Thank you to Stéphane Thiry for his technical expertise and his excellent laboratory management. I also thank Dr. Sandra Pauli for preparing antibodies and her scientific discussions. Thank you to my good friend Dr. Nives Selak Bienz for her generous help in all aspects of my research and for her creative advice and mental support thoughout these years.

Finally, I sincerely thank all my family members and friends who had been so supportive throughout my life.

Ching Janice LAI

e-mail: Janice.lai@fmi.ch
Hong Kong (China)

RESEARCH EXPERIENCE

10/2005 – 08/2010

PhD student, Friedrich Miescher Institute, Part of Novartis Research Foundation, Basel, Switzerland (Group Nagamine).
Project: RHAU is essential for embryogenesis and hematopoiesis

10/2004- 09/2005

Research assistance, Cancer Biology, The Chinese University of Hong Kong.
Project: Study of apoptotic pathway induced by newly designed novel drugs for photodynamic therapy

07/2002 – 09/2004

Master of Philosophy (Biochemistry) student, Chinese University of Hong Kong, Hong Kong.
Project: Alternation of lipid metabolism in glial cells under cerebral hypoglycemia

06/2001 – 08/2001

Trainee of the International Association for the Exchange of Students for Technical Experience (IAESTE)**,** Institute of Enzyme Technology, Juelich, the Forschungszentrum Jülich Germany
Project: Crystalization of L-amino acid oxidase from Rhodococcus Opacus

06/2000 – 08/2000

Laboratory assistance**,** Hong Kong Herbarium.

EDUCATION & TRAININGS

10/2005 – 08/2011

PhD (Cell biology), University of Basel

08/2010

Patent puzzle course (Novartis), *8 hours*

09/1999- 06/2002

BSc (Second Class Honours, [Division I]) in Applied Biology with Biotechnology, Hong Kong Polytechnic University

AWARDS

1. International PhD scholarship from Friedrich Miescher Institute
2. Full studentship at the Department of Biochemistry (Science) of the Chinese University of Hong Kong, 2002
3. Hong Kong Plastics Manufacturers Association Limited 40th Anniversary Scholarship, 2001-2002

PATENTS

International Patent Application PCT/EP2010/056226, Patent: 'DHX36 / RHAU knockout mice as experimental models of muscular dystrophy', Date of Filing: 07.05.2010, Applicant: Novartis Forschungsstiftung Zweigniederlassung Friedrich Miescher Institute for Biomedical Research, Inventors: **Lai, J.,** Nagamine Y., Wu P.

PUBLICATIONS/PRESENTATION

1. **Lai JC**, Ponti S, Pan D, Kohler H, Skoda RC, Matthias P, Nagamine Y. The DEAH helicase RHAU (DHX36) is an essential gene and critical for hematopoiesis (Blood, accepte).
2. **Lai JC**, Lo PC, Ng DK, Ko WH, Leung SC, Fung KP, Fong WP. (2006). BM-SiPc, a novel agent for photodynamic therapy, induces apoptosis in human hepatocarcinoma HepG2 cells by a direct mitochondrial action. Cancer Biol Ther. 5(4):413-8
3. Huang JD, Lo PC, Chen YM, **Lai JC,** Fong WP, Ng DK. (2006). Preparation and in vitro photodynamic activity of novel silicon(IV) phthalocyanines conjugated to serum albumins. *J Inorg Biochem.* 100(5-6):946-51.
4. Wong HY, Chu TS, **Lai JC**, Fung KP, Fok TF, Fujii T, Ho YY (2005). Sodium valproate inhibits glucose transport and exacerbates Glut1-deficiency in vitro. *J Cell Biochem.* 1:96(4):775-85.
5. **Lai JC**, SC Tsang, YY Ho. (11th July 2003) Glucose deficiency alters growth and metabolic properties of glial cells. Poster presented at the Sixth IBRO World Congress of Neuroscience. Prague, Czech Republic.

REFERENCES

Dr. Yoshikuni Nagamine
Senior group leader
Friedrich Miescher Institute
Maulbeerstrasse 66,
CH 4058, Basel, Switzerland
Tel. +41 (61) 6974499
nagamine.yoshikuni@gmail.com

Dr. Patrick Matthias
Senior group leader
Friedrich Miescher Institute
Maulbeerstrasse 66,
CH 4058, Basel, Switzerland
Tel. +41 (61) 6975046
patrick.matthias@fmi.ch